U.PORTO

CICLO DE ESTUDOS

BIOTECNOLOGIA MOLECULAR E CELULAR APLICADA ÀS CIÊNCIAS DA SAÚDE

Targeting of Human CD44v6 with Engineered Nanoparticles for Gastrointestinal Cancer Diagnosis and Therapy

Patrick Joseph Kennedy

D

2018

U.PORTO

Patrick Joseph Kennedy. Targeting of Human CD44v6 with Engineered Nanoparticles for Gastrointestinal Diagnosis and Therapy

D.ICBAS 2018

Targeting of Human CD44v6 with Engineered Nanoparticles for Gastrointestinal Cancer Diagnosis and Therapy

Patrick Joseph Kennedy

SEDE ADMINISTRATIVA

INSTITUTO DE CIÊNCIAS BIOMÉDICAS ABEL SALAZAR

FACULDADE DE FARMÁCIA

Patrick Joseph Kennedy

Targeting of Human CD44v6 with Engineered Nanoparticles for Gastrointestinal Cancer Diagnosis and Therapy

Thesis as a candidate for the Doctoral Program on Cellular and Molecular Biotechnology Applied to Health Sciences (BiotechHealth) submitted to the Instituto de Ciências Biomédicas Abel Salazar da Universidade do Porto

Supervisor:
Dr. Bruno Filipe Carmelino Cardoso Sarmento
Principal Investigator/Auxiliary Professor
i3S – Instituto de Investigação e Inovação em Saúde, INEB - Instituto Nacional de Engenharia Biomédica, Universidade do Porto & IUCS – Instituto Universitário de Ciências da Saúde

Co-Supervisors:
Dr. Pedro Lopes Granja
Principal Investigator/Associate Professor
i3S – Instituto de Investigação e Inovação em Saúde, INEB - Instituto Nacional de Engenharia Biomédica, FEUP - Faculdade de Engenharia, ICBAS - Instituto de Ciências Biomédicas Abel Salazar, Universidade do Porto

Dr. Carla Oliveira
Principal Investigator/Associate Professor
i3S – Instituto de Investigação e Inovação em Saúde, IPATIMUP - Instituto de Patologia e Imunologia Molecular da Universidade do Porto, FMUP - Faculdade de Medicina da Universidade do Porto

To my Family and Friends around the world...

The work presented in this thesis was developed at:

Nanomedicines and Translational Drug Delivery Group
Biomaterials for Multistage Drug and Cell Delivery Group and the
Expression Regulation in Cancer Group
i3S - Instituto de Investigação e Inovação em Saúde
INEB - Instituto Nacional de Engenharia Biomédica and
IPATIMUP - Instituto de Patologia e Imunologia Molecular
Universidade do Porto, Porto, Portugal
Rua Alfredo Allen, 208
4200-135 Porto, Portugal
www.i3s.up.pt | www.ineb.up.pt

and

Department of Microbiology and Immunology, Miller School of Medicine
University of Miami, Miami, Florida, USA
1600 NW 10th Avenue. Miami, FL 33136
www.micro.med.miami.edu

FINANCIAL SUPPORT

Patrick Joseph Kennedy was supported by a national PhD grant (SFRH/BD/99036/2013) from Fundação para a Ciência e Tecnologia (FCT).

This work was financed by the project NORTE-01-0145-FEDER-000012, supported by Norte Portugal Regional Operational Programme (NORTE 2020), under the PORTUGAL 2020 Partnership Agreement, through the European Regional Development Fund (ERDF).

This work was financed by FEDER - Fundo Europeu de Desenvolvimento Regional funds through the COMPETE 2020 - Operacional Programme for Competitiveness and Internationalisation (POCI), Portugal 2020, and by Portuguese funds through FCT - Fundação para a Ciência e a Tecnologia/ Ministério da Ciência, Tecnologia e Ensino Superior in the framework of the project "Institute for Research and Innovation in Health Sciences" (POCI-01-0145-FEDER-007274). This work was also supported by the FCT PhD Programmes and by Programa Operacional Potencial Humano (POCH), specifically by the BiotechHealth Programme (Doctoral Programme on Cellular and Molecular Biotechnology Applied to Health Sciences).

PUBLICATIONS

Ao abrigo do disposto do nº 2, alínea a) do artigo 31º do Decreto-Lei n.º 115/2013 de 7 de Agosto, fazem parte integrante desta tese de doutoramento os seguintes trabalhos já publicados ou submetidos para publicação:

- **Kennedy P.J.**, Sousa, F., Ferreira D., Nestor M., Oliveira C., Granja P.L. and Sarmento B. 2018. Targeting of Fab-conjugated PLGA nanoparticles to cancer cells expressing human CD44v6. Under review.

-**Kennedy P.J.**, Pereira I., Ferreira D., Nestor M., Oliveira C., Granja P.L. and Sarmento B. 2018. Impact of surfactants on the target recognition of Fab-conjugated PLGA nanoparticles. *Eur J Pharm. Biopharm.* 127:366-70.

-**Kennedy P.J.**, Oliveira C., Granja P.L. and Sarmento B. 2018. Monoclonal antibodies: Technologies for early discovery and engineering. *Crit Rev Biotech*. 38(3):394-408.

-**Kennedy P.J.**, Oliveira C., Granja P.L. and Sarmento B. 2017. Antibodies and associates: Partners in targeted drug delivery. *Pharmacol Ther*. 177:129-145.

CHRONOLOGY AND COLLABORATIONS

Chronology:

This thesis research occurred between the periods of May 2014 and October 2017 in the labs outlined below. The specific chronology of this work progressed as follows. The collaboration with Dr. Marika Nestor for the rights to use the anti-CD44v6 Fab, AbD15179, was initiated in the very beginning of this period to allow for time to generate material transfer agreements and to commercially re-engineer and produce the recombinant Fab. The re-engineered Fab was first characterized for binding to CD44v6- and non-expressing cells to ensure that the re-engineering did not alter its specificity and affinity and to ensure that our cancer cell-based system of CD44v6 presentation was an appropriate tool.

In the beginning of 2015, studies with FluoSpheres® were initiated and used as a model nanoplatform to optimize the site-directed conjugation of the validated Fab. These studies persisted throughout most of 2015.

In September 2015, the training and studies on the identification of a novel RNA aptamer based on SELEX was initiated at University of Miami. These studies persisted until the end of 2015 in Miami and were continued throughout the first half of 2016 at i3S.

During the summer of 2016, the studies with the v6 Fab-PLGA nanoparticles (NPs) were initiated and continued well into 2017. Many unsuccessful attempts to demonstrate CD44v6-specific binding were performed. All aspects of the formulation process were addressed to decipher the reason for the lack of specificity. In the middle of 2017, the surfactant that is used during the NP production was altered, and this lead to the specific binding that was expected. This allowed for the planned biological and technological experiments to proceed and thus to fully characterize the v6 Fab-PLGA NPs until the end of the study period.

Collaborations:

In the framework of this thesis, the majority of the work was completed at i3S. INEB was the main host institution while supervision was also provided by IPATIMUP. The Nanomedicines and Translational Drug Delivery group at i3S/INEB has tremendous expertise in the encapsulation of therapeutics (e.g. insulin) in a wide variety of nanomaterials (e.g. chitosan and PLGA) with the purpose of protecting the drug from the

harsh mucosal (e.g. gastrointestinal tract) environment for systemic delivery. The group also has expertise in developing cryopreservation technologies aimed at increasing nanoparticle-associated biologic shelf-life and in developing cell-based models that better mimic the intestine. The Biomaterials for Multistage Drug & Cell Delivery group at INEB was certainly instrumental in the design and initiation of the project, and the insights gained prior to my integration were surely valuable. The Expression Regulation in Cancer group at IPATIMUP has extensive expertise in gastric cancers and in CD44v6 in particular. Their scientific input and model cells were instrumental in the success of this thesis. The combined expertise of the three i3S-related groups was invaluable as a sturdy base from which to develop the thesis as well as to help overcome inevitable obstacles within and outside of the lab.

Part of this work was also in collaboration with the Miller School of Medicine, Department of Microbiology and Immunology at the University of Miami, USA. This group has expertise in the role of myeloid-derived suppressor cells (MDSCs) in cancer, and at the same time has gained expertise in identifying novel RNA aptmers that are able to target and limit tumor progression caused by MDSCs. Their in-depth knowledge of aptamers and the systematic evolution of ligands by exponential enrichment (SELEX) process was key in helping to understand the intricacies of both technologies.

Lastly, the collaboration formed with Dr. Marika Nestor was indispensable for the success of the project. Granting us the rights to use AbD15179 allowed for the proof-of-concept targeting NP studies to advance should a novel anti-CD44v6 ligand not have been discovered.

ACKNOWLEDGEMENTS

Science has been an integral part of my whole life. Witnessing the wondrous beauty of the ocean and its life as a child instilled the importance of understanding and appreciating the natural world around me. The journey during my time as a PhD student has been filled with excitement and heartbreak and filled with blood, sweat and tears. Though, in the end, I feel like a true scientist. One who is able to understand all the prior studies that have been performed by me and the countless researchers before and to apply that knowledge to progressing the specific field of study. With that being said, I use this space to acknowledge those who have been instrumental, either directly or indirectly, in helping me along this journey.

First and foremost, I thank Dr. Bruno Sarmento for giving his precious time and for guiding me through the good and bad times. I've enjoyed our lively discussions inside and outside the lab. I appreciate, now, the necessary times where he had to push me to demonstrate my full potential. Importantly, he exposed me to all aspects of being an independent scientist from writing and reviewing manuscripts and grant proposals to colleague mentorship and supervision and beyond. Thank you from the bottom of my heart!

Dr. Pedro Granja deserves significant acknowledgment as well. First, for his idea and development of the project for which I was involved in. Secondly, for his guidance as a co-supervisor by providing fresh insight into my research. Thirdly, and most importantly, for saying "yes" when I needed it. Yes to the reagents. Yes to the conferences. Yes to the experiments. I will always remember your smile and presence that is essential to the "INEB experience".

I thank Dra. Carla Oliveira for her precious time and experience. Her expertise in CD44v6 and cancer was invaluable. Also, her role as a scientist and pragmatist helped to focus the story and to keep me grounded. Much love to Carla.

To Dr. Paolo Serafini, I give tremendous thanks for accepting me in his lab and to work with RNA aptamers and SELEX. I also wish to give thanks and praises to Dr. Dimitri Van Simaeys, a post-doc in Dr. Serafini's lab, for his time and sharing of knowledge that was critical in helping to understand some of the intricacies of aptamers and SELEX. I also thank Agata Levay in the Dr. Eli Gilboa lab for the help with setting up the emulsion PCR protocol.

Similar to life in general, a scientist is not able to achieve his/her success without the direct help of others. Here, I would like to acknowledge those who have performed

experiments or assays that were essential in the success of this thesis. The MKN74 cells that Daniel Ferreira developed during his time in Dr. Oliveira's lab proved to be a wonderful tool to biologically characterize my targeted nanoparticles (NPs). I thank Flavia Sousa for producing the NPs by double emulsion and for the help with the cryopreservation studies. Inês Pereira was a huge help in performing the tedious HPLC and zetasizer analysis. I also thank Carla Pereira for performing the tissue section studies that did not make it into the final story.

In the same vein, I thank the wonderful technicians of the i3S/INEB services. In no particular order, I thank Ricardo Silva for help with the zetasizer, Maria Lazaro for help with the confocal microscope, Dalila Pedro and Susana Carillho for help with cell culture, Rui Fernandes for help with the TEM, and Catarina Leitão and Catarina Miereles for help with flow cytometry. I also thank Hugo Osorio and Carlos Fernandes for help with MS and FTIR studies, respectively, that did not make into the thesis.

A huge amount of thanks goes to the members of the Nanomedicines and Targeted Drug Delivery group. These thanks are for your help, big or small, and for your patience with me when I "go critical". I hope that I have been a positive influence on your lives, both professionally and personally. Special thanks go to José das Neves for his insight in the drug delivery field and explaining things in a simplistic manner. I also thank Francisca Araujo for being the glue of the team and beyond.

There are several groups within i3S/INEB that deserve my gratitude as well…in no particular order. Dra. Ana Paula Pêgo, her group and their combined expertise in nanomedicine is a nice complement to the group of Dr. Sarmento. Pedro Moreno deserves special thanks due to our discussions about the exploitation of nucleic acids in drugs and drug delivery. The group of Pedro Granja was essential not only for the use of the physical space, but also for their scientific expertise. Here, Tiago Santos and Bianca Lourenço were key in the beginning of the project to be able to learn from their previous studies with CD44v6 and nanomaterials. As our lab co-inhabitants, the group of Dra. Cristina Martins provided a comfortable and wonderful environment for me to work in.

There are many that were not directly related to the thesis and my overall PhD that deserve my thanks and gratitude…

To my children, Daniel and Lia… you are the light of my life! You have been the inspiration for me to better myself…as seen with this thesis and PhD. You are the reason I wake up in the morning. I thank you for your patience for the many nights and weekends that I have been in the lab or at the computer and not able to devote the time to you. You both are very different and special people that may one day become scientists yourselves. I love you with all my heart!

Aos pais da Susana, Luís e Luísa…Obrigado por sua ajuda com as crianças e com o apoio físico e emocional. A sua paciência comigo foi fundamental durante de este epoca. Um dia, eu espero que posso reembolsar o seu generosidade. Vocês são “priceless”!

Of course, I thank Susana for all her support and love as well. You were great in keeping me on track while we built our lives together with the rest of the family. You were also the instigator and coordinator of many great trips across Portugal and Europe. My life has been forever changed since the first day I laid eyes on you at Scripps. I will always love you!

Finally, I thank my parents for their love and support during my entire life. My childhood and early adult experiences have molded me into the person I am today. As a biomedical engineer/biotechnologist, I am definitely a mix of my dad, an electrical engineer, and my mom, a pharmacist. I am forever indebted to you.

“The Earth does not belong to Man.
Man belongs to the Earth”
(Chief Seattle)

TABLE OF CONTENTS

ABSTRACT

CD44 receptor isoforms containing exon v6 (CD44v6) have been implicated in many cancer associated processes including metastasis and exosome-mediated pre-metastatic niche formation. CD44v6 is a co-receptor for human growth factor (HGF) and vascular endothelial growth factor (VEGF), together with c-Met and VEGF receptor 2, respectively. CD44v6 isoforms are expressed in cancer stem cells and (pre-)malignant gastric lesions. Therefore, CD44v6 has potential as a target for early cancer diagnosis and/or for therapeutic intervention.

Targeted therapy has been instrumental in the oncology clinic for several years now. Targeting specific molecules has helped to reduce patient side effects commonly associated with classic chemotherapy. These molecules are mostly of biological origin with monoclonal antibodies (mAbs) representing the largest fraction. Antibodies, with their high specificity and affinity, are nature's molecular recognition machines designed to aid the immune system in destroying extracellular and intracellular threats. A mAb is a unique species of antibody with affinity to only one specific part of a target molecule. Genetic engineering and recombinant protein technologies are providing a wonderful alternative to animal-derived antibody sources and allowing for fully human constructs. Recombinant mAbs can also be constructed from their associated fragments/domains and (re-)engineered with more desirable pharmacological qualities. Though, other biologics in targeted therapy can also be composed of amino acids (i.e. peptides or proteins) or nucleic acids (e.g. antisense oligonucleotides). Aptamers are an emerging, nucleic acid-based technology with the potential for high specificity and affinity to a wide array of molecules with some advantages over the dominating class of antibodies.

Targeted drug delivery borrows from the targeted therapy concept but takes it one step further. Here, the aim is to drive a drug to the specific site of action with the help of a vehicle. The vehicle can be a biomolecule (e.g. antibody) that is specific to, for example, a cell surface receptor or extracellular matrix molecule, or the vehicle can be based on nanotechnology. Bioconjugates based on antibodies are now emerging in the clinic as viable and potentially powerful agents in targeted drug delivery.

Nanotechnology applied to medicine (nanomedicine) is being exploited in the treatment of cancer and beyond, mainly as carriers for the delivery of drugs and/or diagnostics. Nanoparticles (NPs) can enhance a drug's pharmacology through mechanisms such as controlled release, a capacity to harbor a plethora of

therapeutic/diagnostic payloads, intracellular delivery, multi-functionality, and responsiveness to environmental stimuli. NPs can also be engineered to overcome biological barriers such as the mucosa. Additionally, NPs can be conjugated with ligands allowing for cell/tissue-specific targeting. Thus, targeted drug delivery with ligand-decorated NPs offers an attractive strategy for the treatment and/or diagnosis of a wide range of human diseases including (metastatic) carcinoma.

The main goal of this thesis was to develop polymeric NPs that are decorated with a biologic-based ligand for targeting CD44v6-expressing human cells. The first task was to identify a novel RNA aptamer with high specificity and affinity to human CD44v6. The second task was to develop and characterize ligand-decorated, polymeric NPs that target human CD44v6. Ideally, the novel ligand identified in the first task would be used to decorate the NPs in the second task.

A novel RNA aptamer against human CD44v6, presented as a peptide or on the cell surface, was attempted to be identified through selected evolution of ligands by exponential enrichment (SELEX). Twelve rounds of peptide-based and seven rounds of cell-based SELEX were performed, and each output was quality controlled by spectrophotometry and gel electrophoresis. Various rounds of the peptide-based SELEX outputs were fluorescently-labelled and tested for binding to the CD44v6-derived peptide and to CD44v6-expressing cells. No CD44v6-specific enrichment was detected by either of the binding assays. A post-hoc assay that replicated the capture step of the peptide SELEX using a positive control anti-CD44v6 ligand failed suggesting that the SELEX protocol was compromised. Alternative methods, such as high-throughput sequencing and bioinformatics technologies, may be able to reveal sequence enrichment, but for now, a novel aptamer against human CD44v6 was not identified needing further inquiry.

Development of proof-of-concept NPs was attempted by exploiting AbD15179, a well-characterized, human recombinant Fab fragment with high specificity and affinity to human CD44v6 (v6 Fab). Initial studies using polystyrene latex microspheres (FluoSpheres®) had many problems with aggregation and demonstrated no specific binding to CD44v6-expressing cells. Though, secondary attempts at developing Fab-decorated, poly(lactic-co-glycolic acid) (PLGA)-based NPs (v6 Fab-PLGA NPs) were successful. The v6 Fab-PLGA NPs displayed spherical morphology around 300 nm and negative charge. They strongly bound to a CD44v6-derived peptide and, more importantly, to cells that endogenously and exogenously express CD44v6, but not to non-expressing cells and cells expressing the standard form of CD44. v6 Fab-PLGA NPs produced in 2% polyvinyl alcohol (PVA) were unable to bind to the cells, and NPs

produced in 2% Pluronic F127 demonstrated the highest binding compared to those produced in sodium cholate or Tween-80. Empty and paclitaxel-loaded v6 Fab-PLGA NPs had nominal cytotoxicity at 50 µg/mL. Lastly, v6 Fab-PLGA NPs resisted simulated intestinal fluid exposure and cryopreservation.

Overall, the thesis-related research achieved the overall goal of developing CD44v6-specific polymeric NPs. Although a novel ligand that is specific to human CD44v6 was not identified; the second aim of developing a human compatible, polymeric nanocarrier that targets human CD44v6 was completely achieved. In their present form, the v6 Fab-PLGA NPs demonstrated favorable physicochemical, biological and technological qualities that allow them to potentially be used in the oncology clinic as an (*in vivo*) diagnostic tool. Though, their use in drug delivery requires further investigation and optimization. In conclusion, NPs targeting CD44v6 have potential as *in vivo* diagnostic agents and/or as anti-cancer drug delivery agents in patients previously stratified with $CD44v6^{+}$ carcinomas.

RESUMO

As isoformas do receptor CD44 contendo o exão v6 (CD44v6) foram implicadas em muitos processos associados ao cancro, incluindo metástases e formação de nicho pré-metastático mediada por exossomos. O CD44v6 é um co-receptor para o fator de crescimento humano (HGF) e fator de crescimento endotelial vascular (VEGF), juntamente com o receptor c-Met e receptor VEGF 2, respectivamente. As isoformas de CD44v6 são expressas em células-tronco de câncer e lesões gástricas (pré-) malignas. Portanto, o CD44v6 tem potencial como alvo para o diagnóstico precoce do câncer e/ou para intervenção terapêutica.

Terapia direcionada tem sido fundamental na clínica oncológica há vários anos. A segmentação de moléculas específicas ajudou a reduzir os efeitos colaterais do paciente comumente associados à quimioterapia clássica. Estas moléculas são principalmente de origem biológica com anticorpos monoclonais (mAbs) representando a maior fração. Anticorpos, com sua alta especificidade e afinidade, são máquinas de reconhecimento molecular da natureza projetadas para ajudar o sistema imunológico a destruir ameaças extracelulares e intracelulares. Um mAb é uma espécie única de anticorpo com afinidade para apenas uma parte específica de uma molécula alvo. As tecnologias de engenharia genética e proteína recombinante estão fornecendo uma alternativa maravilhosa às fontes de anticorpos derivados de animais e permitindo construções totalmente humanas. Os mAbs recombinantes tambem podem ser construidos a partir dos seus fragmentos/dominios associados e (re-)manipulados com qualidades farmacolicas mais desejeis. No entanto, outros produtos biológicos na terapia alvo podem também ser compostos por aminoácidos (i.e. péptidos ou proteínas) ou ácidos nucleicos (por exemplo, oligonucleótidos antisense). Os aptâmeros são uma tecnologia emergente baseada em ácido nucléico, com o potencial de alta especificidade e afinidade para uma ampla gama de moléculas com algumas vantagens sobre a classe dominante de anticorpos.

A entrega direcionada de medicamentos toma emprestado do conceito de terapia direcionada, mas dá um passo adiante. Aqui, o objetivo é dirigir um medicamento para o local específico da ação com a ajuda de um veículo. O veículo pode ser uma biomolecula (por exemplo, anticorpo) que especica para, por exemplo, um receptor da superficie celular ou molecula da matriz extracelular, ou o veículo pode ser baseado em nanotecnologia. Os bioconjugados baseados em anticorpos estão agora surgindo na

clínica como agentes viáveis e potencialmente poderosos no fornecimento direcionado de drogas.

A nanotecnologia aplicada à medicina (nanomedicina) está sendo explorada no tratamento do câncer e além, principalmente como portadores para a entrega de medicamentos e/ou diagnósticos. As nanopartículas (NPs) podem melhorar a farmacologia de um medicamento por meio de mecanismos como liberação controlada, capacidade de abrigar uma infinidade de cargas terapêuticas/diagnósticas, entrega intracelular, multifuncionalidade e capacidade de resposta a estímulos ambientais. NPs também podem ser projetados para superar barreiras biológicas, como a mucosa. Adicionalmente, os NPs podem ser conjugados com ligandos, permitindo a segmentação específica de células/tecidos. Assim, a distribuio direccionada de farmacos com NPs decoradas com ligandos oferece uma estratia atractiva para o tratamento e/ou diagnostico de uma vasta gama de doencas humanas incluindo carcinoma (metastico).

O objetivo principal desta tese foi desenvolver NPs poliméricos que são decorados com um ligante biológico para o direcionamento de células humanas expressando CD44v6. A primeira tarefa foi identificar um novo aptâmero de RNA com alta especificidade e afinidade para o CD44v6 humano. A segunda tarefa foi desenvolver e caracterizar os NPs poliméricos, decorados com ligantes, que têm como alvo o CD44v6 humano. Idealmente, o novo ligante identificado na primeira tarefa seria usado para decorar os NPs na segunda tarefa.

Um novo aptâmero de RNA contra CD44v6 humano, apresentado como um peptídeo ou na superfície celular, foi tentado para ser identificado através de evolução selecionada de ligantes por enriquecimento exponencial (SELEX). Foram realizadas doze rodadas de base de peptídeos e sete rodadas de SELEX baseado em células, e cada resultado foi controlado com qualidade por espectrofotometria e eletroforese em gel. Varios ciclos dos outputs de SELEX baseados em peptidos foram marcados de modo fluorescente e testados quanto ligacçao ao ptido derivado de CD44v6 e a culas que expressam CD44v6. Nenhum enriquecimento específico para CD44v6 foi detectado por qualquer um dos ensaios de ligação. Um ensaio post-hoc que replicou o passo de captura do péptido SELEX utilizando um ligando anti-CD44v6 de controlo positivo falhou sugerindo que o protocolo SELEX estava comprometido. Métodos alternativos, como o sequenciamento de alto rendimento e as tecnologias de bioinformática, podem revelar o enriquecimento da sequência, mas, por enquanto, um novo aptâmero contra o CD44v6 humano foi identificado sem sucesso.

O desenvolvimento de NPs de prova de conceito foi tentado explorando AbD15179, um fragmento Fab recombinante humano bem caracterizado com elevada especificidade e afinidade para CD44v6 humano (v6 Fab). Estudos iniciais utilizando microesferas de látex poliestireno (FluoSpheres®) tiveram muitos problemas com agregação e não demonstraram nenhuma ligação específica a células que expressam CD44v6. No entanto, tentativas secundárias de desenvolver NPs com base em poli (ácido láctico-co-glicólico) (PLGA) com decoração de Fab (v6 Fab-PLGA NPs) obtiveram sucesso. Os NPs v6 Fab-PLGA apresentaram morfologia esférica em torno de 300 nm e carga negativa. Ligam-se fortemente a um péptido derivado de CD44v6 e, mais importante, a células que expressam endogenamente e exogenamente CD44v6, mas não a células não expressantes e a células que expressam a forma padrão de CD44. As NPs de v6 Fab-PLGA produzidas em álcool polivinílico a 2% (PVA) foram incapazes de se ligar às células, e as NPs produzidas em Pluronic F127 a 2% demonstraram a maior ligação em comparação com as produzidas em colato de sódio ou Tween-80. Os v6 Fab-PLGA NPs vazios e carregados com paclitaxel tinham citotoxicidade nominal a 50 µg/mL. Ultimamente, as v6 Fab-PLGA NPs resistiram a exposição a fluido intestinal simulado e criopreservição.

No geral, a pesquisa relacionada à tese alcançou o objetivo geral de desenvolver NPs poliméricos específicos para CD44v6. Embora um novo ligando específico para o CD44v6 humano não tenha sido identificado; o segundo objetivo de desenvolver um nanocarreador polimérico compatível com humanos que atinja o CD44v6 humano foi completamente alcançado. Na sua forma atual, os v6 Fab-PLGA NPs demonstraram qualidades físico-químicas, biológicas e tecnológicas favoráveis que permitem que eles sejam potencialmente usados na clínica de oncologia como uma ferramenta diagnóstica (*in vivo*). No entanto, seu uso na entrega de medicamentos requer mais investigação e otimização. Em conclusão, as NPs direcionadas para CD44v6 têm potencial como agentes de diagnóstico *in vivo* e/ou como agentes de liberação de drogas anticâncer em pacientes previamente estratificados com carcinomas CD44v6+.

ACRONYMNS AND ABBREVIATIONS

AA	Amino acid
ABC	Antibody-biologic conjugate
AbD15179	Human, anti-human CD44v6 Fab
ADC	Antibody-drug conjugate
ADCC	Antibody-dependent cell-mediated cytotoxicity
ADIN	Antibody-dependent intracellular neutralization
ANC	Antibody-nanoparticle conjugate
BSA	Bovine serum albumin
CD44	Cluster of differentiation 44
CD44std	Standard isoform of CD44
CD44v	Variant isoform of CD44
CD44v6	Variant isoforms of CD44 containing exon v6
CDC	Complement-dependent cytotoxicity
CDR	Complementarity-determining region
CDR H3	CDR 3 from the heavy chain
CH	Constant region of the heavy chain
CL	Constant region of the light chain
CP	Cytoplasmic portion of CD44
CR-CSC	Colorectal cancer stem cell
CSC	Cancer stem cell
CTC	Circulating tumor cell
DCM	Dichloromethane
DDS	Drug delivery system
DLS	Dynamic light scattering
dox	Doxirubicin
EC50	Half maximal effective concentration
ECM	Extracellular matrix
EGFR	Epidermal growth factor receptor
ELISA	Enzyme-linked immunosorbent assay
EMT	Epithelial-to-mesenchymal transition
ePCR	Emulsion PCR
EPR	Enhanced permeability and retention
ERK	Extracellular related kinase
ERM	Ezrin, radixin, moesin
F127	Pluronic F127 (aka Poloxamer 407)
Fab	Fragment antigen binding
FACS	Fluorescence-activated cell sorting
FBS	Fetal bovine serum
Fc	Fragment crystallizable
FcR	Fc receptor
FcRn	Neonatal Fc receptor
FcγR	Fc gamma receptor
FKR648	Fluorescent dye with emission at 648 nm
FluoSpheres®	Polystyrene latex microspheres at 200 nm with yellow/green fluorescence
GC	Gastric cancer

GFP	Green fluorsecent protein
GP202	Gastric cancer cell line endogenously expressing CD44v6
HA	Hyaluronic acid
HER2	Human epidermal growth factor receptor 2
HGF	Hepatocyte growth factor
HIV	Human immunodeficiency virus
HNSCC	Head-and-neck squamous cell carcinoma
HPLC	High pressure liquid chromatography
HRP	Horse radish peroxidase
HuCAL	Human combinatorial antibody library
ICAM-1	Intercellular adhesion molecule-1
Ig	Immunoglobulin
IgG	Immunoglobulin G
LDA	Laser Doppler anemometry
mAb	Monoclonal antibody
Mal	Maleimide
MEK	Mitogen-activated protein kinase kinase
MTT	3-(4,5-dimethylthiazol-2-yl)-2,5-diphenyltetrazolium bromide
MKN74	Gastric cancer cell line that does not express CD44
Na Chol	Sodium cholate
NaN3	Sodium azide
NGS	Next-generation sequencing
NPs	Nanoparticles
OPN	Osteopontin
PBS	Phosphate buffered solution
PBST	PBS + 0.1% Tween-20
PCR	Polymerase chain reaction
PdI	Polydispersity index
PEG	Polyethylene glycol
PI3K	Phosphoinositide 3-kinase
PLGA	Poly(lactic-co-glycolic acid)
PTX	Paclitaxel
PVA	Polyvinyl alcohol
RT	Room temperature
scFv	Single-chain variable fragment
sdAb	Single-domain antibody
SDF	Stromal-derived factor
SELEX	Systematic evolution of ligands by exponential enrichment
SIF	Simulated intestinal fluid
siRNA	Small interferring RNA
SPR	Surface plasmon resonance
SMCC	Succinimidyl 4-(N-maleimidomethyl)cyclohexane-1-carboxylate
SM(PEG)24	Sulfo-SMCC linker containing 24 polyethylene glycol chains
T/E	Trypsin/EDTA
TAC	Tumor-associated cell
TB	Tuberculosis
TEM	Transmission electron microscopy
TM	Transmembrane region of CD44

TRIM21	Tripartite motif-containing protein 21
TCEP	Tris(2-carboxyethyl)phosphine
v6 Fab-PLGA NPs	PLGA NPs tethered with the anti-CD44v6 Fab
VEGF	Vascular endothelial growth factor
VEGFR-2	VEGF receptor 2
V_H	Variable domain from the heavy chain
VHH	Hypervariable domain from heavy chain-only antibodies (camelids)
V_L	Variable domain from the light chain
VLP	Virus-like particle
VNAR	Variable new antigen receptor (sharks)
w/o/w	Water-in-oil-in-water
YSD	Yeast surface display
(-) Fab-PLGA NPs	PLGA NPs tethered with the negative control Fab

CHAPTER I

Literature review

Parts of this chapter were based on the following publications:

-**Kennedy P.J.**, Oliveira C., Granja P.L. and Sarmento B. 2018. Monoclonal antibodies: Technologies for early discovery and engineering. *Crit Rev Biotech*. 38(3):394-408.

-**Kennedy P.J.**, Oliveira C., Granja P.L. and Sarmento B. 2017. Antibodies and associates: Partners in targeted drug delivery. *Pharmacol Ther*. 177:129-145.

1. CD44v6 biology and its role in carcinoma

1.1. General biology and structure of CD44 and its variant isoforms

Cluster of differentiation 44 (CD44) is a transmembrane glycoprotein expressed on the surface of many types of cells. CD44 functions in cell-cell adhesion, cell communication and cell-extracellular matrix interactions [1], and it is considered a biomarker for (cancer) stem cells [2]. CD44 is also a receptor for the extracellular matrix (ECM) molecules hyaluronic acid (HA), osteopontin (OPN) and many others. A hallmark of the *CD44* gene is its very high amount of alternative splicing (**Figure 1**) [3].

The *CD44* gene is composed of a total of 20 different exons. The standard and smallest form of CD44 (CD44std) is composed of 10 exons, termed s1-s10, of which all CD44-associated gene products contain. Exons s1-s7 codes for the extracellular domain, exon s8 codes for the transmembrane region, and exons s9-s10 code for the C-terminal cytoplasmic tail. CD44std is ubiquitously-expressed on the membrane of most mammalian cells. It is best known as a receptor for hyaluronic acid (HA); however, it also contains binding domains for collagen, fibronectin, and CD62 [1].

Variant isoforms of CD44 (CD44v) express one or more additional exons termed v1 through v10 in a wide array of flavors, and their expression is typically restricted to epithelial cells and carcinomas [1]. These variant exons can also be glycosylated and fall between exons s5 and s6 placing them close to the cell surface. All of the possible variant isoforms coupled with different glycosylation patterns results in hundreds of, if not more, different possible biomolecules generated from the one *CD44* gene. Depending on which tissue it is expressed in, a given CD44v often plays a well-defined role. Variant isoforms of CD44 containing exon v6 (CD44v6) have received a significant amount of interest since the early 1990's due to their role in cancer biology.

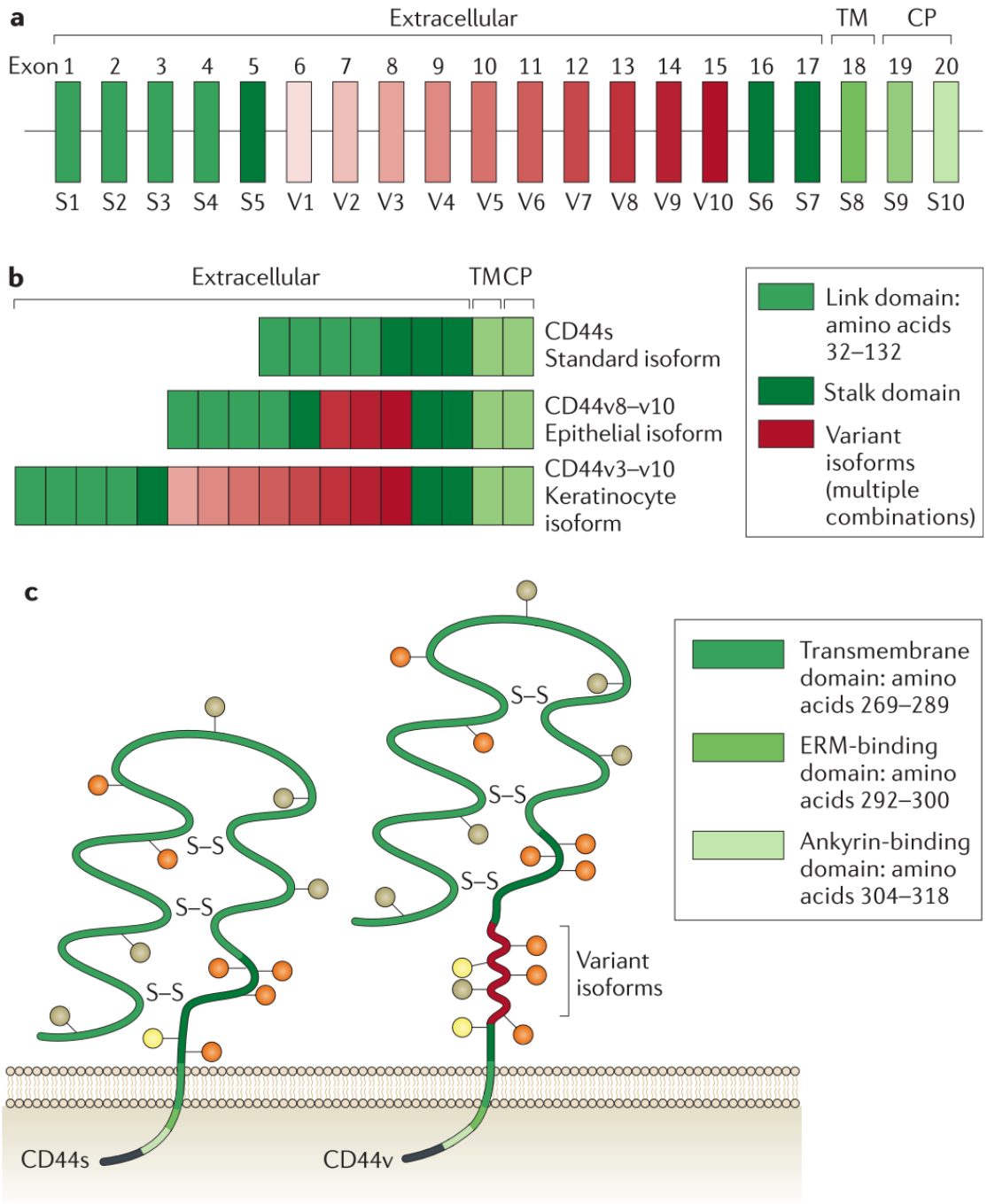

Figure 1. Structure of the CD44 gene and protein. a-b) *CD44* is composed of 20 different exons that are subjected to intense alternative splicing. Ten are included in all isoforms (s1-s10; green bars) and make up the extracellular and transmembrane (TM) domains as well as the cytoplasmic portion (CP). b) Variant isoforms of CD44 (CD44v) contain one or more additional exons (v1-v10; red bars) that are spliced into the stalk domain (s5-s6) in a wide array of combinations. c) The resulting gene products also become heavily glycosylated (colored circles) leading to more isoform diversity. Used with permission from [1].

1.2. CD44v6 biology

Clinical interest in CD44v6 began when Günthert and co (1991) demonstrated that rat pancreatic cancer cells expressing CD44v6 displayed a metastatic phenotype [4]. Additionally, non-metastatic cells forced to express CD44v6 took on a metastatic phenotype, and treatment of rats orthotopically expressing these cells with a CD44v6 blocking antibody halted lymph node and lung metastases. This initiated several studies into exploring the biology of CD44v6 and its potential as a therapeutic target [5, 6] and as a prognostic marker [7] for cancer. Since then, much has been discovered in all of the above aspects of CD44v6. Here, it is important to reiterate that “CD44v6” refers to many different CD44 glycoproteins that contain exon v6 alone or in combination with other variant exons.

CD44v6 expression is mainly restricted to proliferative tissue such as the skin and intestine [6] but can also be found in the endothelium and activated lymphocytes [8]. Through direct interaction [9], CD44v6 is required for hepatocyte growth factor (HGF) activation [10] and internalization [11] of the essential receptor tyrosine kinase c-Met in epithelial [10] and endothelial [12] cells (**Figure 2**). c-Met induces proliferation, differentiation, migration, survival and branching morphogenesis, and its deregulation often results in cancer and metastasis [13]. Though, it has been shown that c-Met recruits intercellular adhesion molecule-1 (ICAM-1) to compensate for loss of CD44v6 [14]. CD44v6 is also a co-receptor, again through direct interaction [9], of vascular endothelial growth factor A (VEGF-A) along with VEGF receptor 2 (VEGFR-2) [12]. In both c-Met [10] and VEGFR-2 [12], signal propagation is mediated by the association of the cytoplasmic tail of CD44v6 with ezrin, radixin and moesin (ERM) proteins (**Figure 2**). This couples CD44v6 to the cytoskeleton to control endothelial cell migration, sprouting and tubule formation [12] as well as Ras, MEK and ERK activation [15]. Importantly, HGF-induced Ras signaling promotes CD44v6 alternative splicing which in turn sustains Ras signaling thus creating a positive feedback loop and stimulating cell cycle progression [16]. Although more is known, the biology of CD44v6 is extremely relevant in cancer as explained below.

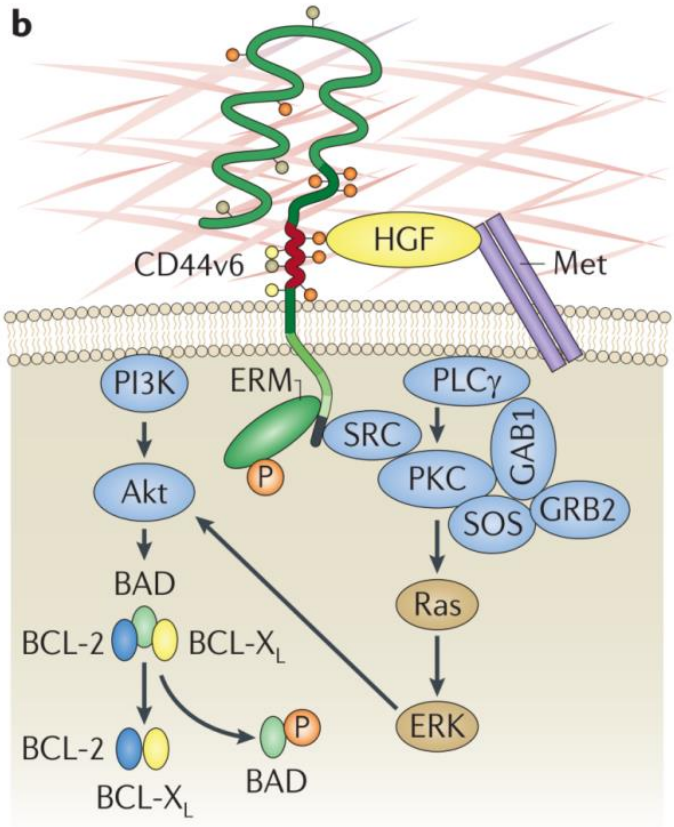

Figure 2. CD44v6 and c-Met association. Hepatocyte growth factor (HGF) activation of c-Met (Met) requires CD44v6. The signaling cascade is initiated with the binding of the cytoplasmic tail of CD44v6 to the assemble the ezrin, radixin and moesin (ERM) proteins and SRC for downstream Ras-ERK and PI3K-Akt activation important for cell proliferation. Used with permission from [1].

1.3. Role of CD44v6 in cancer

The role of CD44v6 in cancer was established with the first metastasis studies on rat pancreatic carcinoma cells [4]. Since then, the role of CD44v6 in cancers from other tissue types, as well as different cancer-related processes, has been investigated.

In order for metastases to form, the secondary tissue often first needs to be primed to be a conducive environment to receive the incoming tumor cells [17]. Among other ways, this pre-metastatic niche can be initiated by exosomes or extracellular vesicles secreted by tumor cells which carry specific biomolecules that act as messengers for tissue remodeling. Jung *et al*. (2009) demonstrated that exosomes from the same CD44v6+ rat pancreatic cancer cells used in the Günthert *et al*. (1991) [4] study strongly promote metastases in the lung and lymph nodes *in vivo* [18].

While investigating the splicing pattern of *CD44* and more in normal stomach and gastric cancer (GC), da Cunha and colleagues (2010) showed that CD44v6 expression was nominal in histochemical staining of normal stomach but increased as the severity of GC increased (**Figure 3**) [19]. Additionally, expression of CD44v6 was inversely correlated with that of E-cadherin, which has a functional pivotal role in GC [20]. This supports the role of CD44v6 in the epithelial-to-mesenchymal transition (EMT) [21], an integral process in metastasis [22]. It was also shown that the highest levels of the CD44v6 transcript in a GC cell line panel was found in GP202 (relevant for the studies in Chapter IV).

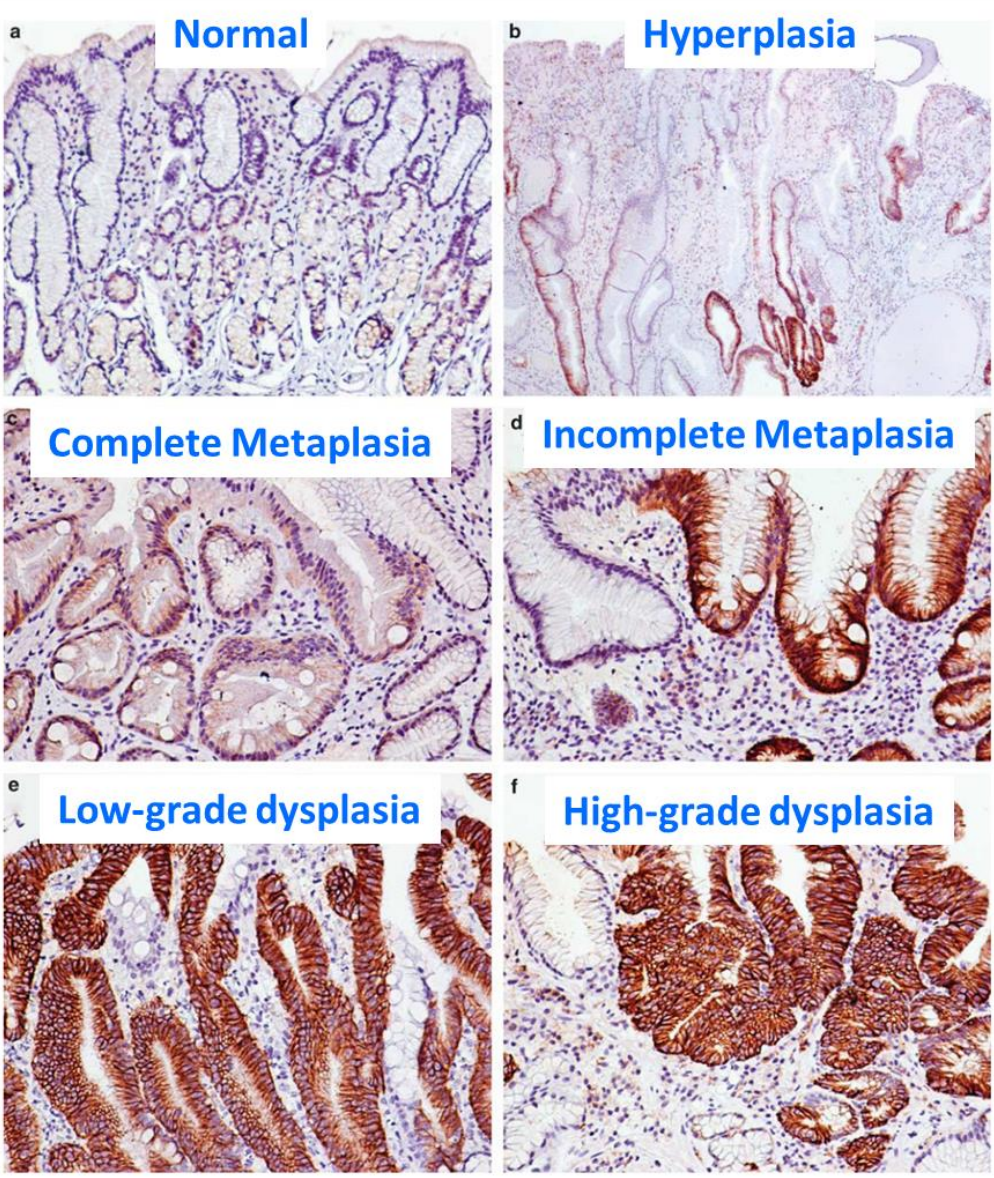

Figure 3. Immunohistochemical staining of CD44v6 in patient-derived gastric (cancer) tissue. a) Normal stomach tissue expresses nominal levels of CD44v6. b) Low-to-moderate levels of CD44v6 is observed in hyperplasia. CD44v6 expression increases as the severity of GC increases as seen in complete metaplasia (c) to incomplete metaplasia (d) with very high levels seen in low-grade (e) and high-grade (f) dysplasia. Adapted with permission from [19].

Cancer stem cells (CSCs), also called cancer initiating cells, are a set of rare cells in a tumor that are, debatably, initiators and drivers of tumor growth and metastasis and resist conventional therapeutics [23, 24]. CD44 has been recognized as a CSC marker for many years now [1, 2]. Of course this biomarker assessment is dependent on antibody

staining. Though, given the extensive alternative splicing of *CD44* and the antibody reliance, it seems probable that designating CD44 as a stem cell marker may be referring to CD44v and not CD44std. A thorough study clearly demonstrated that colorectal cancer stem cells (CR-CSCs) [25] express CD44v6 (**Figure 4**) [21]. CD44v6- progenitor cells do not lead to metastases; however, stimulation of these cells with the cytokines HGF, OPN and stromal-derived factor (SDF) that are secreted by cancer associated fibroblasts acquire CD44v6 expression and a metastatic capability. Inhibition of phosphatidylinositol 3-kinase (PI3K), actively-targeted in cancer therapy [26] (**Figure 2**), lead to specific killing of CD44v6+ CR-CSCs and reduced metastatic growth. A parallel patient cohort study revealed that survivability was increased with low levels of CD44v6 in CRC. This work validated CD44v6 as a functional biomarker and a therapeutic target. Supporting the previous study, cultured circulating tumor cells (CTCs) derived from stage IV CRC patients were shown to express hallmarks of CR-CSC such as CD44v6 [27].

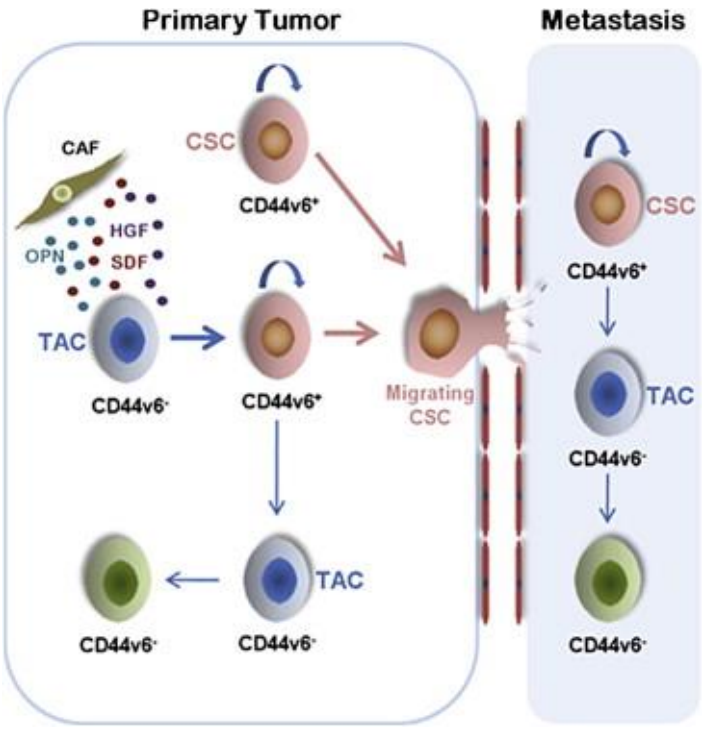

Figure 4. All colorectal cancer stem cells (CSC) express CD44v6. CD44v6- tumor associated cells (TACs) when stimulated by hepatocyte growth factor (HGF), osteopontin (OPN) and stromal-derived factor (SDF) secreted by cancer-associated fibroblasts (CAFs) start to express CD44v6. CD44v6-expressing cells take on a CSC phenotype which includes migration and dispersal to secondary sites to initiate metastasis. Used with permission from [21].

1.4. CD44v6 as a prognostic marker or therapeutic/diagnostic target

Because CD44v6 is associated with metastasis, many studies mainly in the early 2000's looked into the prognostic value of CD44v6 expression [7, 28-31]. Unfortunately, the results were varied; though, most studies showed a positive correlation with Dukes stage and CD44v6 expression. It is probable that the mixed results were caused by a technical problem, such as antibody choice during immunohistochemical staining, and not a biological one. Though, the more recent Todaro *et al*. (2014) study cited above did demonstrate the prognostic value of CD44v6 in CRC [21].

The therapeutic value of CD44v6 has also been investigated over the last few decades [6, 32, 33]. As mentioned above, the initial rat pancreatic carcinoma studies used an anti-CD44v6 mAb to block metastatic spread [4]. The first clinical therapeutic was an antibody-drug conjugate of the anti-CD44v6 monoclonal antibody, bivatuzumab coupled with the cytotoxic microtubule inhibitor mertansine [34, 35]. Two phase I trials were

conducted on patients with head and neck squamous cell carcinoma (HNSCC). Although it seems that the ADC had targeted the tumors in some of the patients, many of them developed skin rashes, exfoliation, or worse. One patient developed toxic epidermal necrolysis and died [34]. Most likely bivatuzumab mertansine targeted the skin keratinocytes causing the severe side effects. The use of this drug in the clinic was terminated due to the above toxicity reasons.

When Orian-Rousseau *et al*. (2002) identified that c-Met activation by HGF required presentation by CD44v6, they were able to inhibit that activation using mAbs directed towards specific CD44v6 epitopes [10]. Mutating three specific residues in the v6 exon disrupted the c-Met co-receptor activation [36]. This work lead to the discovery of a five amino acid peptide containing these three residues that could also disrupt this activation. The same peptide could also disrupt VEGFR-2 binding thus providing a therapeutic to block angiogenesis in relevant pathologies [12]. Lastly, this peptide was able to inhibit tumor growth and metastasis in pancreatic cancer *in vivo* models [37]. It is important to note that, because this peptide is derived from the v6 exon, it does not bind to CD44v6 and functions by interfering with its co-receptor functions with c-Met and VEGFR-2. Therefore, clinical studies should not see the same skin toxicities that were seen with bivatuzumab mertansine [34, 35] but still result in inhibiting tumor growth and/or metastasis. In fact, this drug (AMC303) is currently in Phase I/Ib clinical trials for the treatment of patients with solid tumors (ClinicalTrials.gov #NCT03009214).

CD44v6 may also be amenable to *in vivo* diagnostics of some or all of the cancers outlined above. Thus, the anti-human CD44v6 Fab, AbD15179, was developed and characterized with the intent to target a radionuclide to CD44v6-expressing HNSCC cells [38]. AbD15179 is a fully human, recombinant Fab (see section 3.1.2 for more information about this term) that was selected and screened from the HuCAL® PLATINUM library [39] (see section 3.1.3 for more information about these terms) against a peptide derived from the v6 exon (see Chapters III and IV for its application in this thesis), and it has a binding affinity around 5-50 µM depending on whether the antigen is a biomolecule or expressed on the cell surface. *In vivo*, radiolabeled AbD15179 demonstrated a moderate tumor-to-organ ratio [40], and this Fab was further engineered as a $F(ab')_2$ for improved avidity and slower dissociation rate [41]. Given its specificity, affinity, fully human structure and *in vivo* targeting, AbD15179, or its derivative, has clinical potential to diagnose HNSCC or other CD44v6-expressing human cancers.

All of the above knowledge about the biology and therapeutic/diagnostic/prognostic value of CD44v6 makes it a prime candidate for the

targeted delivery of a drug and/or diagnostic for use in the oncology clinic. Specifically, one could inhibit metastases [4, 37] or could target CR-CSCs [21] or early-stage GC [19].

2. Nanomedicine and targeted drug delivery

Classic drugs in modern medicine are typically based on natural products derived from bacteria, plants or fungi. The active ingredient is often a purified small molecule frequently acting on the whole body. Depending on the mechanism of action and dose, these drugs may have (sometimes serious) side effects. As an example, 20th century chemotherapy drugs are active against proliferating cells which are good at targeting tumors that are growing out of control. However, they also kill other proliferating cells like blood cells, epithelial cells found in the stomach and intestine and hair follicles. Thus, there is a fine line between killing the tumor and killing the patient. 21st century medicines are a result of applying current technology with our vastly improved knowledge of genetics, molecular and cellular biology, biochemistry and materials science.

2.1. General nanomedicine

Nanotechnology applications in medicine (nanomedicine) promise to greatly advance diagnosis and treatment of disease. Nanoparticles (NPs) are extremely versatile and can be engineered to display a multitude of pharmacological properties. In the context of drug delivery, nanotechnology is used to encapsulate the drug, or payload, for enhanced pharmacokinetics, bioavailability, and drug release to increase the therapeutic index by increasing efficacy and/or reducing side effects. As an example, Doxil® is an approved nanomedicine that encapsulates doxorubicin (dox) within PEGylated liposomes [42]. Doxil is not more effective in reducing tumor volume; however, the nanoformulation helps to greatly reduce the cardiotoxicity common with free dox [43]. Importantly, nanoparticles can be engineered to overcome biological barriers [44] and target specific tissues or cells, enhancing drug delivery to its therapeutic destination. There are several NPs already in the clinic [45] with many more on the horizon.

Nanomedicine can impact a large spectrum of human diseases, including cancer [46], HIV [47] and TB [48], and can be engineered with many nanomaterials (**Figure 5**) to harbor many payload types (e.g. small to big (bio-)molecules). Small molecule drug candidates with high therapeutic potential often have poor solubility leading to poor bioavailability [49], and several formulation strategies exist to increase solubility (e.g. solid

dispersion [50] and nanoencapsulation [49]). Though biologics usually do not have solubility issues, they do face other problems associated with biology such as immunogenicity and difficulty to surpass biological barriers (e.g. gastrointestinal tract). Nanovaccines have also been developed for immunotherapy of cancer and beyond [51]. Administration of photosensitizers [52] and multiple therapeutics [53] is also possible with NPs. Beyond drug delivery, NPs can be used in *in vivo* diagnostics either as contrast agents themselves (e.g. quantum dots or gold NPs) or harboring them as payloads [54].

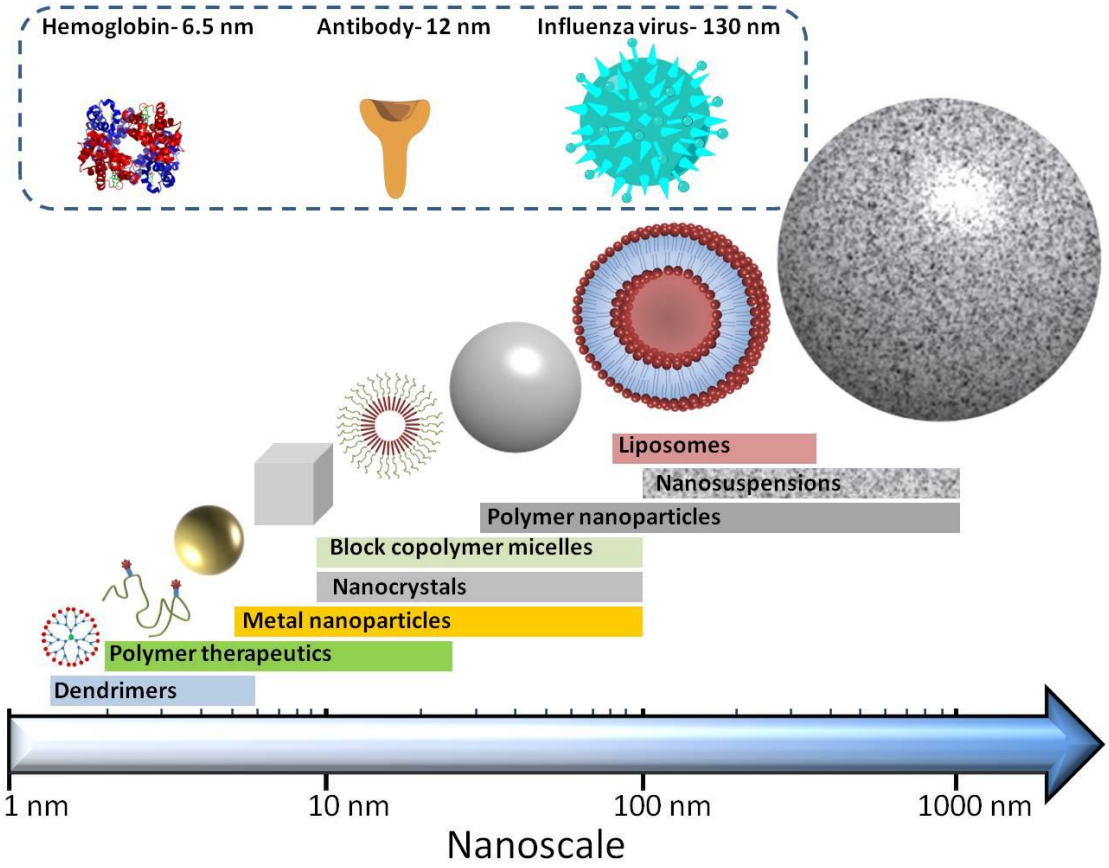

Figure 5. Illustration of the different materials and resulting nanoscale carriers that are found in current nanomedicine. Taken from the British Society for Nanomedicine website: www.britishsocietynanomedicine.org.

The lifespan of a biopharmaceutical is severely dependent on the mode of administration. For example, insulin is mainly administered by painful injection. Patients prefer to take drugs by less invasive means (e.g. mucosal); however, most biopharmaceuticals do not bode well in these environments. Nanotechnology is currently

being exploited for systemic drug delivery by non-parenteral routes [55]. The Nanomedicines and Translational Drug Delivery Group has extensive experience in the nanoencapsulation of macromolecular biotherapeutics based on proteins (e.g. insulin [56]), peptides (glucagon-like peptide [57]) and nucleic acids (e.g. siRNA [58]).

2.2. General targeted drug delivery

Having a drug work at a specific site of action (e.g. tumor) while avoiding normal host tissue has many benefits for the patient such as reduction of side effects and greater therapeutic index. This “targeted therapy” has seen tremendous strides in the clinic impacting many disease indications, but none more so than cancer [59]. Here, the aim is to have the drug target a specific biomolecule that is in circulation or on the surface of, or within, a cell.

Two examples of blockbuster drugs demonstrating this targeted therapy in cancer treatment are bevacizumab and cetuximab. Bevacizumab is a mAb that blocks angiogenesis by inhibiting VEGF-A, an extracellular molecule [60, 61]. Because most solid tumors rely on increased angiogenesis to help supply nutrients, bevacizumab essentially starves the tumors and increases patient survival. Cetuximab is a mAb that binds and blocks epidermal growth factor receptor (EGFR), a cell surface receptor, for the treatment of metastatic cancer [62, 63]. Both targeted therapy agents can also be used in combination with traditional cancer therapy for enhanced efficacy (e.g. [64]).

Targeted drug delivery borrows from the targeted therapy concept but takes it one step further [65]. Here, the aim is to drive a drug to the specific site of action with the help of a vehicle. The vehicle can be a biomolecule (e.g. antibody) that is specific to, for example, a cell surface receptor or extracellular matrix molecule, or the vehicle can be based on nanotechnology (see below). Some of the best drugs that have been discovered also have tremendous side effects to the patient due to undesirable impact to the remaining host tissues thus negating their use in the clinic. Implementing the concepts of targeted drug delivery could enable these drugs to have clinical utility just by concentrating their activity at the site of action and reducing normal host tissue exposure. Designing novel systems always needs to take into account the properties and potential side effects of the drug, route of administration, the intended site of action and the disease indication.

2.3. Combining targeted drug delivery and nanomedicine

Targeted drug delivery and nanomedicine are now close friends [66]. One helps make up for where the other might be lacking. Targeted drug delivery systems (DDSs) can greatly increase the type, capacity and protection of their payload (e.g. cytotoxic drug) through the use of NPs. Nanomedicine can achieve greater localization to the site of action with the use of targeting agents (e.g. antibodies). Targeted nanomedicines can be decorated with a plethora of surface ligand types. These targeting agents are often composed of small molecules [67], nucleic acids (e.g. aptamers [68] (see Chapter III for many more details) or amino acids (i.e. peptides/proteins). However, antibodies are probably the most commonly-used ligand type to decorate NPs due to their high specificity, affinity and availability to a vast swath of molecules (see section 3.1.1), their ability to function as fragments (see section 3.1.2), their robust discovery technologies (see section 3.1.3) and their capacity for engineering (see section 3.1.4) to accommodate the demands of the developer.

Targeted DDSs based on nanotechnology come in two flavors (**Figure 6**) [65]. “Passive” DDSs are successful due in part to their circulation times. Use of stealth agents (e.g. polyethylene glycol (PEG)) help to reduce phagocytic uptake to help the drug bypass elimination machinery. Another example in tumor therapy is the exploitation of the enhanced permeability and retention (EPR) effect to concentrate the drug in the tumor. Though, years of research have concluded that the EPR effect is prominent in rodent models but highly heterogenous in human tumors [69, 70] and should be determined prior to administration of nanomedicines in the clinic [71]. “Active” DDSs use ligands to a specific molecule (e.g. antibodies) to concentrate the drug to the site of action (e.g. tumor). See section 4 for full details on these and other technologies currently found in targeted drug delivery.

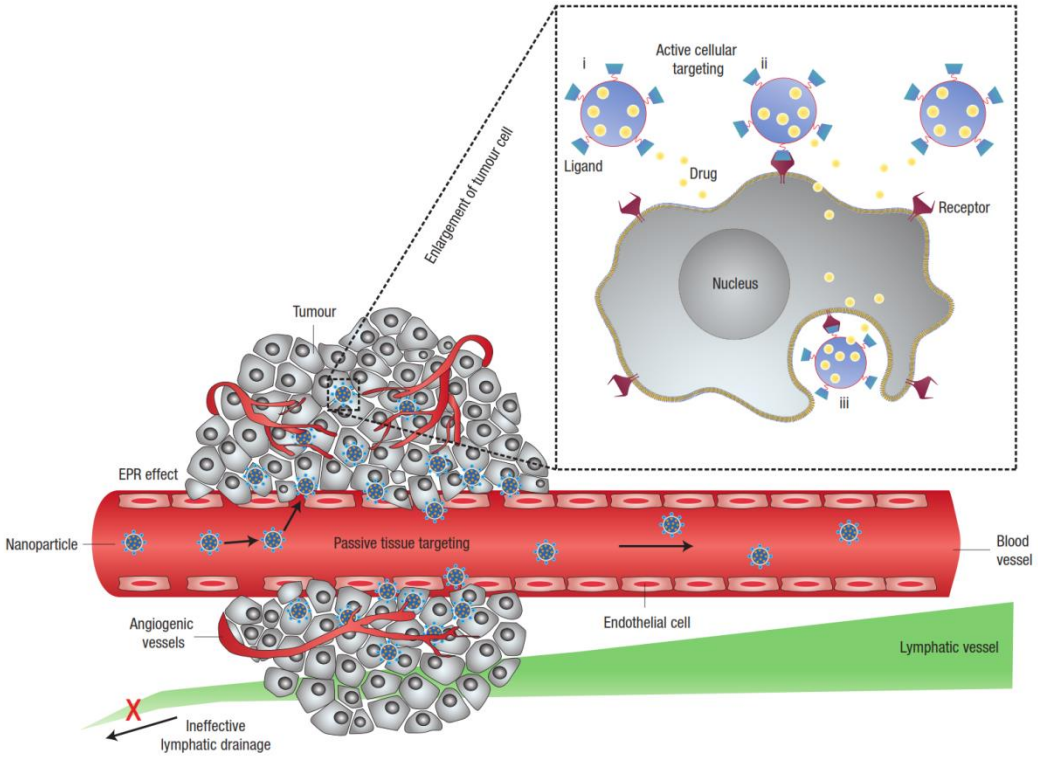

Figure 6. Schematic of "passive" (via enhanced permeability and retention (EPR) effect) and "active" targeted drug delivery for the treatment of solid tumors. Used with permission from [72].

The studies in Chapter IV were designed on the aforementioned qualities associated with targeted DDSs and NPs for the treatment/diagnosis of gastrointestinal tract cancers.

3. Ligands used in targeted therapy

3.1. Monoclonal antibodies (mAbs)

To better understand how monoclonal antibodies (mAbs) can be utilized in the targeted DDSs detailed below, it is first necessary to introduce basic antibody biology. Once the biology has been established, the technologies used to discover novel antibodies and how they can be further engineered are presented.

3.1.1. Antibody biology

The core antibody, or immunoglobulin (Ig), structure is composed of a few domains/regions with their own unique role in the adaptive immunity process (**Figure 7a**) [73]. Ig contains two heavy (H) chains and two light (L) chains that are further subdivided into the constant (C_H/C_L) and variable (V_H/V_L) domains, and the overall structure is stabilized by interspersed disulfide bridges. Two fragment antigen-binding (Fab) regions are connected by a flexible hinge to one fragment crystallizable (Fc) region. One Fab expresses six complementarity determining regions (CDRs), three from each of the V_H/V_L domains, which are responsible for direct physical interaction with the target antigen (i.e. immune-stimulating molecule) and dictate binding affinity. The third CDR from the heavy chain (CDR H3) is particularly important. The glycosylated Fc, entirely composed of constant domains, is responsible for communication with the immune system through binding to various Fc receptors (FcRs). Fc is also necessary for the long circulation times of IgG, the most common Ig isotype, due to lysosomal degradation escape mediated by the neonatal Fc receptor (FcRn). FcRn also aids in the transfer of maternal IgG across the placental and intestinal barriers to the fetus and neonate, respectively [74, 75].

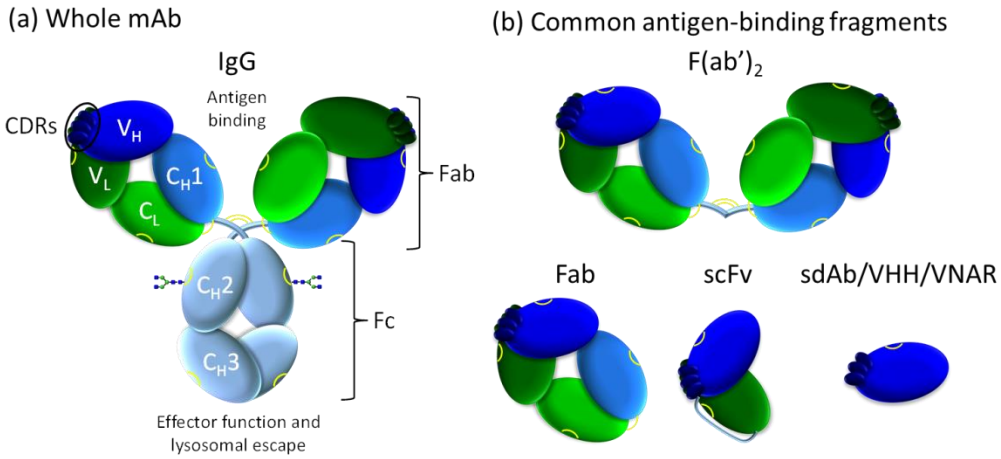

Figure 7. The structural components of (a) a whole monoclonal antibody (mAb)/IgG include the fragment antigen-binding (Fab) and fragment crystallizable (Fc) regions that are composed of the constant (C_H and C_L) and variable (V_H and V_L) domains each containing a disulfide bridge (yellow curves). Direct antigen binding to the target antigen is made through the complementarity determining regions (CDRs) of the Fab fragment and immune effector function is mediated by the Fc fragment. (b) The most common antibody fragment derivatives are: F(ab')$_2$, Fab, single chain variable fragment (scFv) and single-domain antibodies (sdAbs) from llamas (VHH), sharks (VNAR) or other species.

Antibodies identify and destroy the vast array of pathogens (e.g. viruses, bacteria and diseased host cells) in several ways. Outside the cell, they can simply disrupt cellular entry or recruit the help of FcR-expressing immune effector cells mainly through antibody-dependent cell-mediated cytotoxicity (ADCC) or complement-dependent cytotoxicity (CDC) [76]. Inside the cell, antibody-coated pathogens are recognized by tripartite motif-containing protein 21 (TRIM21) [77], a high affinity cytosolic FcR [78], which recruits the proteasome through auto-ubiquitination for pathogen degradation to prevent fatal infection [79]. This immune mechanism is termed antibody-dependent intracellular neutralization (ADIN) [80]. The plethora of pathogens/antigens one can encounter necessitates an on-demand, diverse antibody repertoire (~10^{12} possible unique antibody sequences) made possible by V(D)J recombination of only three Ig genes [81].

3.1.2. Antibody fragments

Targeted DDSs with mAbs relies only on the antigen-binding variable domains and can dispense with the Fc, as long as FcR-dependent effector function is not a consideration. Many antibody fragment-based formats exist that mainly revolve around the V_H/V_L domains [82]. The most common ones are the single-chain variable fragment (scFv), Fab and F(ab')2 (**Figure 7b**). Their smaller size is advantageous, because they are easier to produce by recombinant protein expression, which is useful during selections and screens (see section 3.1.3), and it helps to reduce the overall size of the downstream nanocarrier.

Interestingly, camelids [83] and some sharks [84] express heavy-chain only antibodies, making it possible to isolate the V_H domain as VHH (i.e. nanobody) and VNAR, respectively. It is also possible to isolate the V_H or V_L domains from normal antibodies, and all these formats are considered as single-domain antibodies (sdAbs) (**Figure 7b**).

3.1.3. Antibody discovery

The original technology to create mAbs started by fusing myeloma cells (B cell cancer) with spleen cells from sero-positive mice immunized with the target antigen resulting in hybridoma cells that are both immortal and secrete the antibody of interest [85]. As the gene can be sequenced from a single clone, genotype can then be linked to phenotype.

The true power of mAbs was unleashed in the late 1980's when the genes encoding the variable domains extracted from a population of B cells (i.e. antibody library) were able to be cloned [86, 87], recombinantly-expressed [88], and *in vitro* displayed [89]. Depending on their source of origin, antibody libraries come in several flavors: naïve, immune, semi-synthetic or fully synthetic. Importantly, the functional diversity of an animal-derived library is typically 10^{7-8}. Fully synthetic libraries are designed and constructed to include synthetic genes derived from known (human) antibody frameworks with the capacity to generate a large diversity in appropriate regions, such as CDRs [90]. The HuCAL® (Human Combinatorial Antibody Library) [91] library was a first generation synthetic library consisting of 10^{10} fully human Fab fragments with further improvements from the GOLD® [92] and second generation PLATINUM® [39] versions. The anti-human CD44v6 Fab in Chapter IV was, in fact, derived from the HuCAL PLATINUM® library.

Enrichment of target-specific affinity binders is possible through a process of selection [93-95], and in a way mimics the *in vivo* immune selection process [96] (**Figure 8**). Briefly, the displayed library of antibodies is incubated in the presence of the target antigen. After removal of non-binders, the remaining antigen-bound clones are subjected to subsequent amplification. This "biopanning" is repeated several times to generate an enriched, yet still polyclonal, pool of binders. Finally, single clones are isolated and individually screened for reduction to a lead panel and further characterization. The selection and screening of recombinant antibodies process can be tailored to help maximize the amount of potential high affinity molecules, and many different strategies exist for antigen presentation, library construction, selection and screening, species cross-reactivity and automation [97].

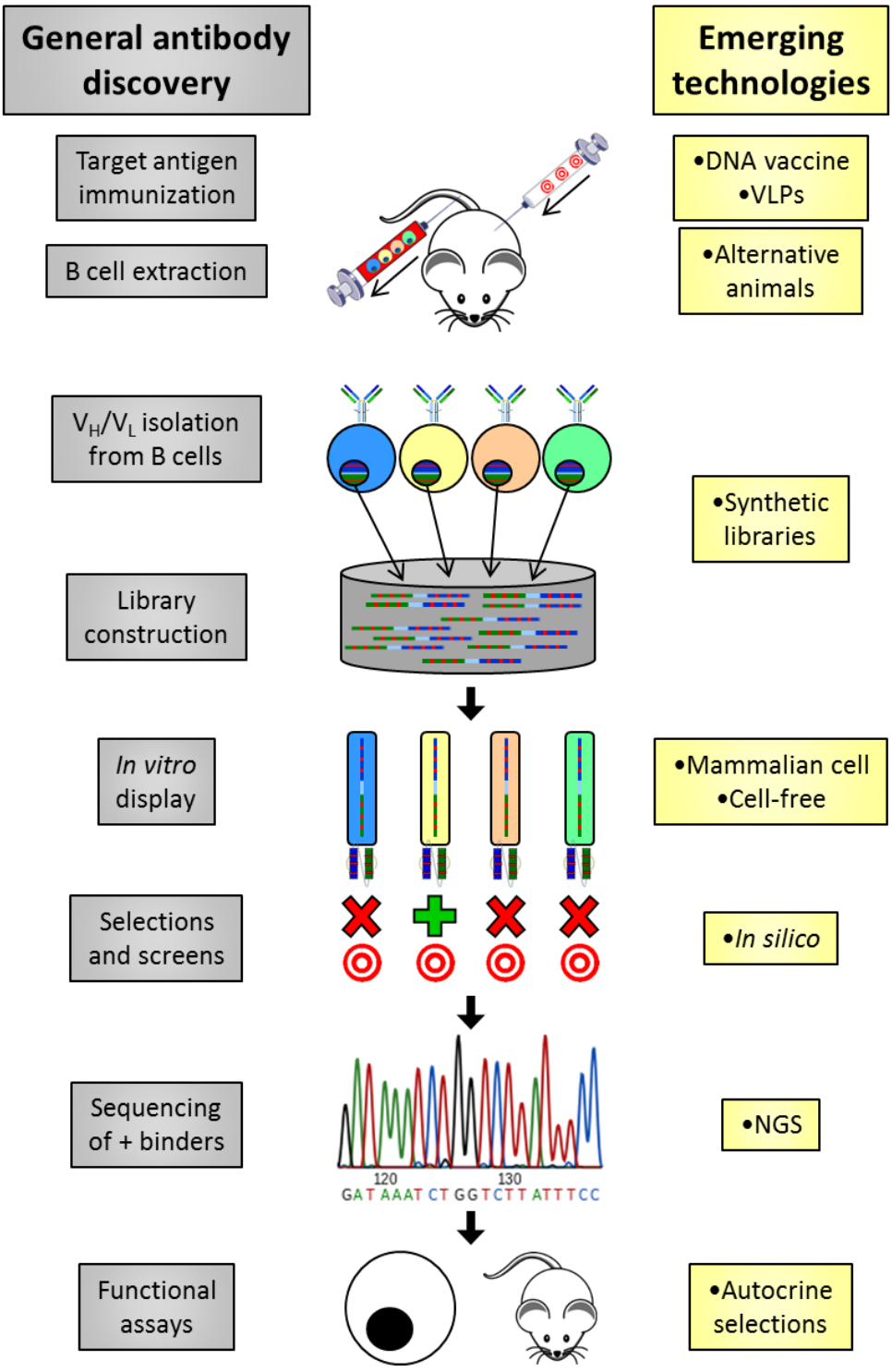

Figure 8. Schematic depicting the early stages of the general antibody discovery process and the emerging technologies that aim to improve each step of the process. Once a target molecule (e.g. cell surface receptor) is defined, an immunoglobulin (Ig)-producing animal (e.g. mouse) is immunized with the target antigen (e.g. peptide) to initiate the antibody response. The variable genes (V_H/V_L) are then isolated from the antibody-producing B cells of positive responders, and polyclonal libraries, often in the single-chain variable fragment (scFv) format, are constructed and packaged into the one of the many

in vitro display technologies (e.g. phage). The displayed libraries are then selected (polyclonal) and screened (monoclonal) for binding to the target antigen. Positive binders are sequenced, recloned, purified and further characterized in functional assays on cells and in animal models. Improvements in the discovery process that have emerged are the use of: DNA vaccines and virus-like particles (VLPs) to enhance immunogenicity, alternative animals to increase repertoire diversity, fully synthetic libraries (e.g. HuCAL®) to eliminate the need for immunized animals, mammalian cell display to have more native presentation, cell-free display and *in silico* analysis coupled with high-throughput technologies (e.g. next generation sequencing (NGS)) to decrease discovery time and, lastly, autocrine-based selection systems to bypass the target binding process and directly select for antibodies with a defined functional phenotype. Figure not drawn to scale.

In vitro display technologies opened up a whole new realm of possibilities in antibody/protein discovery and engineering. A handful of different display technologies used in the discovery process are following (**Table 1**). Phage display technology [98] allows a foreign gene to be inserted within a filamentous bacteriophage coat protein for display on the virion surface while still retaining infectivity [99]. In this genotype-to-phenotype format, the entire repertoire of variable or Fab fragment genes, from mice [89] and humans [96, 100] for example, can be packaged into the phage as a library, and library sizes can be quite large ($>10^{10}$). Yeast surface display (YSD) is the most popular display method after phage display [101]. Here, a library of antibody fragments (e.g. scFv) are expressed on the surface of yeast cells and selected for target binding through successive rounds of mutagenesis and fluorescence-activated cell sorting (FACS) selection [102, 103]. An advantage of YSD is the eukaryotic post-translational processing of secreted proteins (e.g. glycosylation [104]). Mammalian virus/cell surface display systems have begun to offer some advantages in mAb discovery where FACS is also used [105, 106]. Recently, an elegant system whereby candidate antibodies are selected based on a designated phenotypic output was developed [107, 108]. Updated versions of this autocrine-based selection system incorporated a reporter construct and FACS for selection [109] and later anchored the antibody to a membrane protein to maintain receptor co-localization [110, 111]. Intracellular antibodies can also be functionally selected as seen by survival of cell death induced by rhinovirus [112]. Some display/protein synthesis systems eliminate the cell altogether [113] and have been applied to mAb production [114]. These cell-free systems display the antibody on a ribosome [115] or mRNA [116, 117], usually as an scFv or Fab [118] in translation

systems mainly based on *E. coli* [119], wheat germ, rabbit reticulocyte [120] or insect cell [121] lysates.

Table 1. Novel mAbs can be identified using any of the different *in vitro* display technologies listed here. As with any technology, there are advantages and disadvantages to each. Selected references are presented that provide more details and/or demonstrate the power of each technology.

Display technology	Advantages	Disadvantages	Selected references
Phage/ bacteria	•Established •Successful •Robust	•Prokaryotic translation •μM affinity	[89], [98], [122]
Yeast surface	•Eukaryotic translation •Established •FACS selection	•Limited library sizes	[101, 102], [123]
Mammalian virus/cell	•Mammalian translation •Full length IgG possible •FACS selection •Accounts for downstream manufacturing	•Emerging, thus not established •Specialized	[105, 106, 124]
Autocrine	•Selections based on a functional phenotype •Unnecessary prior target knowledge	•Specialized •Patent protected	[107], [111, 112]
Cell-free	•Rapid •Ability to incorporate unnatural amino acids •Ability to couple to microfluidics	•No post-translational modifications	[114, 115, 125]

3.1.4. Antibody engineering

Once a lead candidate is identified that binds to a specific target by one or more of the means detailed above, it can be further engineered for enhanced pharmacology and beyond due to their recombinant nature. Many strategies can improve antibody pharmacokinetics/dynamics in humans (**Figure 9**). Chimerization/humanization aims to lower immunogenicity by replacing the non-antigen binding parts of the antibody that were derived from another animal source with human versions [126]. Affinity maturation aims to increase the affinity of the mAb by selecting and screening for mutants of the original lead mAb with higher binding to the target [127]. Fc modification aims to enhance immune effector function or circulation times by increased engagement with Fcγ receptors [128] or

FcRn [74], respectively. Engineering strategies aimed at improving stability and aggregation are mostly a manufacturing and storage concern that conveniently results in lowered immunogenicity [129]. Some of the above strategies can also be aided by computational tools.

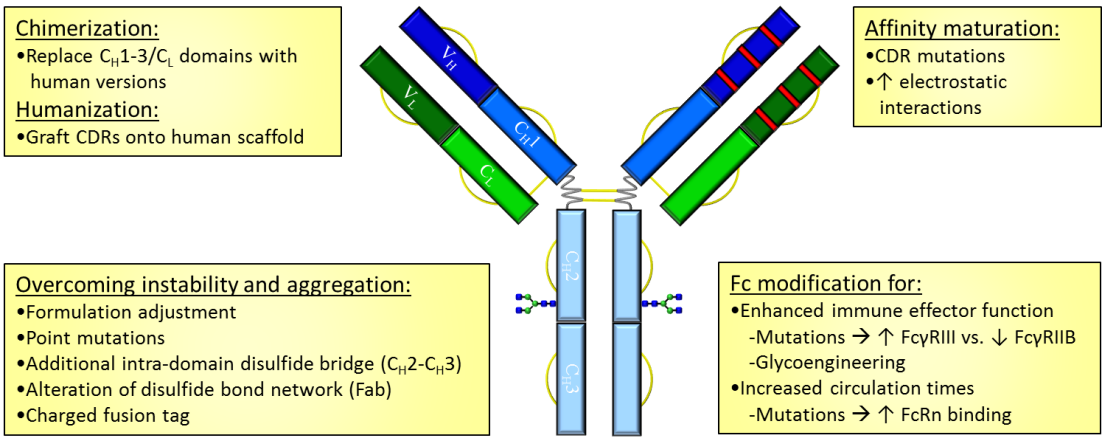

Figure 9. Engineering mAbs for enhanced pharmacology and storage are possible with several strategies. Chimerization and humanization aim to reduce immunogenicity associated with mAbs originating from non-human sources by replacing the constant domains or the entire mAb scaffold with human versions, respectively. Increasing the binding kinetics of a mAb is driven by *in vitro* affinity maturation strategies focusing on point mutations, usually within the complementarity determining regions (CDRs), which often replace uncharged amino acids (AAs) with charged ones to increase electrostatic interactions. Immune effector function is enhanced by modifying Fc with engineered glycosylation groups or with specific AA mutations for increased binding to Fcγ receptor (FcγR) III and decreased binding to FcγRIIB. Circulation times can be extended with AA mutations that enhance binding of Fc to the neonatal Fc receptor (FcRn). Long-term storage of mAbs can lead to instability and/or aggregation that often cause increased immunogenicity. This can be overcome through simple formulation adjustment or by incorporating specific point mutations, an additional intra-domain disulfide bridge between the C_H2 and C_H3 domains, an altered disulfide bond network within the Fab and/or a charged fusion tag.

3.2 Aptamers and SELEX

Nucleic acid-based aptamers (single-stranded DNA or RNA) are an alternative and emerging class of molecules [130] that can act as therapeutics alone [131] or as targeting

ligands [132, 133] (**Figure 10)**. Aptamers are functionally similar to antibodies but present some added advantages such as smaller size, easier production and modification, desirable storage properties, nominal immunogenicity, and the ability to conjugate to biomolecules/nanoparticles [131].

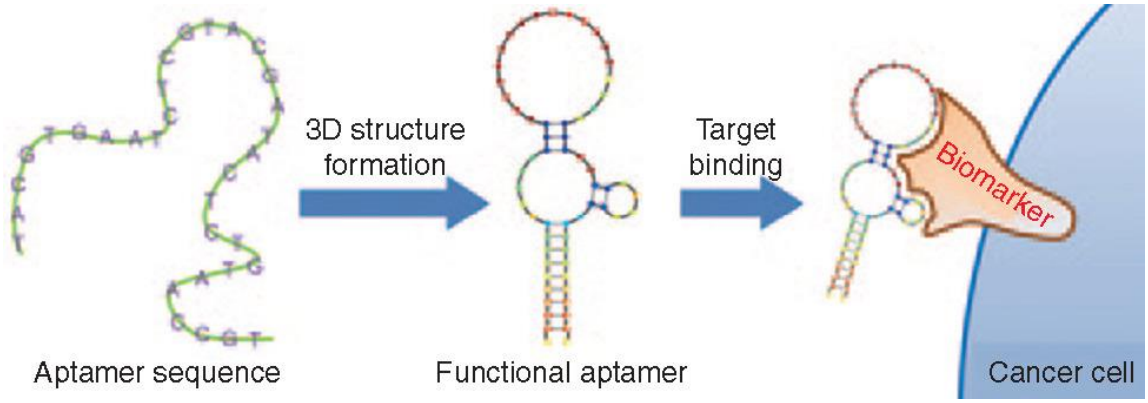

Figure 10. Schematic diagram of an aptamer binding to its target. The sequence of the aptamer defines its three-dimensional conformation that is based on areas of base-pairing and non-pairing. Used with permission from [134]

The aptamer discovery process is relatively similar to the antibody discovery process. For both antibodies and aptamers, novel ligand identification occurs through a repetitive enrichment process of incubating a very large and diverse polyclonal pool of potential ligands on a pre-defined target (e.g. receptor), removing unbound/non-specific ligands, amplifying the target-specific ligands and repeating the process over several cycles.

Novel aptamers are identified through a process termed selected evolution of ligands by exponential enrichment (SELEX) (**Figure 10**) [135, 136]. Basically, the process starts with incubating a synthetic polyclonal library with the target. The target, for example a cell surface receptor like CD44v6, can be presented in a number of ways such as a peptide, a recombinant or purified protein, or on the surface of a cell. Each target presentation has advantages and disadvantages. Once specific aptamers bind to the target, unbound aptamers are washed away. Target-specific aptamers are then amplified by the polymerase chain reaction (PCR). This process is then repeated for several cycles, typically 8-20 cycles. Assuming the SELEX process was successful, we end with an enriched polyclonal pool of aptamers with varying affinities and specificities to the target.

Individual clones are then sequenced, synthesized and characterized for their affinity and specificity to the target. Unlike antibody discovery that typically need 2-3 rounds of selection, one drawback of aptamer discovery is that many more rounds of SELEX need to be performed before one is able to test for target enrichment.

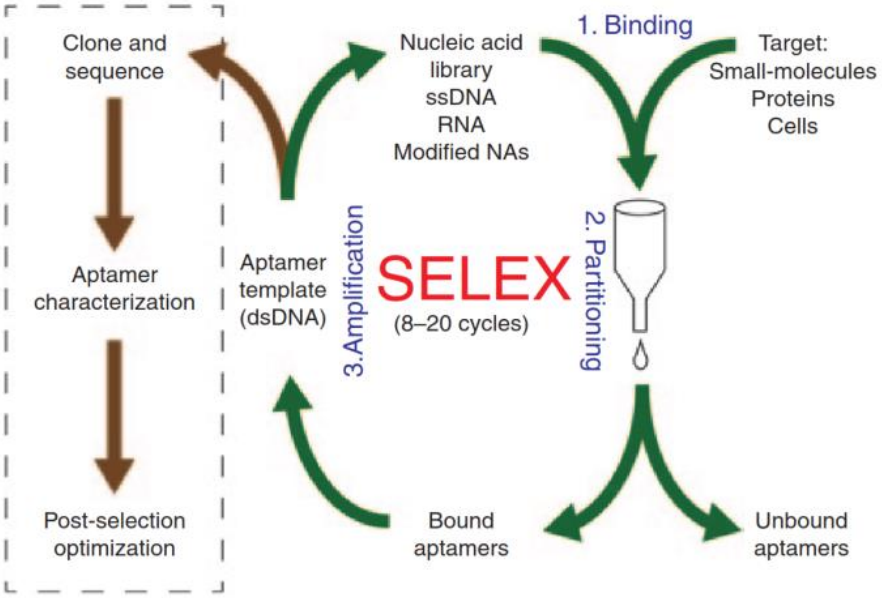

Figure 10. Schematic depicting the systematic evolution of ligands by exponential enrichment (SELEX) procedure. Briefly, a library of ~10^{14} short, single-stranded DNA/RNA-based oligonucleotides (aptamers) is incubated with the target molecule. Unbound aptamers are washed away and bound aptamers are converted to a double-stranded DNA by polymerase chain reaction (PCR) for amplification. The dsDNA is then converted back to the original ssDNA/RNA format ready for another round of selection. This process is then repeated for several more cycles to enrich for target-specific aptamers. Poly- or monoclonal aptamers are then sequenced and screened for binding to the target ready for downstream applications. Used with permission from [136].

The above SELEX description is a very simplified version of the overall procedure. Importantly, SELEX is very malleable and can, and needs to, be adjusted according to the oligonucleotide composition (i.e. DNA or RNA) and/or the target molecule type (e.g. peptide or cell) [137]. For example, when identifying RNA-based aptamers, two extra steps of converting the RNA to DNA for PCR amplification and back to RNA are necessary, because PCR is limited to DNA only. Recently, high throughput sequencing and bioinformatics technologies have been implemented to allow for sophisticated

protocols that can reduce cycle number, and ultimately discovery time, as well as identification of rare binders not detected with traditional methods (e.g. [138, 139]).

4. Antibody-decorated nanoparticles

Targeted therapy of cancer with mAbs holds tremendous promise in the specific elimination of tumor cells without the systemic toxicity associated with conventional chemotherapeutic agents (e.g. rituximab and B cell lymphomas). Unfortunately, only modest success has been achieved in patients with solid tumors, as the immunological mechanisms associated with tumor cell elimination have not proven to be as effective as expected [140]. To address this, several technologies have been developed that combine the specificity and affinity of antibodies with other drugs based on small molecules (antibody-drug conjugates (ADCs)) or biologics (antibody-biologic conjugates (ABCs)) or nanocarriers (antibody-nanoparticle conjugates (ANCs)). In the context of this thesis (see Chapter IV), an introduction to ANCs is presented below.

The early NP-based cancer therapeutics (e.g. Doxil) focused on “passive targeting” to tumors by avoiding the reticuloendothelial system and exploiting the enhanced permeability and retention effect, a consequence of leaky tumor vasculature [66, 141]. However, a major goal for nanomedicine is to drive the therapeutic directly to the site of action (e.g. receptor-overexpressing tumor cell) through decoration with ligands that bind to a specific target molecule (e.g. receptor), often termed “active targeting” [66]. Although no targeted NPs have been approved yet, close to 20 are in clinical trials. BIND-014, one example that completed phase II trials for the treatment of prostate and lung cancer, is a PEGylated polymeric NP harboring docetaxol and decorated with a small molecule specific to prostate-specific membrane antigen [142]. Given the vast multitude of targeting ligands, drugs and nanomaterials, the possible combinations of the three are boundless.

Many factors contribute to the overall success or failure of targeted NPs including: a) route of administration, b) biological barriers [44], c) adsorption of host proteins to the NP surface [143], d) conjugation chemistry, e) hydrophobicity of the NP, f) composition, size, shape and charge of both the ligand and NP, g) density and orientation of the conjugated ligand [66] and h) ligand affinity/avidity (**Figure 11**). Additionally, the properties of the drug to be incorporated will dictate the method of nanoencapsulation. Antibodies serve as ideal targeting ligands for their affinity, specificity and engineering malleability [144].

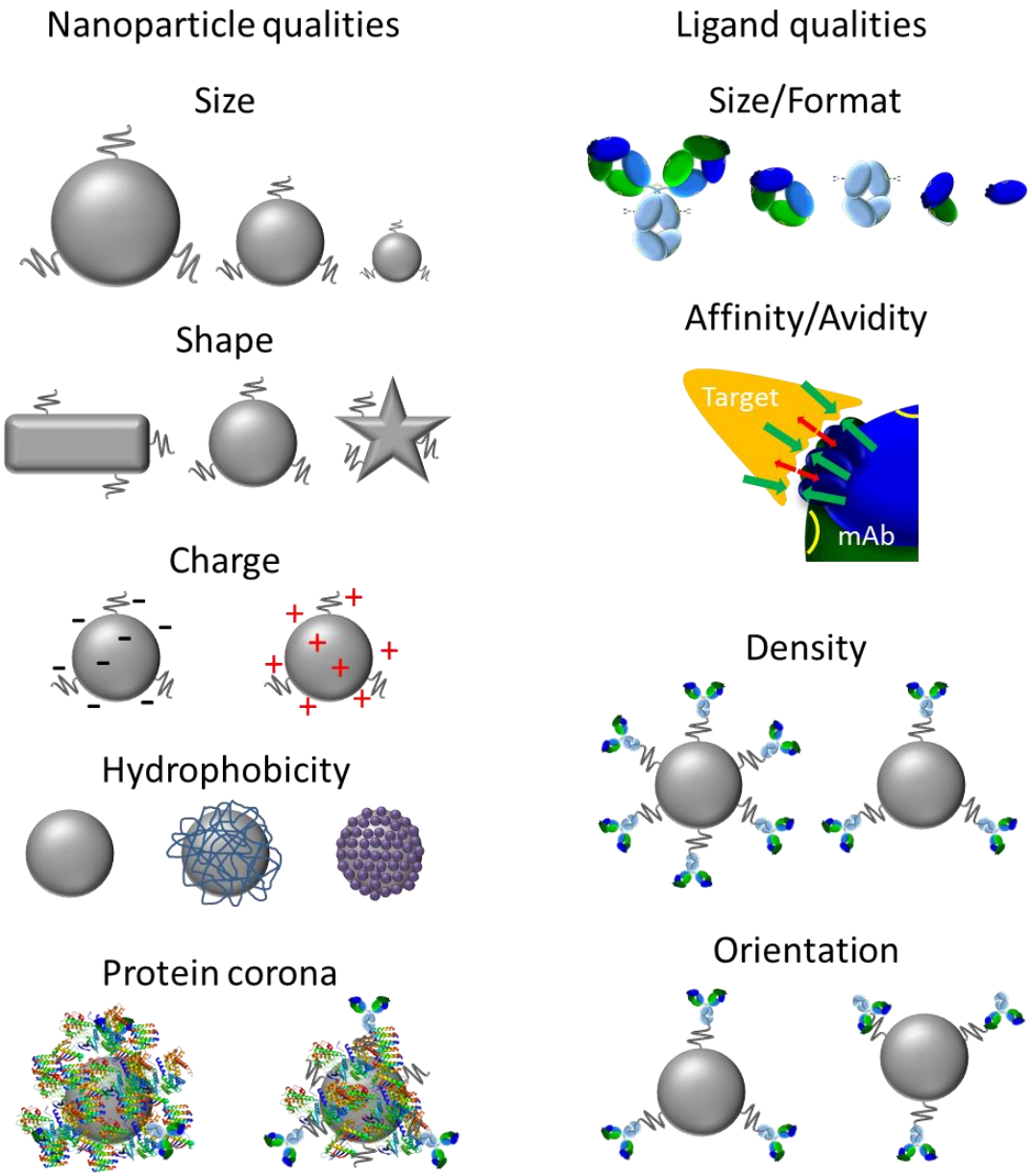

Figure 11. Many factors dictate the *in vivo* behavior of ligand-decorated nanoparticles (NPs) including those associated with the nanoparticle (NP; left) as well as the ligand (right). The specific NP qualities to keep in mind are size, shape, charge and hydrophobicity, and these properties can also dictate the amount and composition of the protein corona. The specific ligand (i.e. mAb) qualities to consider are size and affinity, as well as density and orientation when coupled to the NP. Drawings are not to scale. Inspired by [66].

Active targeting of nanocarriers is possible through decoration with ligands, and antibodies or associated fragments have been proven to be quite viable for this purpose (**Figure 12**) [66]. These systems are often designed to target cell surface receptors and degrade and release their payload once the NPs enter the cell by a number of means. Fortunately, it seems that P-glycoprotein does not recognize the NPs, thus resulting in enhanced intracellular accumulation and nominal drug resistance [145].

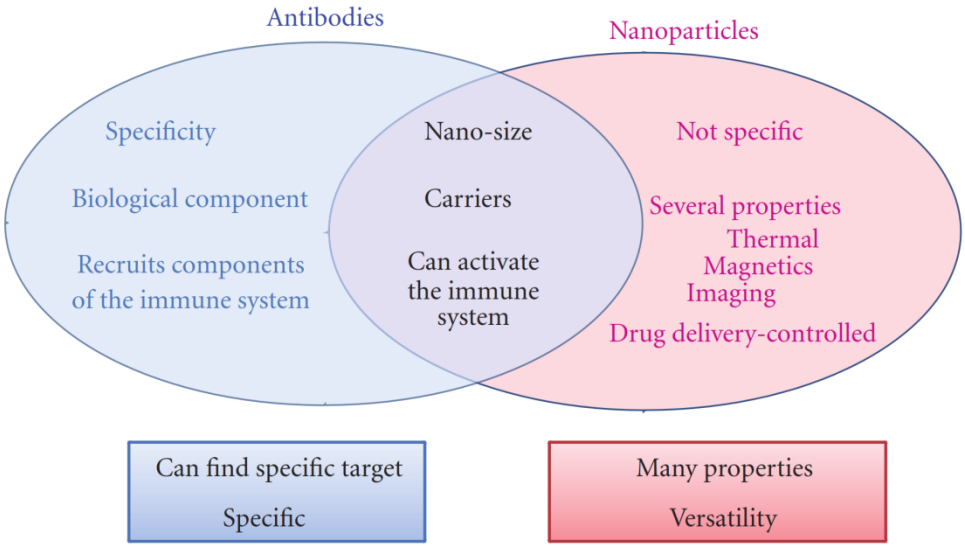

Figure 12. The advantages and disadvantages of antibodies and nanoparticles demonstrating how the two systems can complement each other to further increase their therapeutic efficacy. Used with permission from [145].

Early studies with targeted NPs focused on encapsulating classic chemotherapy agents to increase therapeutic index, mainly by lowering systemic toxicity. Park and colleagues demonstrated that immunoliposomes harboring dox and decorated with anti-HER2 (Fab or scFv) had more tumor targeting efficacy and lower toxicity than all the other control treatments [146].

Unlike ADCs and ABCs, the antibody (~10-20 nm) in this case is usually much smaller than the conjugated NP "cargo" (~100 nm), opening the possibility to attach many antibodies to a single NP. Similar to natural and bispecific antibodies, avidity may be exploited to enhance overall binding and/or specificity to the target antigen(s). A site-specific conjugation strategy using expressed protein ligation and copper-free click chemistry was used to decorate anti-HER2 affibodies to superparamagnetic iron oxide

NPs at controlled ligand densities [147]. In fact, intermediate ligand density resulted in the highest cell binding, and this was confirmed with an alternative (non-antibody) ligand. Thus, optimal ligand density must be empirically determined for highest efficacy.

Ligand orientation on the NP can also affect antigen binding. Conventional chemistries do not afford control of where on the mAb (e.g. amines) the conjugation bridge is formed [148]. This leads to non-ideal conditions where many of the antibodies may be oriented on the NP such that the antigen-binding domains are unavailable for direct antigen contact. Engineering and recombinant strategies can overcome this disorientation and maximize antibody functionality. Whole IgG can be coupled to gold NPs through the Fc domain with the heterobifunctional linker, hydrazide-polyethylene glycol-dithiol [149]. Another example is to engineer a Fab with a C-terminal cysteine and use a maleimide-based linker (e.g. succinimidyl 4-(N-maleimidomethyl)cyclohexane-1-carboxylate (SMCC)) to couple to amine groups commonly found on various nanomaterials (e.g. chitosan [150]). This was the strategy used in a part of this thesis research (see Chapter IV).

In vivo diagnostics can also benefit from targeted NPs. Anti-EGFR-coated gold NPs were developed to aid in endoscopic tumor imaging [151]. Furthermore, combining a diagnostic agent along with the therapeutic payload (i.e. theranostic) offers the advantage of monitoring a treatment regimen during NP administration [152]. It should be noted though that more complexity added to a nanocarrier imposes greater cost (e.g. regulatory); thus, the trade-off should be considered before embarking on (pre-)clinical studies [153].

Although the overall strategy of “active targeting” has been criticized, highlighting the dearth of clinical evidence [154], the current literature points to the extreme validity of this strategy. Yet, clearly more research efforts must be dedicated into ways to identify and overcome the biological barriers inhibiting the targeting [44]. For example, the protein corona [155] is a well-characterized phenomenon known to disrupt targeting [156]. When in biological fluids (e.g. serum), biomolecules adsorb as a “hard” or “soft” layer onto the NP surface. The composition of this corona is dependent on the biological environment but also on the NP qualities (size, shape, charge, hydrophobicity, etc) [143]. These proteins can thus mask the ligand overriding any targeting capabilities, as seen in transferrin-coated NPs [156]. One way to overcome the inhibitory effects of the protein corona is through backfilling with PEG once the ligand has been conjugated to the NP [157].

The infinite combinations of drugs, ligands/antibodies, nanomaterials, encapsulation and conjugation methods and specific disease indications can frustrate the initial planning stages. On one hand, making decisions about the ideal system is quite challenging, but, on the other hand, these technologies can bring unprecedented possibilities. Regardless, the antibody-decorated nanocarrier platform is emerging as a highly promising tool in targeted drug delivery.

This chapter has set the stage for the basis of the research associated with this thesis. Section 1 demonstrated that CD44v6 is a valid therapeutic/diagnostic target for gastrointestinal cancers. Section 2 demonstrated that combining targeted drug delivery with nanomedicine currently offers the most promising strategy for driving a therapeutic/diagnostic to CD44v6-expressing cancers. Section 3 introduced two types of ligands, antibodies and aptamers, that are very promising as NP decorating agents for targeted drug delivery. This section discussed a bit of their structure and function as well as their methods of identification. Section 4 expanded on the use of antibodies as ligands for targeted NPs, a major theme of this thesis.

CHAPTER II

Aims of the thesis

The overall aim of this doctoral thesis was to develop and characterize NPs able to delivering a drug and/or diagnostic agent to human cells/tissues that express CD44v6, while minimizing recognition of normal (non-CD44v6-expressing) cells/tissues. The downstream application of these NPs was intended to be for the treatment and/or diagnosis of gastrointestinal tract-related cancers that express CD44v6.

The specific objectives of this research were:

i) To identify a novel RNA aptamer specific to human CD44v6 by SELEX and to characterize that aptamer in biochemical and cell-based experiments (Chapter III).
ii) To conjugate the novel ligand identified in Chapter III, or an established anti-CD44v6 ligand as proof-of-principle, to polymeric NPs and characterize their physicochemical qualities such as size, polydispersity index, zeta-potential and morphology (Chapter IV).
iii) To biologically characterize the developed NPs for binding specificity and affinity to CD44v6 presented as a biomolecule and on the surface of a cell as well as cell internalization and cytotoxicity (Chapter IV).
iv) To technologically characterize the developed NPs for the ability to be produced by different methods and for resistance to simulated intestinal fluid and cryopreservation (Chapter IV).

This thesis research aimed to translate the scientific knowledge of CD44v6, nanomedicine and targeted drug delivery into a novel polymeric nanosystem that is capable of specifically recognizing human gastro-intestinal tract cancer cells that express CD44v6 while minimizing interactions with normal host tissues. This nanosystem is expected to be fully compatible in humans and to deliver a drug and/or diagnostic for *in vivo* therapeutic and/or diagnostic intervention. Lastly, this nanosystem is expected to display technological qualities that are amenable to pharmaceutic formulation beyond systemic administration (e.g. oral delivery or cryopreservation).

CHAPTER III

Discovery of anti-CD44v6 RNA aptamers by SELEX

This work was partly performed in the lab of Dr. Paolo Serafini at the Miller School of Medicine, University of Miami (USA) that has expertise in identifying and characterizing novel, cancer-related RNA aptamers [158] and their use with targeted nanoparticles [159].

1. Abstract

Variant isoforms of CD44 containing exon v6 (CD44v6) have been implicated in metastasis and other cancer-related processes. Thus, this cell surface receptor is a potential therapeutic and/or diagnostic target in the treatment of various cancers. Akin to antibodies, aptamers are nucleic acid-based oligonucleotides that can adopt specific three-dimensional conformations with high specificity and affinity to a wide array of targets. With the intention of functionalizing nanoparticles, a novel RNA aptamer against human CD44v6, presented as a peptide or on the cell surface, was attempted to be identified through selected evolution of ligands by exponential enrichment (SELEX). Twelve rounds of peptide-based and seven rounds of cell-based SELEX were performed, and each output was quality controlled by spectrophotometry and gel electrophoresis. Various rounds of the peptide-based SELEX outputs were fluorescently-labelled and tested for binding to the CD44v6-derived peptide and to CD44v6-expressing cells. No CD44v6-specific enrichment was detected by either of the binding assays. Alternative methods, such as high-throughput sequencing and bioinformatics technologies, may be able to reveal sequence enrichment, but for now, a novel aptamer against human CD44v6 was unsuccessfully identified.

2. Introduction

CD44 is a highly alternatively-spliced, transmembrane surface receptor. Variant isoforms containing exon v6 (CD44v6) are associated with many aspects of cancer (e.g. metastasis [4], cancer stem cells [21] and hyperplastic lesions [19]) and are found in several tumor types (e.g. gastric, colorectal and head-and-neck cancers) [1, 32]. The overall aim of the thesis research is to develop nanoparticles (NPs) encapsulating a drug and/or diagnostic agent that specifically target CD44v6-expressing human gastric and/or colorectal cancer cells/tissues. Specific targeting can be achieved by tethering a ligand to the surface of the NP that has high specificity and affinity to human CD44v6.

Targeting ligands are typically based on antibodies, proteins/peptides, small molecules, or nucleic acids. Antibodies are commonly used ligands and offer many advantages such as the aforementioned specificity and affinity as well as availability [160]. Though, antibodies do have a few drawbacks such as potential immunogenicity and high discovery and production expense, among others.

Nucleic acid-based aptamers (single-stranded DNA or RNA) are an alternative and emerging class of molecules that can act as therapeutics alone [131] or as targeting

ligands [132, 133]. Aptamers are functionally similar to antibodies but present some added advantages such as smaller size, easier production and modification, desirable storage properties, nominal immunogenicity, and the ability to conjugate to biomolecules/nanoparticles [131].

Novel aptamers are identified through the process called selected evolution of ligands by exponential enrichment (SELEX) (see section 3.2 of Chapter I) [135, 136]. SELEX is very malleable and can, and needs to, be adjusted according to the oligonucleotide composition (i.e. DNA or RNA) and/or the target molecule type (e.g. peptide or cell) [137]. For example, when identifying RNA-based aptamers, two extra steps of converting the RNA to DNA for PCR amplification and back to RNA are necessary as PCR is limited to DNA only (**Figure 1**).

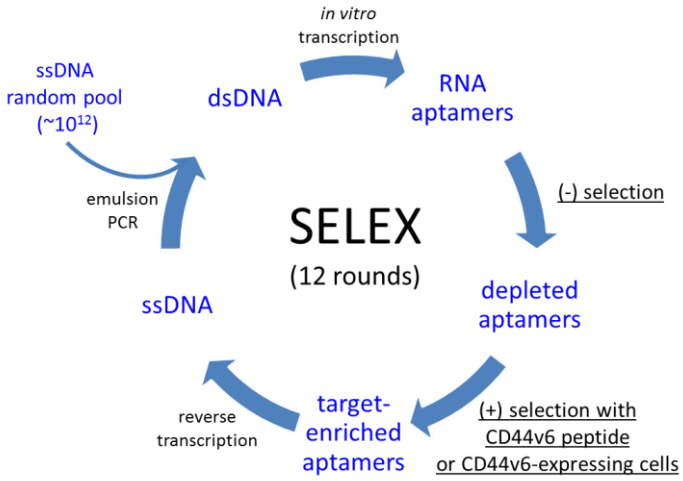

Figure 1. Schematic depicting the SELEX process of anti-CD44v6 RNA aptamer identification that was used herein. Briefly, the Sullenger library was first transcribed into RNA aptamers. The RNA aptamers were then incubated in the presence of the negative selection agent followed by unbound aptamers incubation with the CD44v6-specific selection agent (CD44v6 peptide or expressing cells). Unbound aptamers were washed away, and bound aptamers were either eluted from the magnetic beads or by antibody competition/displacement for the peptide or cell SELEX, respectively. Purified RNA was reverse transcribed into ssDNA and then converted into dsDNA by (emulsion) PCR. Throughout, the quality of the RNA/DNA was confirmed by agarose gel electrophoresis. This process represents one cycle of the SELEX protocol, and 12 peptide-based SELEX cycles were completed. More details about the peptide and cell SELEX protocols can be found in the document text.

PCR is used to convert ssDNA to dsDNA. Unfortunately, many sequences are prone to unequal amplification (aka PCR bias) due to intrinsic differences in the amplification efficiency of templates during multi-template PCR [161]. One way to reduce PCR bias is to emulsify the reaction mixture to compartmentalize the PCR reactions within nano/picoliter water-in-oil emulsion droplets [162, 163]. In essence, a compartmentalized template with higher amplification frequency will exhaust its replication machinery components (e.g. primers and polymerase) and allow templates in other droplets to utilize their own compartmentalized components.

As no aptamers targeting CD44v6 were published in any academic journals or international patents and due to the licensing restrictions of AbD15179 use *in vivo*, SELEX was explored to identify a novel aptamer with specificity and affinity to human CD44v6. It was decided to try two different SELEX approaches based on peptide or cell surface presentation of human CD44v6 (**Figure 1**) intending to increase the rate of success. Emulsion PCR was utilized during the amplification stage to reduce amplification bias. Various rounds of the peptide-based SELEX outputs were then tested, unsuccessfully, for binding to a CD44v6-derived peptide or CD44v6-expressing cells.

3. Materials and methods

3.1. Materials

The cell culture media, penicillin/streptomycin (p/s), geneticin, trypsin/EDTA (T/E), versene, superscript III, Dynabeads MyOne Streptavidin T1, *Taq* polymerase and associated reagents, PCR primers, anti-CD44v6 monoclonal antibody (MA54), Alexa Fluor®647 C2 Maleimide and TMB substrate, were purchased from ThermoFisher Scientific. The fetal bovine serum (FBS) was from Biochrom. The biotinylated rat anti-mouse Ly-6G was purchased from eBioscience, and the biotinylated SDS MW Standard mix was from Sigma. The DuraScribe® T7 Transcription Kit was purchased from Epicentre. The 5 mL cryovials and mini-stir bars were purchased from VWR. The horse radish peroxidase (HRP)-conjugated goat anti-human secondary antibody (anti-human-HRP) and the BIO SPIN P6 (TRIS) size exclusion chromatography columns was from Bio-Rad. Most chemicals were from Fisher Chemical or Sigma-Aldrich.

3.2. Cell culture

The MKN74 cell line was derived from a moderately differentiated tubular adenocarcinoma (intestinal-type carcinoma), and the cells were maintained in RPMI supplemented with 10% (v/v) FBS and 0.5 mg/mL geneticin (to maintain selection pressure; see below) and passaged twice per week diluted 1:10-1:20. The cells were sub-cultured when ~80% confluency was reached, and they were maintained at 37 °C and 5% CO2 in a water-saturated atmosphere. CD44v6 expression was occasionally confirmed by FACS with anti-CD44v6 monoclonal antibody (MA54; Life Technologies) staining (data not shown). Mycoplasma detection by PCR was occasionally performed to ensure no contamination, and once during the studies, a short tandem repeat (STR) profile analysis ensured cell line purity. When relevant, the cells were detached with non-enzymatic Versene to maintain the integrity of the surface-bound receptors; however, trypsin/EDTA was used during sub-culture.

3.3. Generation of transfected MKN74 cell lines

The human stomach adenocarcinoma epithelial cell line MKN74 was purchased from the JCRB Cell Bank (Japanese Collection of Research Bioresources Cell Bank). The parental cell line and isogenic variants were kindly provided by C. Oliveira, a co-supervisor of the author. CD44v3-v10 (variant CD44-04 - ENST00000415148) cloned in a pCMV6-XL5 and pCMV6-AC backbone respectively, were purchased from OriGene. These variants were subcloned into a pIRES-EGFP2 expression vector. These vectors and the empty version (Mock) were transfected into MKN74 parental cells using Lipofectamine 3000 (Life Technologies) according to manufacturer's instructions. After transfection, Mock and CD44v6 expressing cells were selected with geneticin and then sorted by magnetic bead capture using specific anti-CD44v6 (MA54) monoclonal antibody. Transfection and selection efficiency was assessed by immunocytochemistry and flow cytometry (C. Oliveira, unpublished data). For brevity, the MKN74-GFP cells overexpressing CD44v3-v10 are termed "MKN74-v6" and the parental MKN74-GFP cells are termed "MKN74". It should be noted that the GFP expression of the cells dictated the choice of fluorophore used in cell-based studies.

3.4. RNA aptamer (library) and production details

The library was commercially synthesized to contain 40 DNA-based nucleotides (nts) that are degenerate (i.e. containing A, T, C or G) at each position to make up the tremendous diversity of the library. The 40 nts are then flanked at the 5' and 3' ends with ~25 non-degenerate nts that serve as primer binding sites to initiate dsDNA synthesis during PCR. Based on the amount of DNA (1 µg) initially used during the DNA→RNA conversion, this equates to ~10^{12} unique aptamer sequences. DNA was converted to RNA with the DuraScribe® T7 Transcription Kit according to manufacturer's instructions. It is important to note that the reagents must be added in the order specified in the kit. Importantly, the RNA in this kit is resistant to RNase A degradation, because the canonical CTP and UTP are replaced with 2′-Fluorine-dCTP (2′-F-dCTP) and 2′-Fluorine-dUTP (2′-F-dUTP).

Lastly, the RNA that was from the initial library production or eluted from the beads (see section 3.7) or from the supernatant of mAb-competed CD44v6-expressing cells (see section 3.8) was first column purified (Qiagen RNeasy kit) according to manufacturer's instructions. The RNA was then reverse transcribed to single-stranded DNA (ssDNA) with the superscript III kit (ThermoFisher) according to manufacturer's instructions. Here, the Sul3' primer (**Table 1**) was used to form the dsDNA initiation point for the reverse transcriptase. The thermal cycler profile was 65°C for 5 min and then slowly cooled down to 4°C over a one hour period. The enzyme was then inactivated by bringing the temperature to 55°C for 1 hr and 70°C for 15 min. The resultant ssDNA product was used to feed the (emulsion) PCR for conversion to dsDNA (see section 3.5).

Table 1. Sequences of the primers used during RNA to ssDNA conversion and (emulsion) PCR amplification to dsDNA.

Primer	**Sequence (5' → 3')**
Sul3'	TCTCGGATCCTCAGCGAGTCGTC
Sul5'	GGGGGAATTCTAATACGACTCACTATAGGGAGGACGATGCGG

3.5. Emulsion PCR

The emulsion PCR (ePCR) was based on these two references [162, 163]. First, prepared 10 mL of oil mixture containing 9.5 mL mineral oil, 450 uL span 80, 50 uL Tween-80, 5 uL Triton-X-100, mixed thoroughly by gentle inversion, and used within the

day it was made. A typical 250 uL PCR reaction mixture contained 50 pM of the Sul3' and Sul5' primers, 10 pM dNTPs and 25 uM MgCl2. An important component of the PCR mixture is the inclusion of 1% bovine serum albumin (BSA) [162]. The Sul5' primer incorporates T7 RNA polymerase binding site for conversion of dsDNA to RNA. The PCR reaction was emulsified in 2X volume of oil (e.g. 250 uL PCR reaction + 500 uL oil). Emulsion was performed in appropriate sized vessel (e.g. 5 mL Wheaton cryovial) containing a mini stir bar at ~1000 rpm. PCR reaction was added to oil 10 uL at a time and emulsified for a further 5 min. The emulsion was then aliquoted to PCR tubes at 50-100 uL/tube and placed on a thermal cycler as normal. The thermal cycler profile was as follows: (94°C, 30 sec; 52°C, 20 sec; 72°C, 25 sec) 3 times → (94°C, 30 sec; 54°C, 20 sec; 72°C, 25 sec) 20 times → 72°C, 5 min → hold at 10°C.

3.6. Output quality control

After the PCR occurred, all products were recombined into an Eppendorf tube and centrifuged at 13,000xg for 5 min to separate the oil from the PCR mixture, and the top oil layer was carefully removed. One mL of water-saturated diethyl ether was added to the PCR mixture and vortexed. The top ether layer was carefully removed, and the process was repeated with an additional 1 mL ether. The residual ether was evaporated in a fume hood for ~1 hr. The PCR mixture was column purified with QIAquick PCR Purification Kit (Qiagen) according to the manufacturer's instructions. The quantity and quality of the dsDNA was determined by spectrophotometric analysis (NanoDrop 1000) and 2% agarose gel electrophoresis, respectively.

It is relevant to note that ePCR was replaced by normal PCR after round 8 of the peptide SELEX, because the advantage of ePCR was assumed to have been severely reduced after so many rounds.

3.7. SELEX using a peptide derived from human CD44v6

Here, peptide SELEX was based on RNA aptamer binding to a peptide that is derived from human CD44v6. The same peptide sequence that was used to select and screen for an anti-CD44v6 Fab was chosen, as this biochemical tool has a proven track record of successful synthesis and functional anti-CD44v6 ligand discovery [164]. The peptide sequence (N- to C-terminus) = biotin-GNRWHEGYRQTKEDS. The peptide was biotinylated to allow for capture with the streptavidin-coated beads. One SELEX cycle

began by incubating 1 ug of the polyclonal aptamers with ~30 pmol of an irrelevant biotinylated protein (biotinylated rat anti-mouse Ly-6G = rounds 1-7; biotinylated SDS MW Standard mix = rounds 8-12) in 300 uL of peptide SELEX buffer (0.5 mM $MgCl_2$ + 1 mM $CaCl_2$ in 1X PBS; pH 7.4) followed by incubation at 65°C for 5 min and then to room temperature (RT) for 10 min on a rotator. The negatively-selected aptamers were then captured with 200 ug streptavidin-coated magnetic beads (**Figure 1**). The beads were then discarded. In principle, this negative selection should reduce the amount of aptamers that are specific to streptavidin, the magnetic beads, biotin and proteins in general. The biotinylated CD44v6 peptide was then added to the supernatant for 10 min and captured with the beads (**Figure 2**). The beads were washed with increasing stringency with each SELEX cycle. The aptamers were eluted from the magnetic beads using an RNA purification kit (Qiagen) with slight modifications to the manufacturer's protocol. In total, 12 rounds of peptide SELEX were performed.

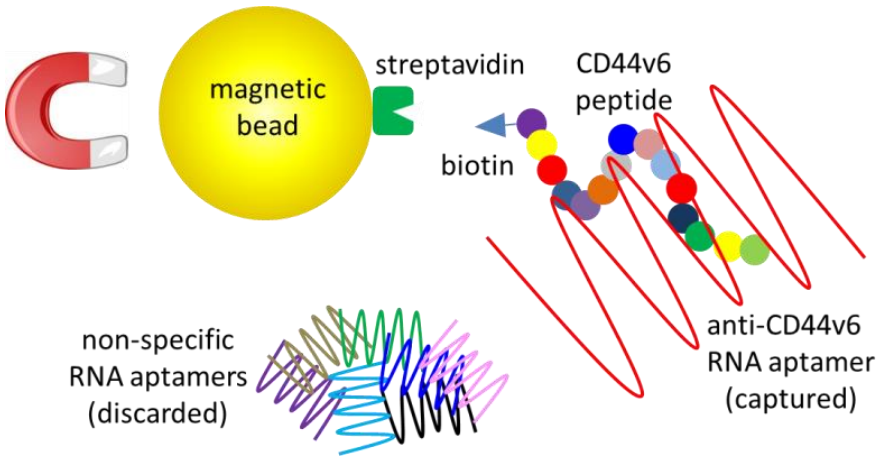

Figure 3. Schematic depicting the positive selection of the peptide SELEX protocol. After the aptamer pool was negatively selected (**Figure 1**), they were incubated with the biotinylated CD44v6 peptide and captured with streptavidin-coated magnetic beads. Increasingly stringent washes were performed to remove non-specific aptamers, and RNA bound to the beads was subsequently purified.

3.8. SELEX using human cells expressing CD44v6

Cell SELEX [165] was also used as an alternative protocol as the cell-based tools were already available. The negative selection involved incubating the polyclonal

aptamers first with MKN74 cells that do not express CD44v6 to deplete aptamers that are specific to the parental cell but not to CD44v6. These cells were centrifuged and discarded. The supernatant containing the depleted aptamers was then incubated with cells that express the variant isoform of CD44 containing exons v3 through v10 (MKN74-CD44v6+). To ensure that only exon v6-specific, and not any of the other exons (v3 through v5 or v7 through v10), aptamers were enriched, the anti-CD44v6 monoclonal antibody (MA54) was used to compete off aptamers that were present on the same epitope of CD44v6 that the mAb recognized. As this mAb has ~1 nM EC_{50} binding (data not shown) to these cells, it was assumed that only aptamers with lower affinity than 1 nM would be displaced by the mAb in equilibrium conditions. The supernatant of mAb-treated MKN74-CD44v6 cells was then used for RNA purification. In total, 7 rounds of cell SELEX were performed.

3.9. Fluorescent labeling of polyclonal RNA aptamers

In order to track the polyclonal RNA aptamers from selected rounds of enrichment, the 5' EndTag Labeling DNA/RNA Kit (Vector Labs) was used according to manufacturer's instructions to fluorescently label the aptamers with Alexa647. Briefly, a thiol group was added to the 5' end of the aptamers with the kit to allow for covalent conjugation to the maleimide group of the Alexa647. Removal of non-conjugated Alexa647 was accomplished by size exclusion chromatography using the BIO SPIN P6 columns according to manufacturer's instructions. The positive conjugation was only inferred since the resultant RNA aptamer product contained a blue color and could be measured by spectrophotometry with the NanoDrop.

3.10. Binding of fluorescent polyclonal RNA aptamers on v6 peptide or cells

To test for enrichment of CD44v6-specificity, fluorescent, polyclonal aptamers from rounds 4, 8, and 12 were subjected to a similar peptide or cell binding procedure as that found during the (+) selection step of the corresponding SELEX (**Figure 1**). Unfortunately, none of the cell SELEX RNA material was tested, and only one replicate was performed throughout due to limited RNA and labeling reagents.

During the peptide binding test, 50 pmoles of each round of aptamers from the peptide SELEX were incubated with either the biotinylated CD44v6-derived peptide or MW standard (negative control) for 1 hr in 300 uL peptide SELEX buffer (see section 3.6).

This was followed by capture with 20 ug of streptavidin-coated magnetic beads for 10 min and 5 rinses before measuring the red channel fluorescence intensity by FACS (FACSCanto II; BD Biosciences).

During the cell binding test, MKN74-CD44v6 or MKN74 (negative control) cells were first non-enzymatically detached from the culture flask, counted, treated with 0.1% sodium azide and 10% FBS and kept on ice. Then, 50 pmoles of each round of aptamers from the peptide SELEX were incubated with 50,000 of either cell line in PBS for 2 hrs. This was followed by two washes with PBS, and fluorescence intensity was measured by FACS.

3.11. Quality control of peptide SELEX protocol with anti-CD44v6 Fab

Based on the peptide SELEX protocol (see section 3.6), 125 nM of the anti-CD44v6 Fab, AbD15179, or a negative control Fab in 300 uL of the peptide SELEX buffer was incubated with 333 nM of the biotinylated v6 peptide for 30 min at RT. The complex was captured with streptavidin-coated magnetic beads for 20 min. The beads were then washed three times and incubated with goat anti-human-HRP at 1:1000 for 30 min with or without 20 min pre-incubation of the beads/peptide/Fab complex in 1% BSA for 20 min. A similar assay was performed, but the peptide was first captured by the beads before incubation with the Fab. In all versions, the beads complex was incubated in 50 uL of TMB for ~15 min, and the reaction was stopped with 50 uL of 2 M sulfuric acid. The absorbance was measured at 450 nm with a microplate reader.

4. Results and discussion

In order to identify novel RNA aptamers to human CD44v6, both peptide and cell SELEX was employed in parallel. A total of twelve rounds of peptide SELEX and seven rounds of cell SELEX were performed. The peptide SELEX strategy was designed to maintain the peptide-aptamer binding in solution conditions as this is usually more optimal during ligand discovery. More rounds of peptide SELEX were performed due to the directed expectation of better success since using this peptide as a selection antigen was essential in identifying an anti-CD44v6 Fab fragment [164]. Emulsion PCR was employed to reduce amplification bias during the dsDNA amplification step [162, 163], and quality controls of the resulting products were performed by gel electrophoresis. If successful,

these aptamers would ultimately be used as ligands to target NPs to CD44v6-expressing cells.

4.1. Quality control of SELEX outputs

Each round of SELEX generated electrophoresis gels at the conversion of amplified dsDNA to RNA aptamers and from the ssDNA, after RNA aptamer enrichment and ssDNA conversion, to dsDNA. These steps were important to control the quality of the resultant products to ensure they were at the correct size. **Figure 3** shows representative examples of gels demonstrating the expected sizes (~100 bp) of the dsDNA (**Figure 3a**) and the RNA aptamers (**Figure 3b**) and no unexpected amplified products. These quality controls (QCs) were performed for every dsDNA and RNA aptamer product for each round of peptide or cell SELEX. During the times where they did not pass QC or quantities were not sufficient, the reaction was repeated, with modifications if necessary, until the expected size or quantity was achieved.

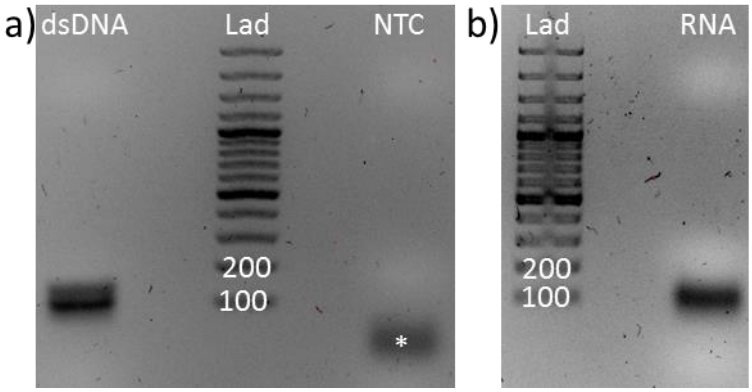

Figure 3. Representative quality control of dsDNA (a) and RNA aptamers (b) by agarose gel electrophoresis. Round 8 from the peptide SELEX is shown to demonstrate that the dsDNA and RNA aptamers (RNA) are migrating at ~100 base pairs (bp), which is at the expected size of 105 bp. Also, only some primer dimer (*) formation for the no template control (NTC) not seen in the dsDNA. Lad = ladder.

4.2. Enrichment of anti-CD44v6 RNA aptamers

Upon completion of the SELEX cycles, enrichment of CD44v6 specificity was attempted by testing for binding of fluorescently-labelled polyclonal aptamers to v6-

expressing cells or the v6 peptide. Positive enrichment would be expected if there was an increase in binding as the round number increased. Since more rounds of peptide SELEX were performed, the focus was on a sampling of those outputs (i.e. rounds 4, 8 and 12).

During the cell binding assay, a very similar protocol to the positive selection step of the cell SELEX was followed except fluorescence intensity of the cell/aptamers complex was measured by FACS (**Figure 4a**). Only a very slight increase in fluorescence was observed on the aptamer-treated MKN74-CD44v6 cells compared to the unstained cells, and the signal did not increase with each higher round number. However, there was higher fluorescence for the MKN74 cells (negative control) than for the positive cells. This suggests that there was no CD44v6 enrichment.

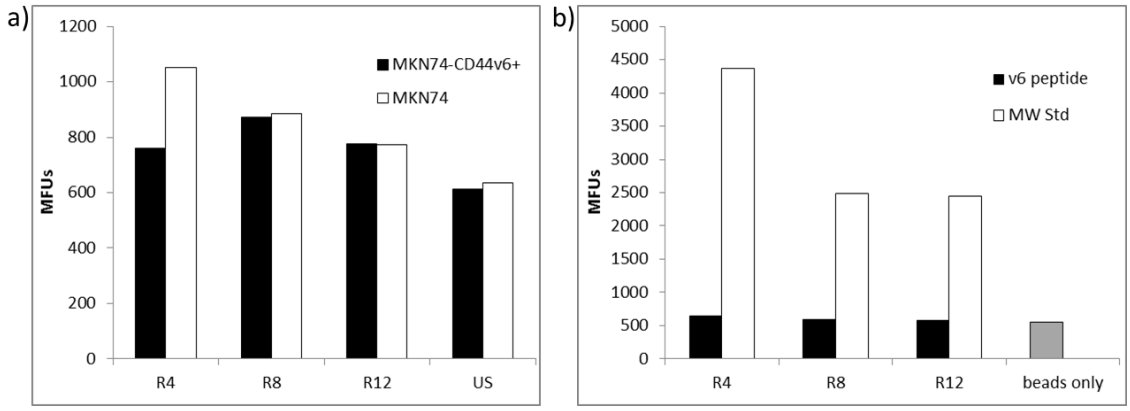

Figure 4. No enrichment of CD44v6-specificity of fluorescent, polyclonal RNA aptamers from rounds 4, 8 and 12 (R4, R8 and R12) of the peptide SELEX outputs on the (a) CD44v6-expressing MKN74 (MKN74-v6) cells or on the (b) CD44v6-derived peptide (v6 peptide). (a) 50 pmoles of Alexa647-labeled aptamers were incubated with either MKN74-v6 or MKN74 cells followed by 2X washes. Unstained cells (US) were used as a baseline of fluorescence. (b) 50 pmoles of Alexa647-labeled aptamers were incubated with either the biotinylated v6-peptide or the negative control, biotinylated MW standard mix (MW Std), and captured with streptavidin-coated, magnetic beads. Fluorescence in both assays was monitored by FACS. MFUs = mean fluorescence units.

During the peptide binding assay, a very similar protocol to the positive selection step of the peptide SELEX (**Figure 2**) was followed except fluorescence intensity of the magnetic bead/v6 peptide/aptamers complex was measured by FACS (**Figure 4b**). No fluorescence was observed in the v6 peptide captured aptamer binding test, suggesting that there was no enrichment. The only fluorescence that was measured was when the aptamers were in the presence of the negative control biotinylated MW standard mix. This

was not expected, but it could be explained that the polyclonal aptamer mix has more places to bind in the many different proteins found in this mixture. If this was true, then the decrease in fluorescence seen with the increase in round number was expected, because this mixture was used as a negative selector to deplete non-specific aptamers. However, this is just speculation.

4.3. Test of peptide SELEX protocol with anti-CD44v6 Fab

After the SELEX procedures and the enrichment were not validated, a quality control test was performed to ensure the robustness of the positive selection step of the peptide SELEX protocol (**Figure 2**). This was accomplished by exploiting a known binder of the CD44v6-derived peptide, an anti-CD44v6 Fab, AbD15179 [40, 164] while using a slightly modified peptide SELEX protocol in an in solution-based ELISA format. To explore the possible issues with, and possible improvements of, the protocol, two variations were investigated: presence/absence of BSA blocking and Fab binding before or after streptavidin-coated magnetic bead capture of the biotinlyated v6 peptide. In order to replicate the initial peptide SELEX protocol, the Fab was tested in equivalent molar amounts as that of the aptamers. The QC assay here that was most similar to the peptide SELEX protocol was the Fab + peptide incubation before capture with the beads without BSA block (**Figure 5a**).

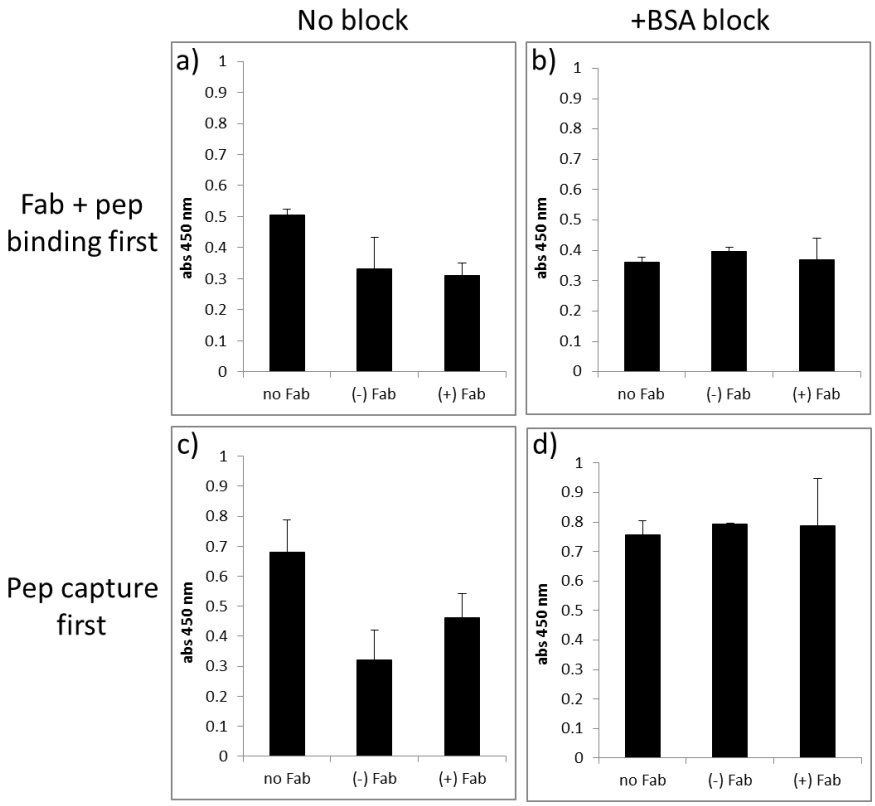

Figure 5. Quality control assay to validate the integrity of the peptide SELEX protocol. An anti-CD44v6 Fab ((+) Fab) vs. a negative control Fab ((-) Fab) was incubated with the biotinylated v6 peptide (pep) either before (a and b) or after (c and d) capture with streptavidin-coated magnetic beads. Fab presence was detected with anti-human-HRP and quantified by measuring absorbance of the TMB substrate. These assays were performed without (a and c) or with (b and d) BSA block before addition of the anti-human-HRP. In all versions, a no Fab control (no Fab) was performed in parallel. Abs 450 nm = absorbance at 450 nm. error bars represent the standard error of n=3 replicates.

No specific binding of the Fab to the v6 peptide, compared to the negative controls, was detected in any of the conditions tested (**Figure 5**). Higher signals were observed in the samples without any Fab (no Fab) present and without BSA block (**Figures 5a** and **5c**). This was probably because of increased non-specific binding of the anti-human-HRP to the beads since they were not previously exposed to any protein (i.e. Fab or BSA). The lack of v6 Fab + peptide specific binding using this protocol suggests that the protocol itself is flawed. Though, it must be noted that even though Fab amounts were similar to those of the aptamers in the SELEX protocol, the assay may have not been sensitive enough to detect the amount of Fab used. Because the Fab can bind to the peptide in a plastic well-based, ELISA format (see Chapter IV) is further evidence that the

peptide SELEX protocol is not a robust method for the discovery of anti-CD44v6 RNA aptamers.

5. Conclusions

In the search for a novel RNA aptamer that targets human CD44v6, two different SELEX methods were attempted. Both strategies were designed to accomplish the same goal but from different approaches. The cell SELEX outputs were not tested for enrichment due to limited time and resources. The focus was placed on the peptide SELEX and the resulting outputs as this was considered the protocol with more likelihood for success based on the selection of the anti-human CD44v6 Fab, AbD15179 [164]. Unfortunately, enrichment of CD44v6 specificity was not observed based on the lack of binding to both CD44v6-expressing cells and to the peptide itself (**Figure 4**). The quality control assay where the positive selection step of the peptide SELEX protocol using AbD15179 (**Figure 5**) highly suggests that the protocol itself is flawed leading to the lack of CD44v6 enrichment. In hindsight, this QC assay should have been performed prior to the laborious and time-consuming 12 rounds of peptide SELEX. Then, the focus could have been on using a plate-based SELEX format which is known to work with AbD15179 (see chapter IV). It is also important to note that just because enrichment for CD44v6 was not measured does not mean that it did not occur. Using high-throughput NGS and bioinformatics techniques may have proven to be a more sensitive method to identify enriched aptamers [138, 139].

CHAPTER IV

Targeting of human CD44v6 with Fab-conjugated, fluorescent nanoparticles

Parts of this chapter were based on the following publications:

- **Kennedy P.J.**, Sousa, F., Ferreira D., Nestor M., Oliveira C., Granja P.L. and Sarmento B. 2018. Targeting of Fab-conjugated PLGA nanoparticles to cancer cells expressing human CD44v6. Under review.

-**Kennedy P.J.**, Pereira I., Ferreira D., Nestor M., Oliveira C., Granja P.L. and Sarmento B. 2018. Impact of surfactants on the target recognition of Fab-conjugated PLGA nanoparticles. *Eur J Pharm. Biopharm.* 127:366-70.

1. Abstract

CD44 isoforms containing exon v6 (CD44v6) have been implicated in many cancer associated processes including metastasis and exosome-mediated pre-metastatic niche formation. It is a receptor for hyaluronic acid (HA) and a co-receptor for HGF and VEGF, together with c-Met and VEGFR-2, respectively. CD44v6 is also expressed in cancer stem cells and (pre-)malignant gastric lesions. Therefore, CD44v6 has potential as a target for early cancer diagnosis and/or for therapeutic intervention. Targeted drug delivery with antibody-decorated nanoparticles (NPs) offers a possible strategy for the treatment and/or diagnosis of metastatic carcinoma. Thus, NPs decorated with an engineered human Fab that specifically target human CD44v6 (v6) were developed and characterized. Initial studies using polystyrene latex microspheres (FluoSpheres®) had many problems with aggregation and demonstrated no specific binding to CD44v6-expressing cells. Though, secondary attempts at developing Fab-decorated, poly(lactic-co-glycolic acid) (PLGA)-based NPs (v6 Fab-PLGA NPs) were successful. The v6 Fab-PLGA NPs displayed spherical morphology around 300 nm and negative charge. They strongly bound to a CD44v6-derived peptide and, more importantly, to cells that endogenously and exogenously express CD44v6, but not to non-expressing cells and cells expressing the standard form of CD44. v6 Fab-PLGA NPs produced in 2% polyvinyl alcohol were unable to bind to the cells, and NPs produced in 2% Pluronic F127 demonstrated the highest binding compared to those produced in sodium cholate or Tween-80. Empty NPs had nominal cytotoxicity at 50 µg/mL. Lastly, v6 Fab-PLGA NPs withstood simulated intestinal fluid exposure and cryopreservation. In conclusion, we envision NPs targeting CD44v6 as potential *in vivo* diagnostic agents and/or as anti-cancer agents in patients previously stratified with $CD44v6^+$ carcinomas.

2. Introduction

Overexpression of alternatively-spliced CD44 containing exon v6 (CD44v6) variants [1, 3] is frequent in carcinomas [5]. Clinical interest of CD44v6 began when studies showed that only metastasizing cell lines from two rat tumor types expressed CD44v6, and a metastatic phenotype from non-metastasizing cells could be gained by overexpressing CD44v6 [4]. These pioneering studies sparked a myriad of subsequent studies devoted to analyzing the role of CD44v6 in cancer biology and as a prognostic biomarker [7]. CD44v6 is a receptor for hyaluronic acid (HA) and is a co-receptor for HGF and VEGF in collaboration with the tyrosine kinases c-Met [10] and VEGFR-2 [12], respectively, both therapeutic targets of clinical relevance [13]. Presentation of the

cytokine HGF by CD44v6 to c-Met activates the Ras/ERK/AKT signaling pathway, thus stimulating cell migration and invasion [10, 15]. Furthermore, in some contexts, Ras signaling promotes CD44v6 splicing, which then leads to more Ras activation, thus resulting in a positive feedback loop stimulating cell cycle progression [16]. CD44v6 is also associated with exosome-mediated, pre-metastatic niche formation [18].

In gastro-intestinal malignancies, CD44v6 is overexpressed in gastric cancer (GC) [19] and colorectal cancer (CRC), particularly in CRC stem cells (CR-CSCs) [21]. Paradoxically, it is overexpressed in pre-malignant gastric lesions as opposed to the normal gastric mucosa [19] and it is associated with chemo-resistance in a model of CD44v6-overexpressing CRC cells treated with common chemotherapeutic agents [166]. Recently, cultured circulating tumor cells (CTCs) derived from stage IV CRC patients were shown to express hallmarks of CR-CSC such as CD44v6 [27]. Gain of CD44v6 is associated with loss of E-cadherin [19, 167] helping to demonstrate its role in the epithelial-to-mesenchymal transition (EMT) [21], an integral process in metastasis [22]. Lastly, CD44v6 has been shown to be a marker of poor prognosis for GC [168, 169] and CRC patients [7, 167, 170]. Thus, CD44v6 holds tremendous promise as an *in vivo* target for therapeutic intervention [32] and/or (early) cancer diagnosis.

Targeted therapy regimens in the oncology clinic are increasingly based on tumor characteristics such as genetic mutations and/or cell surface markers. Antibodies, essential to the vertebrate immune system in pathogen identification and neutralization both outside and inside [77] the cell, dominate targeted therapy due to their exquisite specificity and affinity to countless targets. This is evidenced by the approval of >60 mAbs and >50 more in late-stage clinical trials [171]. Antibodies are quite malleable, often function as fragments, and recombinant antibody production and engineering is now commonplace [144]. More recently, antibodies are being exploited in targeted drug delivery [65] as bioconjugates with small molecule drugs (antibody-drug conjugates (ADCs)), peptides/proteins, other antibodies or nanoparticles (NPs) [172].

Nanotechnology applied to medicine (nanomedicine) promises to greatly impact disease management through pharmacological enhancement mechanisms such as controlled release, a capacity to harbor a plethora of therapeutic/diagnostic payloads, intracellular delivery [173], multi-functionality [174], and responsiveness to environmental stimuli [175]. Importantly, NPs can be engineered to overcome biological barriers [44] such as the mucosa [55], and nanoencapsulation can overcome chemo-resistance [176]. As such, cancer is particularly receptive to nanomedicine [71], and several NPs are already routinely used in the clinic [45]. Classical nanosystems debatably [69] exploit the

enhanced permeation and retention (EPR) effect for “passive targeting” to tumors; however, “active targeting” exploits defined biochemical interactions (e.g. ligand-receptor) for recognizing specific tissues/cells and avoiding healthy tissue [65]. Thus, combining the aforementioned qualities of nanotechnology with antibodies [145, 177] is an extremely viable strategy for targeted drug delivery [172].

Given the clinical relevance of CD44v6 in gastro-intestinal cancers, we set out to develop and characterize NPs with selectivity to human CD44v6 for downstream targeted drug and/or diagnostic delivery. As such, we utilized a well-characterized human Fab fragment specific to human CD44v6, AbD15179 [40, 164], and attempted to tether it to fluorescent NPs. Initial studies with polystyrene latex microspheres failed; however, subsequent studies with poly(lactic-co-glycolic acid) (PLGA) NPs were successful. These NPs were subsequently characterized for their physical parameters, binding to a CD44v6-derived peptide and CD44v6 expressing cells and cytotoxicity. Additionally, the versatility of this nanosystem was explored by investigating their ability to be produced by different formulation methods, withstand simulated intestinal fluid (SIF) exposure and cryopreservation.

3. Materials and methods

3.1. Materials

The RPMI and DMEM cell culture media, penicilin/streptomycin (p/s), geneticin, trypsin/EDTA (T/E), versene, 200 nm green-yellow, amine-modified FluoSpheres®, sulfo-SMCC linker containing 24 polyethylene (PEG) chains (SM(PEG)24), Alexa Fluor 555-labelled, goat anti-human, TMB substrate, Alexa Fluor 546-labelled phalloidin were purchased from ThermoFisher Scientific. The fetal bovine serum (FBS) was from Biochrom. The core PLGA (50:50 LA:GA; 44,000 Da; 5004A) was kindly provided by Corbion. PLGA-FKR648 (20,000-30,000 Da) and PLGA-PEG-Mal (30,000:5000 Da) were from Polyscitech/Akina. The Pluronic F127 (aka Kolliphor Poloxamer 407) was from BASF. The commercially-synthesized CD44v6-derived peptide (biotin-GNRWHEGYRQTKEDS-$CONH_2$) was a kind gift from Dr. Paolo Serafini. The horse radish peroxidase (HRP)-conjugated goat anti-human secondary antibody (anti-human-HRP) was from Bio-Rad. The Amicon centrifuge filters (100 kDa MWCO) was from EMD Millipore. The Mowiol 4-88 mounting media, polyvinylalcohol (PVA), sodium cholate (Na Chol) and Tween-80 was from Sigma. Pancreatin was from Biozym. Most chemicals were from Fisher Chemical or Sigma-Aldrich.

3.2. Cell culture

The MKN74 cell line was derived from a moderately differentiated tubular adenocarcinoma (intestinal-type carcinoma), and the cells were maintained in RPMI supplemented with 10% (v/v) FBS and 0.5 mg/mL geneticin (to maintain selection pressure; see below) and passaged twice per week diluted 1:10-1:20. The GP202 cell line was derived from primary diffuse gastric carcinoma [178], and the cells were maintained in RPMI supplemented with 10% FBS (v/v) and 1% (v/v) p/s twice per week diluted 1:4-1:7. The cells were sub-cultured when ~80% confluency was reached, and they were maintained at 37 °C and 5% CO_2 in a water-saturated atmosphere. CD44v6 expression was occasionally confirmed by FACS with anti-CD44v6 monoclonal antibody (MA54; Life Technologies) staining (data not shown). Mycoplasma detection by PCR was occasionally performed to ensure no contamination, and once during the studies, a short tandem repeat (STR) profile analysis ensured cell line purity. When relevant, the cells were detached with non-enzymatic Versene to maintain the integrity of the surface-bound receptors; however, T/E was used during sub-culture.

3.3. Generation of transfected MKN74 cell lines

The human stomach adenocarcinoma epithelial cell line MKN74 was purchased from the JCRB Cell Bank (Japanese Collection of Research Bioresources Cell Bank). The parental cell line and isogenic variants were kindly provided by C. Oliveira, a co-supervisor of the author. CD44v3-v10 (variant CD44-04 - ENST00000415148) and CD44std (variant CD44-03 - ENST00000263398) cloned in a pCMV6-XL5 and pCMV6-AC backbone respectively, were purchased from OriGene. These variants were subcloned into a pIRES-EGFP2 expression vector. These vectors and the empty version (Mock) were transfected into MKN74 parental cells using Lipofectamine 3000 (Life Technologies) according to manufacturer's instructions. After transfection, Mock, CD44std and CD44v6 expressing cells were selected with geneticin and then sorted by magnetic bead capture using specific anti-CD44v6 (MA54) and anti-CD44std (Cell Signaling) monoclonal antibodies. Transfection and selection efficiency was assessed by immunocytochemistry and flow cytometry (C. Oliveira, unpublished data). For brevity, the MKN74-GFP cells overexpressing CD44v3-v10 are termed "MKN74-CD44v6+", the MKN74-GFP cells expressing the standard form of CD44 are termed "MKN74-CD44std" and the parental

MKN74-GFP cells are termed “MKN74”. It should be noted that the GFP expression of the cells dictated the choice of fluorophore used in cell-based studies.

3.4. EC_{50} binding of re-engineered Fabs to peptide and cells

The human anti-human CD44v6 Fab, AbD15179 [40, 164], was commercially re-engineered (Bio-Rad) to express three cysteine residues near the C-terminus of the Fab to allow for coupling to the maleimide functional groups of the NPs (see below). Henceforth, the re-engineered AbD15179 is termed “v6 Fab”. An irrelevant Fab without specificity to CD44v6 that was identified during the initial monoclonal screening stage and served as a negative control Fab was also re-engineered as above; henceforth, termed “(-) Fab”.

Enzyme-linked immunosorbent assay (ELISA) was performed to determine the binding of the Fabs to a peptide derived from CD44v6. This was the same peptide antigen used in the initial selection and screen [164]. Briefly, 50 µL of 10 µM peptide (~1 µg) diluted in 50 mM bicarbonate/carbonate coating buffer at pH 9.6 (CCB) was added to each well of a 96-well black plate with moderate protein binding capacity for 3 hr. Blocking was achieved with 100 µL of 1% BSA in 1X PBS at pH 7.4 (PBS) for 1 hr. 50 µL of each Fab was serially diluted from 500 nM to 0.02 nM in PBS and incubated with the immobilized and blocked peptide for 3 hr. The Fabs were detected with 50 µL of anti-human-HRP diluted 1:2500 in PBS for 1 hr. 50 µL of TMB substrate was added to the wells, and the reaction was stopped with 50 µL of 2M sulfuric acid. Absorbance at 450 nm was measured with a microplate reader (Synergy Mx; BioTek). Between each of the steps, each well was washed three times with 100 µL of PBS containing 0.1% Tween-20 (PBST). All incubations took place at 37 °C and the reactions were performed in duplicate.

Fluorescence-activated cell sorting (FACS) was performed to determine binding of the Fabs to MKN74 cells with or without overexpression of human CD44v3-v10. Briefly, cultured cells were detached with versene and fixed with PBS supplemented with 10% FBS and 0.1% sodium azide (NaN_3) (FACS buffer) for 1 hr. 10^5 cells were added to a 96-well plate with round-bottom wells (Corning). Pelleted cells were resuspended in 50 µL of each Fab serially diluted from 500 nM to 0.02 nM in FACS buffer for 2 hr. The Fabs were detected with 50 µL of anti-human-Alexa Fluor 555 diluted 1:250 in FACS buffer for 1 hr. Three washes by centrifugation (300xg; 3 mins) of 100 µL of cold FACS buffer occurred between each of the steps, all incubations took place on ice and the reactions were performed with biological duplicates. Fluorescence intensity was measured with the

FACSCanto II flow cytometer (BD Biosciences) using the same voltage settings for all cell lines and between all experiments. The data was analyzed with FlowJo v10 by gating out cellular debris and doublets and determining the geometric mean (mean fluorescence units (MFUs) of the APC signal. Error bars represent the standard deviation of two replicates for both ELISA and FACS.

3.5. Generation of Fab-decorated FluoSpheres®

200 nm green-yellow, amine-modified FluoSpheres® were first treated in a water sonication bath for 30 min prior to downstream preparation. Calculations were based on the number of amine groups per bead (2.4 x 10^6/bead) and the number beads and molecules of SM(PEG)24 linker and Fab in a given concentration of all. No linker and 10^6 SM(PEG)24 linkers/bead were resuspended in PBS containing the experimental amount of FluoSpheres® for one hr. To remove non-associated SM(PEG)24 from the FluoSpheres®, three washes with PBS were performed by centrifugation at 5000xg and removal of supernatant from FluoSphere® pellet. The v6 or (-) Fab was added to the above FluoSpheres® at 10 or 1000 Fab molecules/bead in PBS for 1 hr at RT. To remove non-associated Fab from the FluoSpheres®, three washes with PBS were performed by centrifugation at 5000xg and removal of supernatant from FluoSphere® pellet. The FluoSpheres® were resuspended in PBS and stored at 4°C until further use.

3.6. Generation of PLGA nanoparticles by nanoprecipitation

The base PLGA NPs were generated by nanoprecipitation (modified from [179]) with the following percentages: 80% core PLGA, 10% PLGA-FKR648 and 10% PLGA-PEG-Mal. FKR648, a red channel fluorophore with absorbance at 642 nm and emission at 663 nm, was implemented here so that the GFP from the cells would not interfere with detection of the NP fluorescence. Briefly, 20 mg of total PLGA polymer dissolved in 1 mL acetone were slowly injected (~3-4 mL/min) through a 25g needle into 20 mL 0.5% F127 in ultrapure water while stirring at 300 rpm. The precipitated PLGA was kept stirring for 3-4 hr, and then, the NPs were washed three times with 10 mL ultrapure water using Amicon centrifuge filters (100 kDa MWCO) at 3000xg. The final concentrations before conjugation (see below) equated to ~2 µg/µL of total PLGA and 2.5 µM maleimide. PLGA was stored under argon at -20 °C after usage. During the PTX encapsulation study, 4 mg of Paclitaxel (PTX) was also dissolved in the acetone along with the PLGA components. Downstream assays accounted for the additional mass imparted by the drug.

During the impact of the surfactant on targeting studies, the PLGA NPs were prepared similarly as above. The surfactants were prepared in ultrapure water, and the percentages of PVA, Na Chol and F127 were based on weight:volume while Tween-80 was based on volume:volume. In the initial study, the PLGA NPs were washed three times by centrifugation at 10,000xg for 20 min followed by resuspension in 10 mL ultrapure water. In the follow-up study with different concentrations of F127 and Tween-80, the NPs were washed three times with water using Amicon centrifuge filters (100 kDa MWCO) at 3000xg.

3.7. Generation of PLGA nanoparticles by water-oil-water (w/o/w) double emulsion

PLGA NPs were generated by a modified water-in-oil-in-water (w/o/w) double emulsion technique [180, 181] with the same percentages as for NPs produced by nanoprecipitation. 20 mg of total PLGA were dissolved in 1 mL of dichloromethane (DCM). Then, 80 µL of ultrapure water were added, and the polymeric solution was homogenized for 30 s using a Vibra-Cell™ ultrasonic processor with 70% of amplitude. After this homogenization, 4 mL of 0.5% F127 in water were added into the primary emulsion (w/o) and mixed with similar sonication conditions. Finally, the second emulsion (w/o/w) was added into 7.5 mL of the same surfactant solution. The solvent evaporation and washes of the resultant PLGA NPs were treated similarly as above.

3.8. Fab conjugation to the PLGA nanoparticles

Stock Fabs were diluted to reach a final concentration of 1 µM in 1X PBS pH 7.4. The reducing agent tris(2-carboxyethyl)phosphine (TCEP) was added to the Fabs at a final concentration of 3 µM to allow for mild reduction of the C-terminal cysteines and incubated for 1-2 hours at 4 °C before addition to the NPs. Depending on the experiment, the necessary amount of PLGA was pelleted by centrifugation at 10,000xg for 10 min, and the pellet was resuspended in the 1 µM Fab solution to maintain a PLGA concentration of ~25 µM (1 µg/µL). Initial studies used different molar ratios of Fab to PLGA during conjugation to the base NPs, but the results of this test dictated the use of a molar ratio of 1:25 Fab:PLGA (which equals 1 µg of Fab per 20 µg of PLGA) for all subsequent studies, including the different surfactant study. NPs without Fab conjugation were processed similarly but with buffer only. After overnight incubation at 4 °C, the NPs were washed three times by centrifugation at 10,000xg at 4 °C with 200 µL of ultrapure water. The NPs were then resuspended in water/buffer/media as needed for the subsequent assays. All

NPs were maintained in low light conditions, and each formulation was performed in triplicate. PLGA-FKR648-PEG-Mal NPs were conjugated with the re-engineered, human anti-human CD44v6 Fab are termed “v6 Fab-PLGA NPs“, and those conjugated with the human negative control Fab are termed “(-) Fab-PLGA NPs”. NPs without any Fab conjugation are termed “bare PLGA NPs”.

3.9. Physicochemical characterization of nanoparticles

Size and polydispersity (PdI) were determined by dynamic light scattering (DLS), and charge was determined by laser Doppler anemometry (LDA). Both DLS and LDA were performed with a Zetasizer Nano ZS (Malvern) incorporating the Smoluchowski model, and three measurements were taken for each of the triplicate NP formulations. Around 5 µg of NPs were diluted in 750 µL of 10 mM NaCl pH 7 for each sample yielding count rates around 200 kcps. Data is presented as the average of the triplicate NP formulations including the standard deviation. The association efficiency of PTX within the PLGA NPs was determined by HPLC of the supernatants according to protocol standardized in the Nanomedicines lab [182].

Transmission electron microscopy (TEM) was used to visualize the morphology of the bare and v6 Fab-PLGA NPs. About 0.5 µg of NPs in water were dried onto 200 mesh Formvar Ni-grids without a counterstain. The NPs were observed and imaged at 25,000X and 120,000X magnifications at 80 kV with a JEM 1400 TEM (JEOL). Images were digitally recorded using an 1100W CCD digital camera (Orious).

3.10. Determination of PTX association efficiency

During the toxicity studies (see section 3.15), the supernatant, after the 3 hr acetone evaporation and first centrifugation steps, was retained to monitor the efficiency of the encapsulation of PTX within the PLGA NPs. High pressure liquid chromatography (HPLC) was used to quantify the amount of PTX in the supernatant. A standard curve of known PTX concentrations was also run in parallel. The amount of PTX measured in the supernatant thus indirectly reflected the amount of associated PTX within the PLGA NPs.

3.11. Determination of Fab association efficiency to the PLGA NPs

ELISA was used to monitor the amount of Fab present on the PLGA NPs during the surfactant studies. The overall protocol is similar to that found in the EC_{50} binding of the Fabs only to the CD44v6-derived peptide (see section 3.4). Briefly, 10 µg of Fab-decorated NPs in 50 µL CCB were adsorbed to the 96-well plate well in duplicate, blocked with 1% BSA and detected with anti-human-HRP at 1:5000 with 3X washes of PBST between each step.

3.12. Binding of PLGA NPs to the CD44v6-derived peptide

ELISA was used to measure the binding of 10 µg of the v6 Fab-PLGA NPs to the CD44v6 peptide following a similar protocol as for the EC_{50} binding (see section 3.4).

3.13. Binding of nanoparticles to the surface of cells expressing CD44v6

The protocol and downstream data manipulation was similar to that used during the EC_{50} binding of the free Fab (see section 3.4). Though, NP presence was determined by measuring the intensity of the red channel fluorophore FKR648; thus, forgoing the need for the anti-human secondary. Depending on the experiment, a defined quantity of NPs was incubated with 10^5 NaN_3-fixed and FBS-blocked cells for ~2 hrs followed by 3X washes with 100 µL PBS. During Fab competition study, the cells were incubated with 50 µL of 250 nM v6 or (-) Fab for 1 hr, without subsequent cell washing, prior to addition of the 10 µg v6 Fab-PLGA NPs. During protein corona study, the NPs were incubated with 10% (v/v) FBS for 4 hr, without subsequent NP washing, prior to addition to the cells. Binding studies of w/o/w double emulsion, SIF-treated and freeze-dried NPs were performed with ~10 µg v6 Fab-PLGA NPs on MKN74-CD44v6+ and MKN74 cells as above (see section 3.4).

3.14. Binding of nanoparticles to live cells

MKN74-CD44v6+ and MKN74 were seeded at 20,000 cells/well in 24-well plates and cultured for 3 days, giving ~70% confluency, prior to addition of the NPs. 10 µg of NPs was added to each well of cells in RPMI without the FBS and P/S supplements for 6 hr. The cells were carefully washed 3X with 250 µL PBS.

For the microscopy assay, the cells, plated on glass cover slips, were fixed in 4% paraformaldehyde for 20 min at RT and rinsed 3X with PBS. The cells were then permeabilized with 0.2% Triton-X100 for 7 min at RT and rinsed 3X with PBS. The cells were blocked in 10% FBS in PBS containing 0.1% Tween-20 (PBST) for 30 min at RT. The solution was then replaced with 300 µL PBST + 5% FBS containing 0.3 units of Alexa Fluor 546 labelled-phalloidin and incubated for 4 hrs at RT. The cells were rinsed 3X in PBS and mounted on glass microscope slides with mounting media and dried overnight at RT in the dark. The stained and fixed cells were observed and imaged with an SP5 confocal microscope (Leica) using the appropriate laser and filter combinations. Image analysis was performed with the LAS AF Lite software (Leica). The 20X magnification images are shown as maximum projections of 13-15 Z-stacks with a distance of 2 µm between them. The 63X magnification image of the MKN74-CD44v6+ cells incubated with v6 Fab-PLGA NPs was taken with 16 Z-stacks with 0.29 µm distance between them. One image is shown as a maximal projection of the Z-stack, and the other is shown as an interior Z-stack with the Z-dimension displayed to the right and below.

For the FACS assay, the cells were detached with T/E, pelleted by centrifugation and washed once more with PBS before FACS measurement.

3.15. Cytotoxicity of PLGA NPs

MKN74-GFP/CD44v6+ and GP202 cells were seeded at 4,000 and 10,000 cells/well in 96-well plates, respectively, and cultured for 2 days, giving ~50% confluency, prior to the addition of the NPs. The culture media for all cell lines was replaced with 80 µL of fresh media (containing 10% FBS) followed by the addition of 20 µL of media containing 5 µg of freshly-prepared NPs were added to each well of cells in media. Duplicates of each of the formulation triplicates were tested. Three plates were loaded equally reflecting the three time points. Two were incubated for 6 hrs and replaced with 200 µL fresh media after being rinsed 2X with 100 µL PBS, one plate for 24 hrs and another for 48 hrs total. The third plate was cultured with the NPs for 24 hrs and then rinsed 3X with 100 µL PBS. At the end of each time point, the media or PBS was replaced with 100 µL of media containing 0.5 mg/mL of the 3-(4,5-dimethylthiazol-2-yl)-2,5-diphenyltetrazolium bromide (MTT) solution and incubated for 4 h. Two assay replicates were performed for each of the three formulation replicates. Free PTX was dissolved in DMSO before addition to the media at 10, 1 and 0.1 µg/mL. The PTX levels of free PTX at 10 and 1 µg/mL correspond to similar levels of PTX at 50 and 5 µg/mL for the NPs based on production design. In all plates, six wells each were devoted to 1% Triton-X-treated cells (“background”) or media

only (“untreated”). All culture conditions were maintained as above. The reaction was terminated by replacement of the MTT solution with 100 µL dimethyl sulfoxide. After 15-20 mins, reduced MTT levels were measured with a microtiter plate reader (Biotek Synergy Mx) at 590 nm and 630 nm absorbance (abs). During the calculations, the 630 nm abs was subtracted from the 590 abs, and the % of MTT reduction was calculated from this subtracted value (Equation (1)).

Equation (1) $$MTT\ reduction\ (\%) = \frac{Experimental\ value - background}{untreated - background} \times 100$$

3.16. Simulated intestinal fluid treatment of v6 Fab-PLGA NPs

The simulated intestinal fluid (SIF) was composed of 50 mM KH_2PO_4 and 15 mM NaOH and brought to a pH of 6.8. Pancreatin was added to the buffer at a concentration of 1% (w/v) and mixed for 1 hr. The mixture was then centrifuged at 10,000xg for 10 min. The supernatant was removed and used fresh. It should be noted that much of the pancreatin powder did not go into solution; therefore, the true concentration was unknown. 10 µg of NPs (n=3 formulation replicates) were added to 200 µL of SIF with or without pancreatin for 15 or 60 min at 37 °C. The NPs were then centrifuged and washed 1X with 200 µL PBS followed by resuspension in 50 µL PBS for an immediate cell binding assay (see above). Control NPs were treated with PBS pH 7.4 for 60 min.

3.17. Cryopreservation of v6 Fab-PLGA NPs

A modified cryopreservation protocol based on [183] was used to assess the storage capabilities of the NPs. Freshly-prepared v6 Fab-PLGA NPs were resuspended in 1 mL of 10% (w/v) trehalose in water. NPs resuspended in 1 mL of water were used as a negative control. All formulations were frozen at -80 °C in lobind tubes with perforated caps for 6h and then transferred to a FreeZone lyophilizer (LabConco) set to 0.008 mbar for 24h. NP replicates were either stored in the dark at RT, 4 °C, or -20 °C for two weeks (n=3 for each temperature). The NPs were then resuspended in 1 mL of water for ~1 hr and pelleted by centrifugation at 10,000xg for 15 min. The supernatant was removed, and the NP pellet was resuspended in PBS and maintained on ice for 1-2 hrs before cell binding studies.

3.18. Statistics

GraphPad Prism 6 analysis was used to analyze the significance levels (ANOVA with Dunnet's test) and determine the EC_{50} value. The results represent the mean value with a standard deviation of three replicates.

4. Results and discussion

The general objective of the overall study was to develop and characterize NPs that specifically target cells (over)expressing CD44v6 for the purpose of oncological drug and/or diagnostic delivery. Amine-modified, polystyrene latex microspheres at 200 nm with yellow/green fluorescence (FluoSpheres®) were initially tested as, in principle, they could allow for the directed conjugation of the re-engineered, anti-human CD44v6 Fab using a maleimide-based linker. Additionally, the initial idea was to produce and functionalize chitosan-based NPs, which harbor amine functional groups, and thus, the FluoSpheres® acted as a fluorescent surrogate for proof-of-principle studies. The decision to work with PLGA instead of chitosan was based on the current focus of the Nanomedicines group and the easier production and modification possibilities. For instance, amine- or maleimide-modified PLGA as well as PLGA-conjugated to a fluorophore could be incorporated.

4.1. General nanoparticle design ensures PEGylation and optimal Fab orientation

Antibody recognition of its cognate antigen (e.g. CD44v6) occurs via the antigen-binding, variable regions of the heavy and light chains (see section 3.1, Chapter III) [144]. The commonly-used conjugation methods based on EDC/NHS rely on the amine group of one binding partner to be coupled to the carboxyl group of the binding partner. When conjugating amine-modified NPs with an antibody, this means that all the available carboxyl groups of the antibody (i.e. C-terminus, aspartic acid and glutamic acid) are subject to conjugation to the NP. This results in a randomly-directed conjugation such that the antigen-binding domain of the antibody may or may not be available for antigen recognition, and, ultimately, may reduce binding specificity, affinity and/or avidity.

Conjugating the antibody such that the antigen-binding domain of every molecule is oriented for proper antigen recognition is ideal. Because AbD15179 is a recombinant protein, it was re-engineered to express three C-terminal cysteines to be able to exploit the thiol-Michael addition click reaction based on conjugation to a maleimide functional

group [184]. The thiol group from the cysteines reacts to the activated ester group of the maleimide to form a covalent bond. In this study, the initial plan was designed to use a sulfo-SMCC linker containing 24 polyethylene glycol chains (SM(PEG)24) to bridge the amine functional groups of the NPs to make a maleimide available for conjugation to the thiols of the C-terminal cysteines of the Fab (**Figure 1**). PLGA-based NPs were also attempted by just incorporating PLGA-PEG-maleimide to avoid the need for the linker (see below)

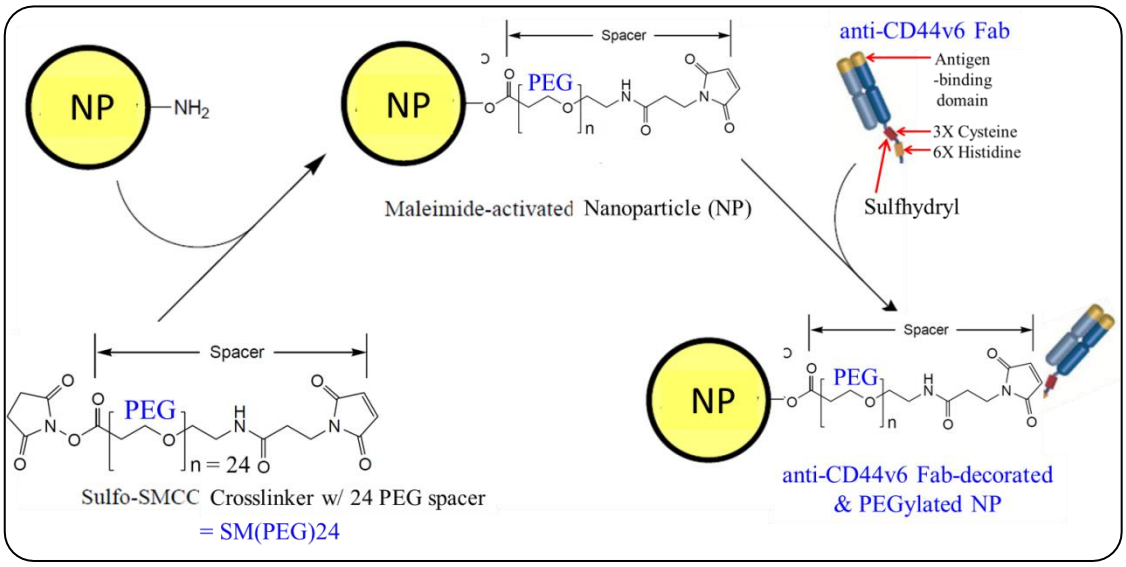

Figure 1. Schematic depicting the conjugation of the re-engineered AbD15179 (anti-CD44v6 Fab) to the nanoparticles (NPs). Briefly, the NHS ester of the SM(PEG)24 linker reacts with the amine group of the NPs, and the maleimide of the linker reacts with the thiols of the C-terminal cysteines of the Fab to form the covalent bridge between the two. This ensures that the NPs are PEGylated and all the conjugated Fabs have their antigen-binding domain available for CD44v6 recognition. Adapted from ThermoFisher Scientific.

4.2. Re-engineered AbD15179 maintains its binding affinity for human CD44v6

AbD15179 is a human Fab antibody fragment from the HuCAL® PLATINUM library [39] that was selected and screened for binding to human CD44v6 for radio-immunodiagnostics of head-and-neck squamous cell carcinoma (HNSCC) [40, 164]. AbD15179 was previously shown to have K_D values (affinity) ranging from ~6-70 nM on proteins derived from CD44v6 and ~2-10 nM on CD44v6-expressing cells as determined by surface plasmon resonance (SPR) and LigandTracer Grey, respectively [164].

Importantly, radiolabelled AbD15179 also demonstrated moderate overall tumor-to-organ specificity in mouse xenograft models [40]. Due to its specificity to CD44v6, human origin and engineering malleability, AbD15179 was exploited as a targeting ligand for drug/diagnostic delivery mediated by PLGA NPs.

In order to ensure gastro-intestinal CD44v6-expressing cell specificity, we used a gastric cancer cell model system based on cells with forced overexpression of CD44v6, previously developed by the group. MKN74 cells are a good model for these studies as the parental cells are naturally devoid of any CD44 expression due to hypermethylation of the promoter [185], and therefore constitute the ideal cell line for overexpression studies. We then used MKN74 cells with forced CD44v6 expression (MKN74-CD44v6+) as the testing model, that were properly controlled with MKN74 cells expressing the empty vector (MKN74) or the standard version of CD44 (MKN74-CD44std), which is a ubiquitously expressed isoform. Furthermore, we used another cell line that endogenously express CD44v6 as well as other CD44 alternative splicing isoforms (GP202), to monitor specificity in a naturally occurring context.

Because ligand orientation impacts the targeting capability of ligand-decorated NPs [172], we had AbD15179 commercially re-engineered to express C-terminal cysteines to allow for ligand conjugation to the NPs via thiol-maleimide based chemistry (more below). We first aimed to ensure that the re-engineering of AbD15179 did not alter its affinity to the CD44v6-derived peptide and CD44v6-expressing cells. Additionally, we needed to ensure that the transfected MKN74 cell-based system could robustly monitor binding of the Fab and Fab-decorated NPs. To do so, we serially diluted the v6 Fab and monitored the binding response to the peptide and to our cell lines by ELISA and FACS, respectively. Importantly, we utilized a negative control Fab ((-) Fab) to ensure that any downstream NP binding is due to CD44v6 specificity and not from the mere presence of a conjugated protein.

The approximate half maximal effective concentration (EC_{50}) of the v6 Fab to the peptide was ~90 nM, and the (-) Fab had nominal binding (**Figure 2a**). The EC_{50} of the v6 Fab to the MKN74-CD44v6+ cells was ~25 nM and ~10 nM to GP202 (**Figure 2b**). As expected, there was nominal binding of the v6 Fab to the parental MKN74 cells at the highest concentration, and the (-) Fab at 500 nM had nominal binding to all three cell lines (**Figure 2c**). The higher overall fluorescence of the v6 Fab on MKN74-CD44v6+ compared to GP202 was expected. Because the original AbD15179 had K_D values ~5-70 nM [164] depending on the biochemical or cellular presentation of CD44v6, the data here confirms that the re-engineering of the Fab had nominal impact on the antigen-binding

specificity and affinity. Additionally, the cell binding assay demonstrated that the MKN74 cell-based system is robust; thus, validating its utility for the NP binding assays.

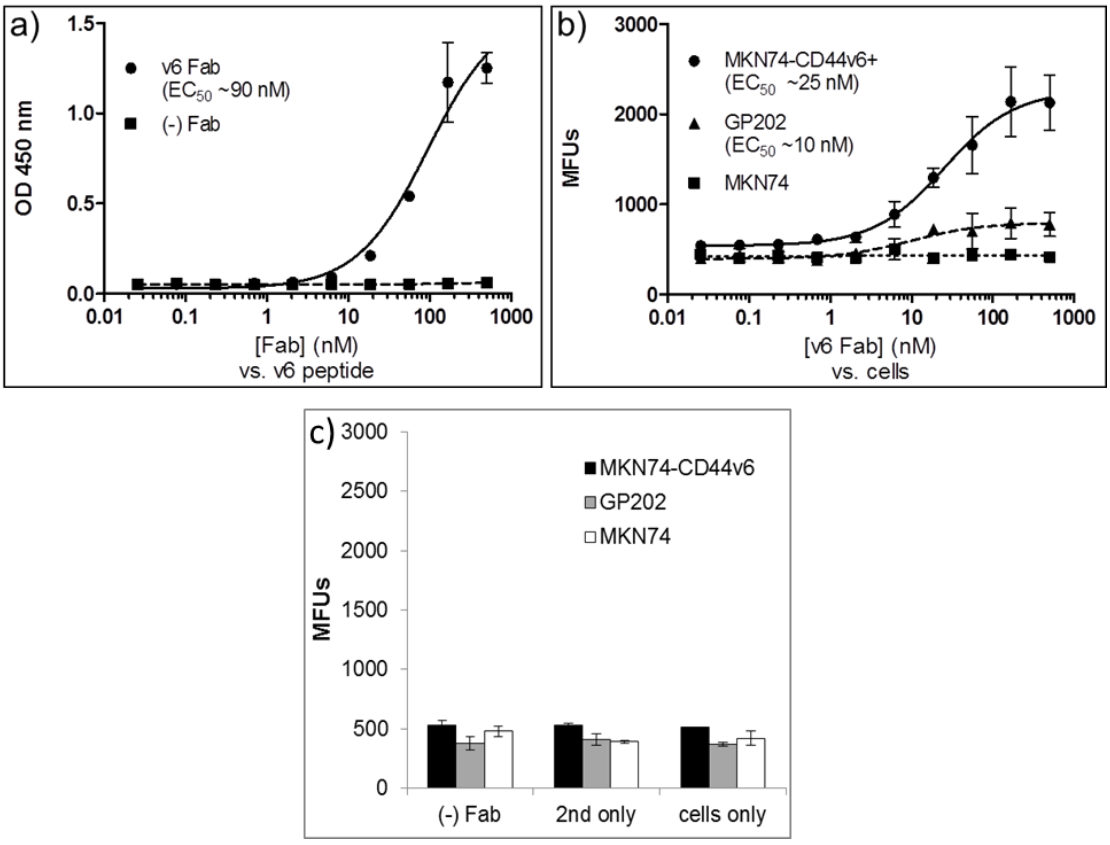

Figure 2. Approximate EC_{50} binding of the v6 Fab to a CD44v6-derived peptide (a) and cells (b). a) ELISA was used to determine the approximate EC_{50} binding of serially-diluted free (-) Fab and v6 Fab (highest Fab concentration = 500 nM) to a CD44v6-derived peptide [164]. FACS was used to determine the EC_{50} binding of serially-diluted v6 Fab to MKN74-CD44v6+, GP202 and MKN74. c) Negative controls of the cell binding assays with the three same cell lines as b) were similarly used to assess the binding profile of the negative control Fab at 500 nM ((-) Fab), anti-human-AlexaFluor555 secondary (2nd only) and unstained cells (cells only). n=2 biochemical/biological replicates. Error bars represent the standard deviation. OD 450 nm = optical density at 450 nm. MFUs = mean fluorescence units.

4.3. Manipulation of FluoSpheres® leads to extensive aggregation

Several attempts were made to conjugate the v6 Fab to the FluoSpheres® following the design outlined in **Figure 1**. The protocol detailed in section 3.5 required the

use of centrifugation to wash the FluoSpheres® in order to remove the unconjugated SM(PEG)24 linker and v6 Fab. The resulting preparations had very high Z-averages (size) and PdIs as well as negative zeta-potentials (**Table 1**). This was even seen in the negative control preparations where no linker and Fab were included. The high Z-averages and PdIs indicate that the FluoSpheres® had extensive aggregation because an individual FluoSphere® itself has no possibility of increasing its 200 nm size. The slightly negative zeta-potential of the non-functionalized FluoSpheres® was also unexpected because they are modified with positively-charged amine groups. During commercial production, the FluoSpheres® begin as being carboxylated and are later amine-modified. Thus, a possible reason for the change in the charge is due to removal of some or all of the amine groups during the washing steps.

Table 1. Physicochemical properties of experimental FluoSpheres®. Attempts were made to conjugate the v6 Fab to the FluoSpheres® with the SM(PEG)24 crosslinker. Parallel studies eliminated the crosslinker to see the effect of Fab adsorption to the FluoSpheres®. FluoSpheres® only were straight from the stock without manipulation/washing. Z-average (size), polydispersity index (PdI) and zeta potential of the different FluoSphere® preparations. 10:1 and 1000:1 = # of Fab molecules per # of FluoSpheres®. (-) Fab = negative control Fab. v6 Fab = re-engineered AbD15179. ± represents the standard deviation of n=3 assay replicates.

Crosslinker	Ligand	Z-average (size, nm)	Polydispersity Index (PdI)	Zeta potential (charge, mV)
SM(PEG)24	1000:1 v6 Fab	1157 ± 60	0.35 ± 0.01	-13.1 ± 1.1
	1000:1 (-) Fab	1527 ± 98	0.41 ± 0.05	-14.7 ± 0.8
	10:1 v6 Fab	1266 ± 163	0.38 ± 0.05	-14.7 ± 1.2
	10:1 (-) Fab	1527 ± 36	0.40 ± 0.02	-15.0 ± 0.7
	No Fab	1232 ± 47	0.37 ± 0.04	-3.0 ± 1.0
no crosslinker	1000:1 v6 Fab	1489 ± 135	0.43 ± 0.06	-14.0 ± 1.7
	1000:1 (-) Fab	1952 ± 123	0.80 ± 0.12	-16.7 ± 3.2
	10:1 v6 Fab	772 ± 62	0.50 ± 0.07	-16.4 ± 0.7
	10:1 (-) Fab	2921 ± 581	0.89 ± 0.19	-12.1 ± 3.1
	No Fab	1700 ± 232	0.90 ± 0.16	-12.3 ± 1.9
	FluoSpheres® only	733 ± 80	0.25 ± 0.01	8.1 ± 1.4

Even though the physicochemical data was disappointing, tests for specific binding to the experimental cells were still attempted. FACS demonstrated very high fluorescence values for the FluoSpheres® with the linker, but low values above background in the absence of the linker (**Figure 3**). A slight increase in binding was seen with FluoSpheres® that had 1000 molecules of adsorbed v6 Fab per FluoSphere® compared to controls. The extensive aggregation and near lack of CD44v6-specificity with the FluoSpheres® prompted the cessation of working with the FluoSpheres®, and the studies with the PLGA were initiated.

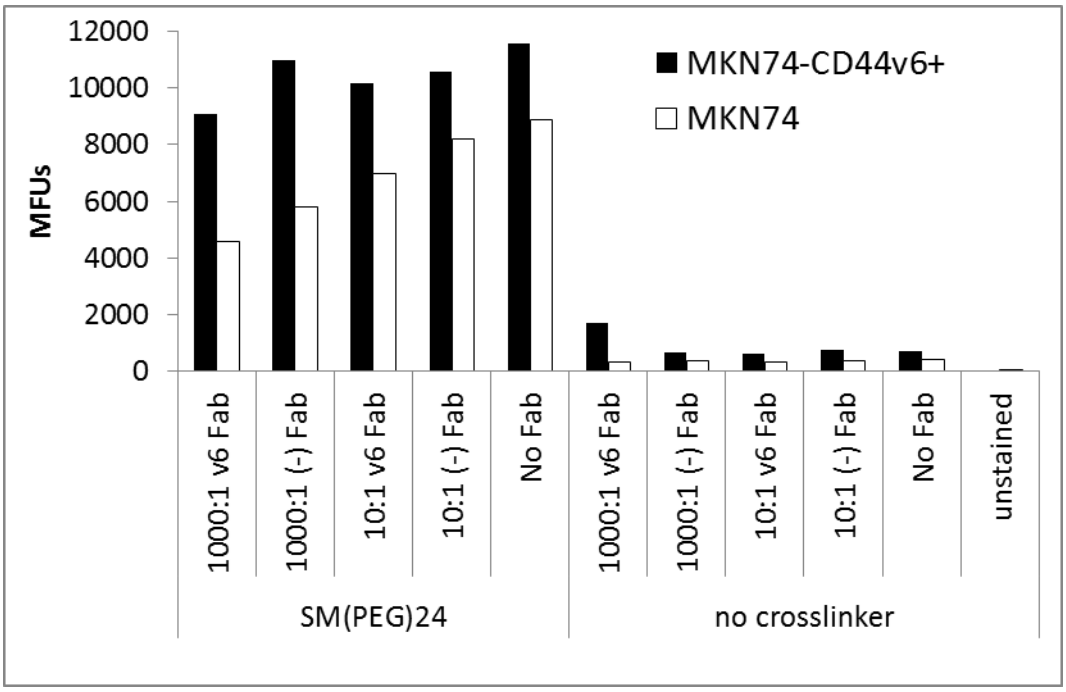

Figure 3. FluoSpheres® with or without the SM(PEG)24 crosslinker and with or without the v6 or (-) Fab were tested for binding to MKN74 cells expressing CD44v6 or not as measured by FACS. 10:1 and 1000:1 = # of Fab molecules per # of FluoSpheres®. No replicates were performed. MFUs = mean fluorescence units.

4.4. CD44v6-targeted PLGA NP design

PLGA was used as the primary material for this study due to its favorable qualities in drug delivery [186, 187] such as biodegradability, biocompatibility, tunable sustained drug release, capacity to harbor a plethora of drug types from small molecules to (large) proteins [180, 183] and nucleic acids [181], the ability to protect the drug from degradation, malleable surface properties for further functionalization (e.g. tethering of targeting ligands) and FDA/EMA approval. FKR648, a fluorophore in the red spectrum, was chosen because the GFP expression of the cells would not interfere with NP detection. PEG was incorporated in the formulation to potentially serve as a stealth agent and/or for mucus penetration in potential *in vivo* characterization [188]. 5000 MW PEG was specifically chosen as it was shown to have maximal reduction in protein corona formation in PLA NPs [189]. The maleimide served as the functional group for covalent Fab conjugation via a thiol-Michael addition reaction [184]. Importantly, conjugating the C-terminus of the Fab to the surface of the NPs via the maleimide helped to ensure that the Fab was oriented such that the N-terminal, antigen-binding domain was available for receptor (i.e. CD44v6) binding (**Figure 4**) [172].

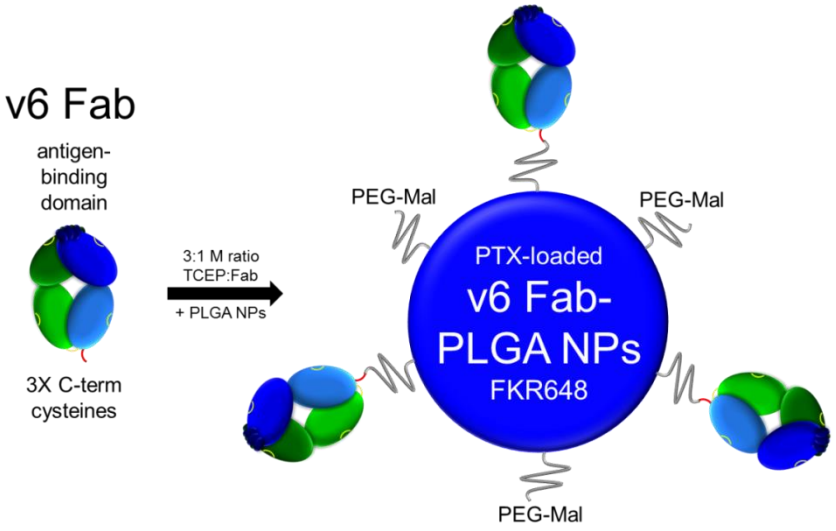

Figure 4. Schematic of v6 Fab-PLGA nanoparticle (NP) design. AbD15179 was re-engineered to express three C-terminal cysteines (v6 Fab). The PLGA NPs were composed of 80% core PLGA, 10% PLGA-FKR648 and 10% PLGA-PEG-Maleimide and nanoprecipitated in 0.5% Pluronic F127 with or without paclitaxel loading (PTX). The v6 Fab was mildly reduced with TCEP and added to the washed PLGA NPs to ultimately produce PLGA-based NPs that were fluorescent, PEGylated and decorated with a human Fab for targeting human CD44v6.

The NPs in this study were produced with the following components and percentages: 80% PLGA (50:50 LA:GA), 10% PLGA-FKR648 and 10% PLGA-PEG-Maleimide. Nanoprecipitation, the primary method for encapsulation of hydrophobic drugs (e.g. PTX), was used for NP construction for its robust and facile protocol. Pluronic F127 was chosen because this surfactant is cytocompatible, and drug-loaded, F127-coated PLGA NPs have higher cancer cell uptake and cell-killing ability and are able to overcome drug resistance [190]. Additional studies incorporated PTX during the production protocol as this served as a model drug and one that is prone to chemoresistance [176]. With the design of the NPs in place, it was then possible to proceed to the physical and biological characterization of the v6 Fab-PLGA NPs.

4.5. Physicochemical properties of v6 Fab-PLGA NPs

The physicochemical qualities of nanoparticles help to predict their *in vivo* behavior. The Z-average (hydrodynamic radius or size) of the PLGA NPs was measured at ~200-400 nm with a polydispersity index (PdI) ~0.2-0.4 and an overall negative zeta-potential (charge) (**Table 2**), as measured by DLS and LDA. As expected, due to its hydrophobic character, the association efficiency of PTX was close to 100% [191]. The v6 Fab-decorated NPs displayed an increase in Z-average and decrease in charge, helping to confirm the presence of the Fab on the NPs. Though, the much larger increase in Z-average for the v6 Fab-PLGA NPs was not expected just based on the presence of the Fab; therefore, the increase may be due to some aggregation even though an additional peak was not observed in the DLS profile (data not shown). TEM imaging confirmed the characteristic spherical morphology of PLGA-based NPs with sizes in the range of 100-300 nm (**Figure 5**). These data are in agreement with the DLS data as well as previous studies from our group [180].

Table 2. Physical characterization of the PLGA NPs. Z-average (size), polydispersity index (PdI) and Zeta-potential (charge) of the Fab-decorated and bare PLGA NPs from nanoprecipitation, with or without Paclitaxel (PTX) encapsulation, as measured by DLS and LDA. n=3 formulation replicates and ± = standard deviation.

NPs	PTX	Z-average (size, nm)	Polydispersity Index (PdI)	Zeta Potential (charge, mV)	Association Efficiency (%)
v6 Fab-PLGA	-	379 ± 48	0.40 ± 0.05	-19.9 ± 0.4	-
	+	293 ± 15	0.32 ± 0.04	-20.0 ± 0.4	100 ± 1
(-) Fab-PLGA	-	234 ± 27	0.21 ± 0.04	-18.2 ± 2.0	-
	+	234 ± 34	0.22 ± 0.06	-19.6 ± 0.1	100 ± 1
bare PLGA	-	205 ± 6	0.16 ± 0.01	-15.6 ± 0.8	-
	+	217 ± 10	0.24 ± 0.03	-17.4 ± 0.1	100 ± 1

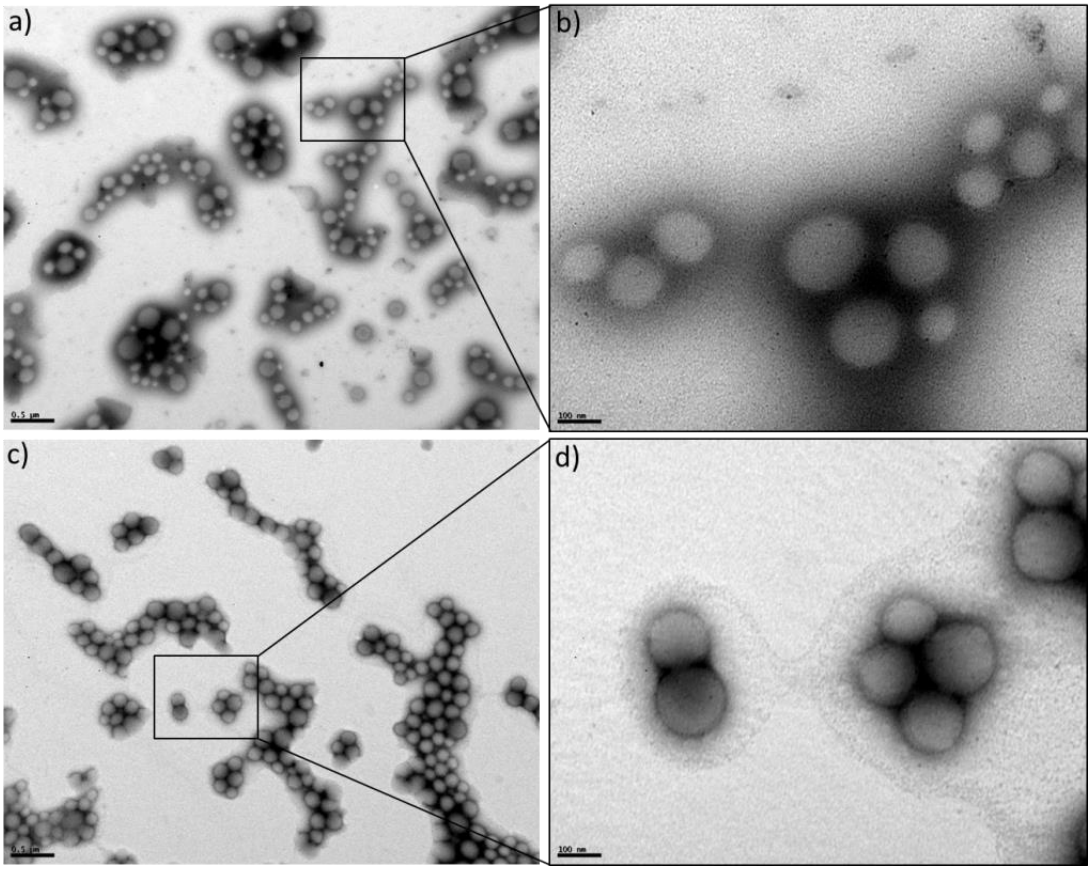

Figure 5. TEM images of the v6 Fab- (a and b) and bare (c and d) PLGA NPs. a and c = 25,000X magnification (scale bar = 0.5 µm). b and d = 120,000X magnification (scale bar = 100 nm). The boxes in each of the 25,000X magnification correspond to the 120,000X magnification for each NP preparation.

4.6. v6 Fab-PLGA NPs specifically bind to a human CD44v6-derived peptide and to the surface of cells expressing CD44v6

After determining that the v6 Fab-PLGA NPs displayed favorable physicochemical qualities, it was then necessary to investigate their specific binding to CD44v6 presented as a biochemical and on the surface of gastric/intestinal cancer cells. **Figure 6** shows the various experiments implemented during the optimization phase of NP construction and specific binding to CD44v6. The main cell-based readout was NP binding to NaN_3-fixed MKN74 cells expressing human CD44v6 as monitored by FACS. The use of NaN_3 fixation and low temperature helped minimize surface receptor recycling. Also, special care was taken to ensure that the proper negative controls (i.e. (-) Fab-PLGA NPs and non-expressing cell lines) were implemented.

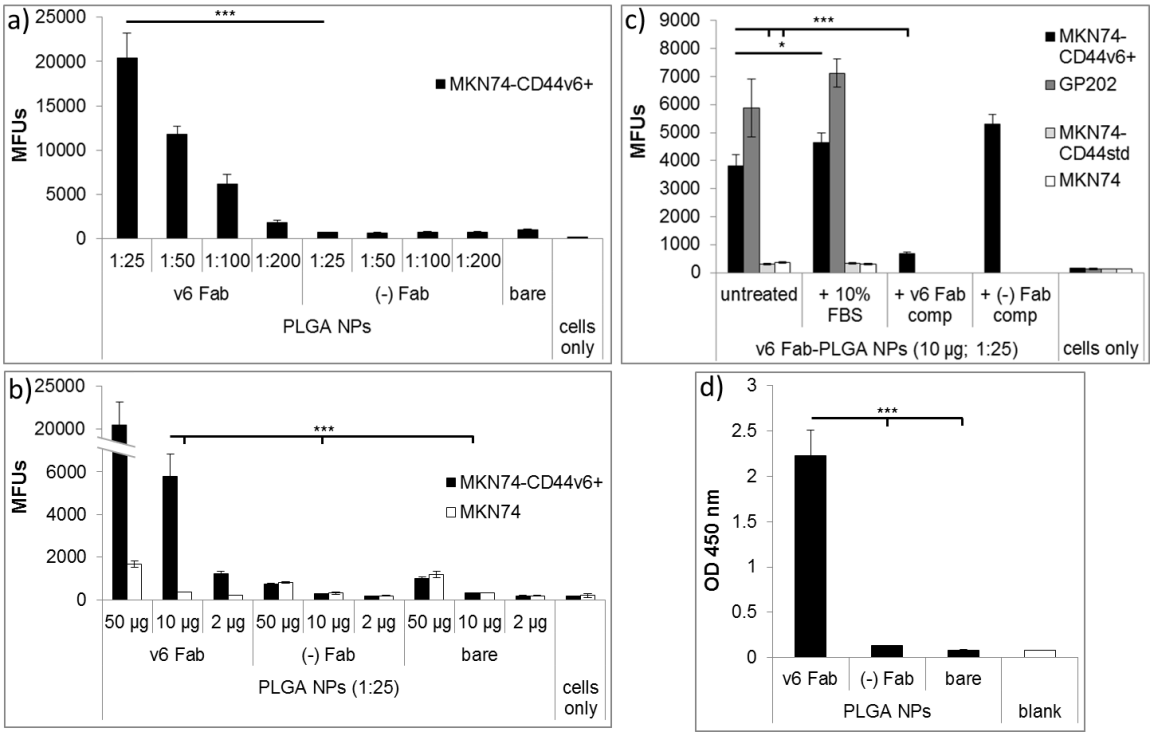

Figure 6. Binding of v6 Fab-PLGA NP to CD44v6 presented on the surface of a cell (a-c) or as a peptide (d) by FACS and ELISA, respectively. a) 50 µg of Fab-decorated NPs were developed with different molar ratios of Fab:PLGA during conjugations and tested for binding to 10^5 fixed MKN74-CD44v6+ cells. b) 50, 10 and 2 µg of NPs at 1:25 Fab:PLGA ratio were tested for CD44v6+ cell binding. Non-expressing cells (MKN74) were used as a dosing control. c) 10 µg of the v6 Fab-PLGA NPs at 1:25 were pre-incubated with 10% v/v FBS. In parallel, the MKN74-CD44v6+ cells were pre-treated with free v6 Fab or the (-) Fab at 250 nM before incubation of the v6 Fab-PLGA NPs. d) 50 µg of Fab-decorated or bare PLGA-FKR648-PEG-Mal NPs were incubated in 96-well plates containing adsorbed CD44v6-derived peptide and detected with anti-human-HRP. n=3 replicates. Error bars represent the standard deviation. OD 450 nm = optical density at 450 nm. MFUs = mean fluorescence units. ns = P-value >0.05. * = P-value ≤0.05. *** = P-value ≤0.001.

During the initial optimization phase, different molar ratios of Fab:PLGA during Fab conjugation were investigated. 50 µg of v6 Fab-PLGA NPs with the highest amount of Fab:PLGA (1:25) had the strongest binding to CD44v6+ MKN74 cells, and decreasing the amount of Fab to PLGA resulted in reduced binding (**Figure 6a**). This suggests that a "crowding effect" from steric hindrance caused by too many tethered ligands was not reached. It must be noted that significant efforts during the optimization stages to

demonstrate CD44v6+ cell-specific binding with v6 Fab-PLGA NPs produced with polyvinyl alcohol (PVA) as the surfactant were unsuccessful, thus prompting the utilization of F127 (**Figure 7**).

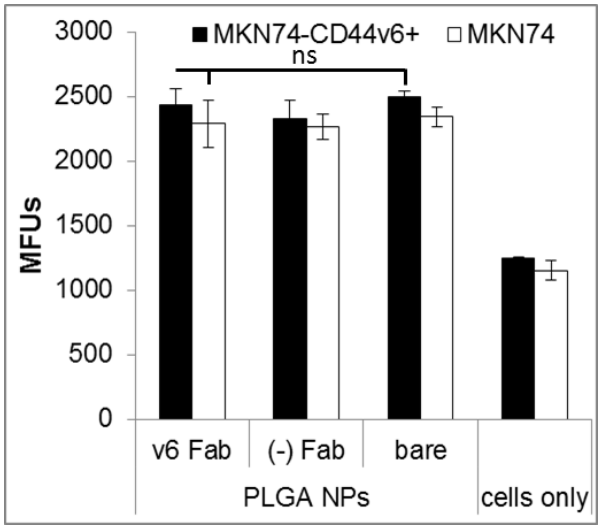

Figure 7. v6 Fab-PLGA NPs produced by nanoprecipitation into polyvinyl alcohol (PVA) do not specifically bind to MKN74-CD44v6+ cells. PLGA NPs were injected into 2% PVA, instead of 0.5% F127, during NP production. Subsequent washes and Fab conjugation methods were identical to those in the rest of this study. The PLGA NPs were then monitored for cell binding by FACS. n=3 formulation replicates. Error bars represent the standard deviation. MFUs = mean fluorescence units. ns = P-value >0.05.

Once it was determined that a Fab:PLGA ratio of 1:25 was sufficient, we tested three quantities of the NPs for cell binding (**Figure 6b**). The highest binding correlated with the highest quantity (50 µg), and signal intensity was dose dependent. Though, 50 µg of the negative control NPs had >50% fluorescent cells compared to cells only (data not shown). It is important to note that there was minimal, but some, binding of the bare and (-) Fab-PLGA NPs to the cells with 10 µg indicating that a large window between positive and negative binding was achieved at this amount. Additionally, the v6 Fab-PLGA NPs had higher binding to the negative cell lines compared to the (-) Fab- and bare PLGA NPs at 50 µg, for reasons that are currently unknown. CD44v6-specificity of the v6 Fab-PLGA NPs was finally validated when pre-treatment of the cells with free v6 Fab, but not the (-) Fab, inhibited most of the v6 Fab-PLGA NP binding (**Figure 6c**). Complete binding

inhibition of the v6 Fab-PLGA NPs with 250 nM of free v6 Fab was not detected, possibly due to binding kinetics and/or incomplete receptor occupation.

The presence of a biomolecule/protein corona, a consequence of NP exposure to a biological environment, is known to potentially reduce/abolish specific targeting of ligand-decorated NPs [156]. Thus, we performed a simple experiment where the v6 Fab-PLGA NPs were incubated with 10% (v/v) FBS for two hours prior to incubation with the MKN74-CD44v6+ cells (**Figure 6c**). There was no difference in binding in the FBS-treated NPs suggesting that they should retain their CD44v6 targeting capability in an *in vivo* setting. Binding may have been maintained due to the presence of the PEG chains, which are known to reduce protein corona formation from non-specific adsorption [189].

Because 10 µg of NPs gave a large window of positive vs. negative binding and 50 µg of control NPs had >50% fluorescent cells, we decided to use 10 µg of NPs for ~10^5 cells for all subsequent NP characterization studies that involved cell binding. Even though NP binding to MKN74-CD44v6+ gave lower fluorescence values than GP202, we chose to use the MKN74 cell system to maintain a robust positive and negative cell-based system with identical backgrounds. As a final confirmation, the v6 Fab-PLGA NPs, and not the negative controls, showed strong binding to the CD44v6-derived peptide as determined by ELISA, thus validating the presence of the Fab on the NPs (**Figure 6d**). The ELISA and FACS data are in agreement with the previous Fab-only data (**Figure 2**). The cell binding optimization allowed for the subsequent biological and technological characterization to proceed.

4.7. Impact of surfactants on the targeting of v6 Fab-PLGA NPs

The use of surfactants in PLGA NP production is critical in maintaining NP stability. Surfactants act by decreasing the interfacial tension between the components in a material system to increase such properties as miscibility and dispersion [192]. Although Menon *et al*. studied the impact of surfactants on the physical and biological properties of PLGA NPs [190], no studies until now have investigated the impact of surfactants on the specific targeting of ligand-decorated NPs.

To confirm that v6 Fab-PLGA NPs produced in PVA do not demonstrate specific binding to CD44v6-expressing cells while those produced in F127 do, a parallel study was performed studying those and two other common surfactants, sodium cholate (Na Chol) and Tween-80. The PLGA NPs, independent of the presence of a Fab or not, produced in 2% Tween-80, 0.5% F127, or 2% PVA had Z-averages around 300-400 nm and

polydispersity indices (PdIs) around 0.3-0.4 (**Table 3**). However, the NPs produced in 1% Na Chol or without surfactant (water only) had Z-averages >1000 nm and PdIs >0.6. These high values were most likely a result of aggregation, and not on actual NP size, as the PLGA was observed to become more difficult to resuspend with each subsequent wash. In general, the presence of a Fab did not cause significant changes in the zeta potential.

Table 3. The physicochemical properties of the PLGA NPs, with or without Fab conjugation, that were produced in different common surfactants as measured by dynamic light scattering and laser Doppler anemometry. ± = standard deviation of n=3 formulations.

Surfactant	Ligand	Z-average (size, nm)	Polydispersity Index	Zeta Potential (charge, mV)
2% Tween-80	v6 Fab	289 ± 23	0.35 ± 0.07	-10.9 ± 0.8
	(-) Fab	340 ± 17	0.33 ± 0.01	-11.0 ± 1.0
	none	385 ± 55	0.46 ± 0.07	-4.9 ± 1.7
0.5% F127	v6 Fab	373 ± 126	0.38 ± 0.08	-10.9 ± 1.1
	(-) Fab	487 ± 121	0.49 ± 0.07	-8.8 ± 2.1
	none	383 ± 34	0.38 ± 0.06	-6.5 ± 3.2
2% PVA	v6 Fab	472 ± 18	0.26 ± 0.06	-4.2 ± 0.1
	(-) Fab	373 ± 62	0.28 ± 0.01	-5.5 ± 0.8
	none	410 ± 21	0.24 ± 0.05	-4.3 ± 1.4
1% Na Chol	v6 Fab	1392 ± 495	0.74 ± 0.07	-13.5 ± 0.3
	(-) Fab	865 ± 161	0.65 ± 0.13	-12.5 ± 2.8
	none	926 ± 54	0.82 ± 0.10	-6.2 ± 1.2
water	v6 Fab	1244 ± 462	0.79 ± 0.15	-6.3 ± 1.2
	(-) Fab	1024 ± 262	0.69 ± 0.11	-5.2 ± 1.1
	none	2282 ± 1163	0.77 ± 0.20	-2.8 ± 0.6

Enzyme-linked immunosorbent assay (ELISA) was used to monitor the presence of the Fab on the surface of the NPs (**Figure 8a**). All the tested formulations demonstrated nearly equivalent amounts of Fab where appropriate. However, Fab-conjugated NPs produced in 2% PVA had significantly reduced detection of the Fab, most likely a result of the PVA blocking maleimide accessibility to the Fab.

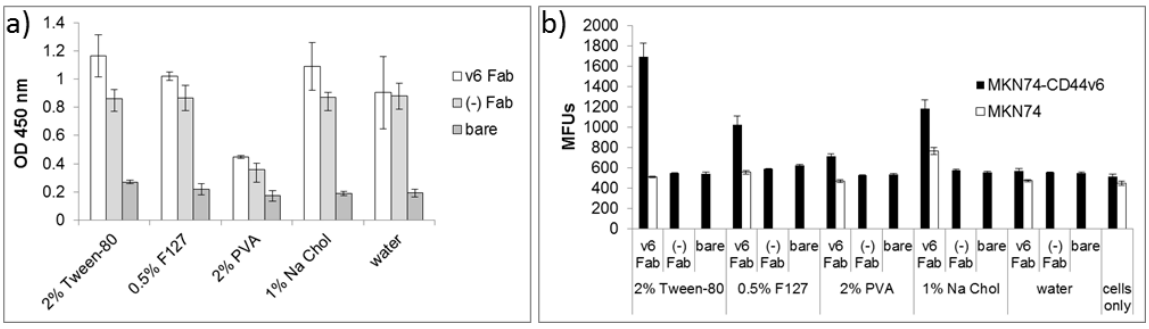

Figure 8. a) Fab presence on PLGA NPs produced in different common surfactants as measured by ELISA. b) Target cell binding of the Fab-conjugated PLGA NPs as measured by FACS. OD 450 nm = optical density at 450 nm and MFUs = mean fluorescence units. Error bars represent the standard deviation of n=3 formulations.

Overall, the v6 Fab-PLGA NPs had nominal binding to the non-expressing MKN74 cells, except for some slight binding seen with the NPs produced in 1% Na Chol (**Figure 8b**). Additionally, all the negative control NPs had nominal binding to the MKN74-CD44v6+ cells. v6 Fab-PLGA NPs produced in 2% Tween-80 had the highest binding to the MKN74-CD44v6+ cells, while the lowest binding was seen with NPs produced in PVA or water only. It is important to note that the presence of the Fab on the NPs did not preclude receptor recognition, as seen with the NPs produced in water. Similarly, a large Z-average did not preclude a lack of cell binding, as seen with the NPs produced in 1% Na Chol. Even though Fab levels were comparable, except for PVA, the varied cell binding levels could be attributed to a possible impact that the surfactant remaining on the NPs may have on the Fab itself (e.g. altered structure, orientation and/or affinity) or on the availability of the Fab to the receptor (e.g. steric hindrance).

Although the v6 Fab-PLGA NPs produced in 1% Na Chol had higher binding to the positive cells than 0.5% F127, their non-specific binding to the negative cells and the large Z-averages disqualified them from further inquiry. Thus, the NPs produced in Tween-80 and F127 were further tested to monitor the effect that surfactant concentration has on the same properties as seen in the initial experiments.

The concentration of the surfactant used during production, and ultimately the amount on the NP surface, may alter downstream target recognition. Therefore, the studies were repeated with Tween-80 and F127 at 2% and 0.5%. Physicochemical characterization demonstrated that the NPs had Z-averages around 250-400 nm, PdIs

around 0.25-0.40 (**Table 4**) and Zeta potentials around -10 to -20 mV. Surfactant percentage had no discernible effect on any of the above qualities.

Table 4. The physicochemical properties of the PLGA NPs, with or without Fab conjugation, that were produced in Tween-80 or F127 at 2% or 0.5% as measured by dynamic light scattering and laser Doppler anemometry. ± = standard deviation of n=3 formulations.

Surfactant	Ligand	Z-average (size, nm)	Polydispersity Index	Zeta Potential (charge, mV)
2% Tween-80	v6 Fab	322 ± 20	0.28 ± 0.05	-11.1 ± 3.4
	(-) Fab	297 ± 11	0.24 ± 0.01	-16.4 ± 1.3
	none	334 ± 11	0.33 ± 0.02	-15.8 ± 0.7
0.5% Tween-80	v6 Fab	282 ± 59	0.32 ± 0.07	-14.1 ± 3.3
	(-) Fab	284 ± 24	0.26 ± 0.02	-18.4 ± 2.4
	none	377 ± 41	0.38 ± 0.01	-20.3 ± 0.6
2% F127	v6 Fab	278 ± 58	0.31 ± 0.10	-17.8 ± 0.6
	(-) Fab	341 ± 49	0.36 ± 0.05	-13.8 ± 2.8
	none	394 ± 56	0.34 ± 0.02	-11.3 ± 0.3
0.5% F127	v6 Fab	349 ± 80	0.34 ± 0.04	-11.5 ± 0.8
	(-) Fab	250 ± 70	0.27 ± 0.05	-11.7 ± 0.9
	none	240 ± 18	0.30 ± 0.03	-10.8 ± 0.7

ELISA again demonstrated the presence of the Fabs on the appropriate NPs (**Figure 9a**). No difference in Fab presence was observed between the two surfactants or concentrations.

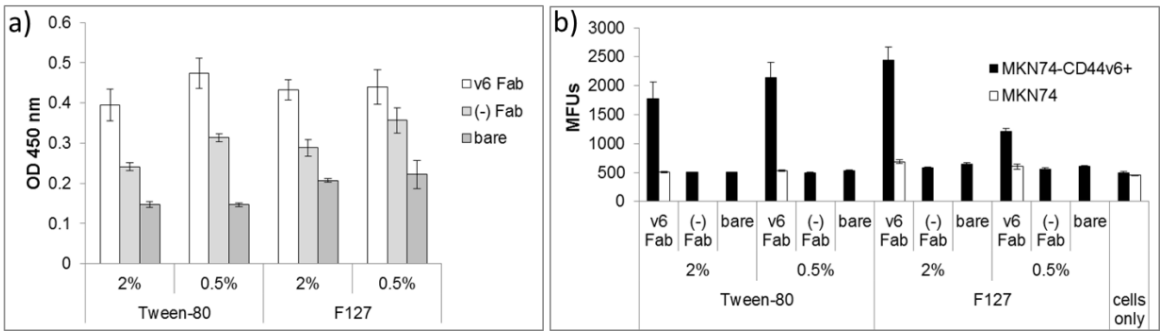

Figure 9. (a) Fab presence on PLGA NPs produced in Tween-80 or F127 at 2% or 0.5% as measured by ELISA. (b) Target cell binding of the Fab-conjugated PLGA NPs as measured by FACS. OD 450 nm = optical density at 450 nm and MFUs = mean fluorescence units. Error bars represent the standard deviation of n=3 formulations.

Cell binding studies demonstrated similar non-binding of the v6 Fab-PLGA NPs on the negative cells as well as the negative control NPs on the positive cells (**Figure 9b**). The two formulations produced in Tween-80 had binding values in between those of F127, but there was no statistical difference between the two concentrations. The highest target binding was seen with the NPs produced in 2% F127 while the lowest was with 0.5% F127. The cause of this difference is unknown, but it may be due to the PEG molecules of F127 acquiring different orientations leading to hindrance or promotion of the proper orientation of the Fab [193].

When compared with the initial study with the four surfactants, the NPs were slightly smaller and with lower Zeta potentials. This may have been due to the more mild washing conditions that incorporated Amicon filters and lower centrifugation speeds. These values coincide with the previous results (**Table 1**). Regardless, the cell binding results of the 2% Tween-80 and 0.5% F127 NPs agree with the initial study. The majority of the experiments performed were with v6 Fab-PLGA NPs that were produced in 0.5% F127. If this surfactant study had been performed prior to those other experiments, 2% F127 would have been used.

4.8. v6 Fab-PLGA NPs demonstrate specific live cell binding and internalization

To ensure that the NPs still maintained CD44v6 specificity in live cells, the binding assays were repeated with MKN74 cells in culture with similar amounts of NPs and cell counts. The microscopy images demonstrate specific binding of the v6 Fab-PLGA NPs to

MKN74-CD44v6+ cells, and there was no detectable fluorescence of the bare PLGA NPs to either cell line (**Figure 10a**). Additionally, some of the NPs appear to have been internalized; though, the majority appears to be associated with the cell surface (**Figure 10b**). The FACS results mostly correspond with the NaN_3-fixed cells in that there was higher binding of the v6 Fab-PLGA NPs to the MKN74-CD44v6+ cells compared to the negative control NPs (**Figure 10c**). Although the overall fluorescence for the v6 Fab-PLGA NPs was similar to that of the fixed cells, there is more fluorescence seen for the negative control NPs. This was not unexpected as live cells normally take up NPs in a dose dependent manner. Also, the use of trypsin during the cell detachment probably removed any NPs associated with the surface that had yet to be internalized.

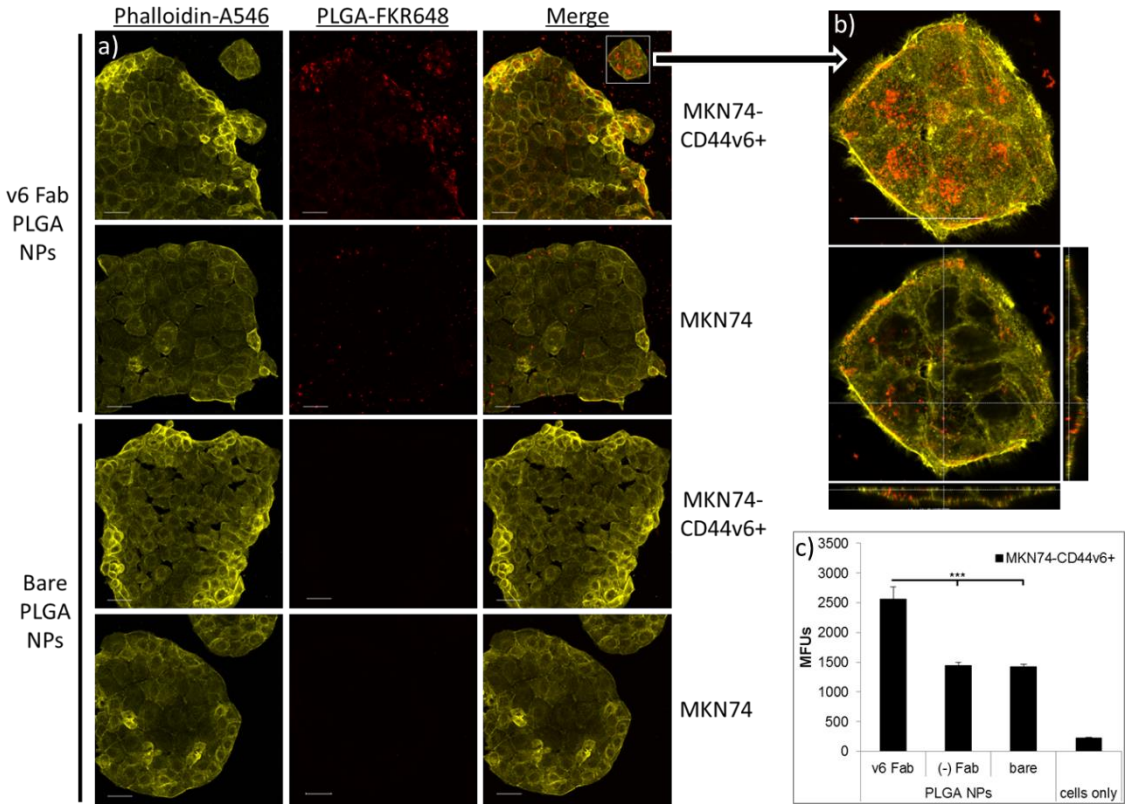

Figure 10. v6 Fab-PLGA NP binding to live cells as detected by light microscopy (a-b) and FACS (c). For both assays, live MKN74-CD44v6+ (and MKN74 for microscopy) cells were incubated with 10 µg of either v6 Fab- or bare PLGA NPs for 6 hrs. For the microscopy assay, the cells were fixed, actin-stained with phalloidin-AlexaFluor 546 (Phalloidin-A546) and imaged by confocal light microscopy. a) 20X magnification and maximal projection images. b) shows the MKN74-CD44v6+ cells incubated with the v6 Fab-PLGA NPs at 63X magnification (corresponding to the white box in the upper right panel of a)). The upper panel shows the maximal projection while the lower panel shows

an interior Z-dimension plane. c) MKN74-CD44v6+ cells were detached with trypsin before FACS measurement. Scale bar = 50 μM. n=3 replicates. Error bars represent the standard deviation. MFUs = mean fluorescence units. *** = P-value ≤0.001.

4.9. v6 Fab-PLGA NPs demonstrate nominal cytotoxicity but not target-specific drug delivery

In order to understand the cytotoxicity of the v6 Fab-PLGA NPs with and without PTX encapsulation, we measured cell viability with the MTT reduction assay (**Figure 11**). The 6 hr NP incubation was chosen to simulate the estimated *in vivo* exposure time, and the additional time (18 or 42 hr) was needed to monitor the antimitotic effects of the PTX. The 24 hr time point (without treatment removal) was chosen to simulate more long-term exposure of residual NPs. The empty NPs, independent of Fab decoration, were not cytotoxic to the MKN74 (+/- CD44v6) cells and only slightly toxic to the GP202 cells. At the 6+18 hr time point, no cytotoxicity was observed for any of the cells when exposed to the PTX-loaded NPs. Though, more cytotoxicity was observed in the 24 hr and 6+42 hr time points for the MKN74 (+/- CD44v6) cells (~40-60% viability) than for the GP202 cells (~80% viability). This loss of viability was similar to free PTX at equivalent PTX concentrations. This was probably due to PTX release into the media when incubated with the cells or previously during storage[194] and not an effect caused by intracellular delivery. Overall, the empty NPs are not cytotoxic, but NP association did not alter the toxicity of PTX.

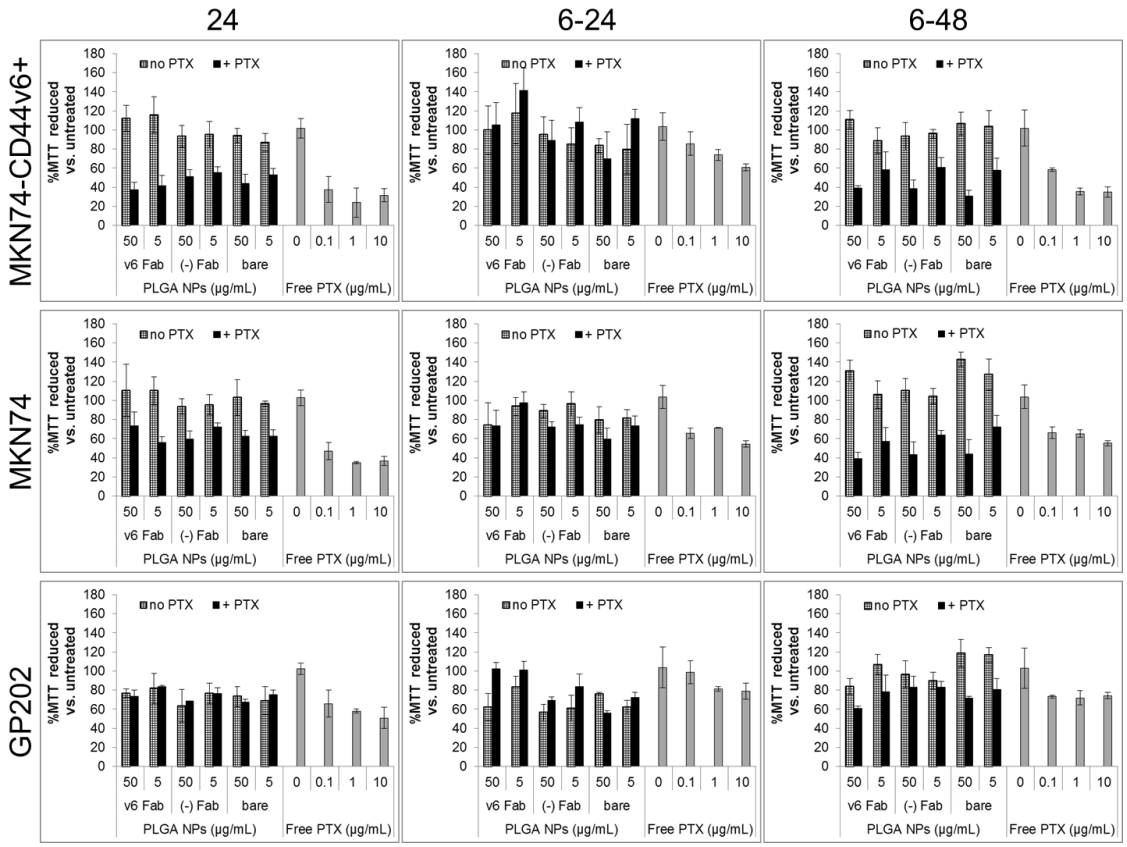

Figure 11. Cytotoxicity of empty PLGA NPs and Paclitaxel (PTX)-loaded PLGA NPs. MKN74, MKN74-CD44v6+ and GP202 cells in 96-well format were incubated with 50 or 5 µg/mL of empty PLGA NPs (no PTX) or PTX-loaded PLGA NPs (+ PTX) with or without (bare) decoration of the v6 Fab or (-) Fab for 24 hrs total (24) or for 6 hrs followed by NP removal and recovery in fresh media for an additional 18 hrs (6+18) or 42 hrs (6+42) before determining cell viability by MTT reduction. Free PTX was used as a control for cytotoxicity and for the PTX-loaded NPs. The levels of PTX in 50 and 5 µg/mL of PTX-loaded NPs was equivalent to 10 and 1 µg/mL of free PTX, respectively. n=6 formulation replicates. Error bars represent the standard deviation.

4.10. v6 Fab-PLGA NPs maintain CD44v6-specific binding when produced by w/o/w double emulsion

PLGA NPs can be produced with a handful of methods depending on the type of (bio)molecule (e.g. hydrophobic vs. hydrophilic) used for nanoencapsulation [186, 187]. The principle method of NP production in this study was nanoprecipitation by injection of the PLGA components dissolved in an organic solvent into water containing 0.5% F127. Here, we aimed to expand the therapeutic/diagnostic potential of our system to be able to

encapsulate hydrophilic molecules such as biopharmaceuticals. Thus, water-in-oil-in-water (w/o/w) double emulsion with an identical Fab conjugation protocol was employed to produce similar NPs [180]. DLS and LDA demonstrated that the NPs have similar physical profiles as those produced by nanoprecipitation (**Table 1**). Importantly, they retained similar cell binding specificity (**Figure 12**).

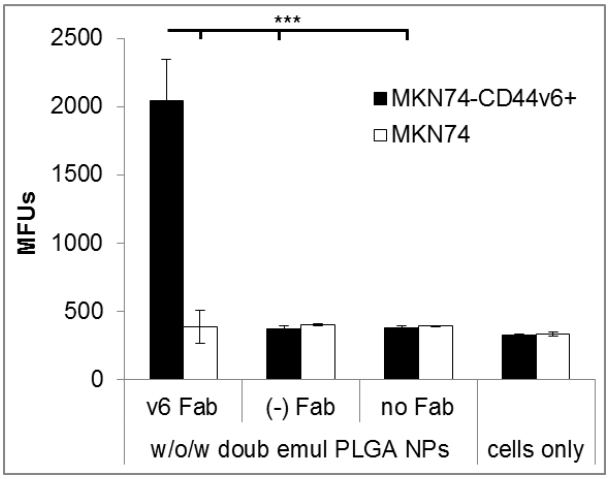

Figure 12. v6 Fab-PLGA NPs produced by w/o/w double emulsion demonstrate CD44v6+ cell-specific binding. 10 µg of PLGA NPs produced by w/o/w double emulsion and the standard Fab conjugation protocol were monitored for binding to MKN74-CD44v6+ or MKN74 cells by FACS. n=3 replicates. Error bars represent the standard deviation. MFUs = mean fluorescence units. *** = P-value ≤0.001.

4.11. v6 Fab-PLGA NPs resist simulated intestinal fluid (SIF) exposure

One possible application for the v6 Fab-PLGA NPs is *in vivo* diagnosis of CD44v6+ (pre-) metastatic CRC [21, 195] by oral administration. To determine whether the v6 Fab-PLGA NPs could withstand the intestinal environment, the NPs were exposed to SIF (pH 6.8), with or without the presence of pancreatin, for 15 or 60 min (**Figure 13**). No difference in cell binding was seen when compared to PBS-only treatment. However, binding was completely abolished when pancreatin was present in the SIF. This is not unexpected as the pancreatin most likely enzymatically degraded, at the very least, the v6 Fab on the surface of the NPs, and probably the PLGA itself, similar to that observed in PLA NPs [196]. Perhaps the NPs could be protected *in vivo* by inhibiting the intestinal enzymes with protease inhibitors or pH decrease [174] and/or through encapsulation within microparticles [57].

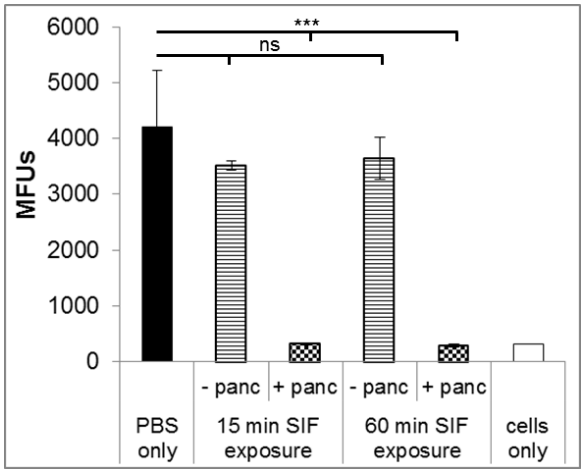

Figure 13. v6 Fab-PLGA NPs exposed to simulated intestinal fluid (SIF) maintain CD44v6+ cell binding. v6 Fab-PLGA NPs were exposed to SIF at pH 6.8 with or without pancreatin (panc) for 15 or 60 min and cell binding was monitored by FACS. n=3 replicates. Error bars represent the standard deviation. MFUs = mean fluorescence units. ns = P-value >0.05. *** = P-value ≤0.001.

4.12. v6 Fab-PLGA NPs resist longer-term storage and cryopreservation

One disadvantage of antibody-based therapy and *in vivo* diagnostics is the frequent need for maintaining cold chain storage. This imposes storage and distribution costs at all stages from post-production to the patient. Antibody-decorated NPs, like those developed here, are also constrained to the same limitations. As polymeric nanoparticles, such as those developed herein, are able to be cryopreserved [197], we aimed to superficially assess different storage conditions of the v6 Fab-PLGA NPs. We also aimed to translate our stability studies of freeze-dried biotherapeutics (e.g. insulin [183] or a therapeutic mAb [180]) encapsulated within PLGA NPs to PLGA NPs with antibodies on their surface.

Parallel studies investigated the effect of mid-range storage times in solution at 4 °C and cryopreservation with two weeks of storage at different temperatures on the v6 Fab-PLGA NP. During the in solution study, NPs were maintained at 1 mg/mL in water. Decreased binding occurred as time progressed, but a plateau was reached after 2-3 weeks (**Figure 14a**). During the cryopreservation study, the NPs were diluted to ~15 µg/mL in water with or without 10% trehalose, freeze-dried, and stored at -20 °C, 4 °C or RT for two weeks. The NPs were then rinsed with water before biological assessment by

FACS. NPs freeze-dried without trehalose had nominal cell binding (**Figure 14b**); though, it should be noted that, unexpectedly, no PLGA pellet was observed upon reconstitution and centrifugation. Importantly, the freeze-drying process did not significantly reduce cell binding when the NPs were stored at -20 °C or 4 °C but did reduce binding when the NPs were stored at RT.

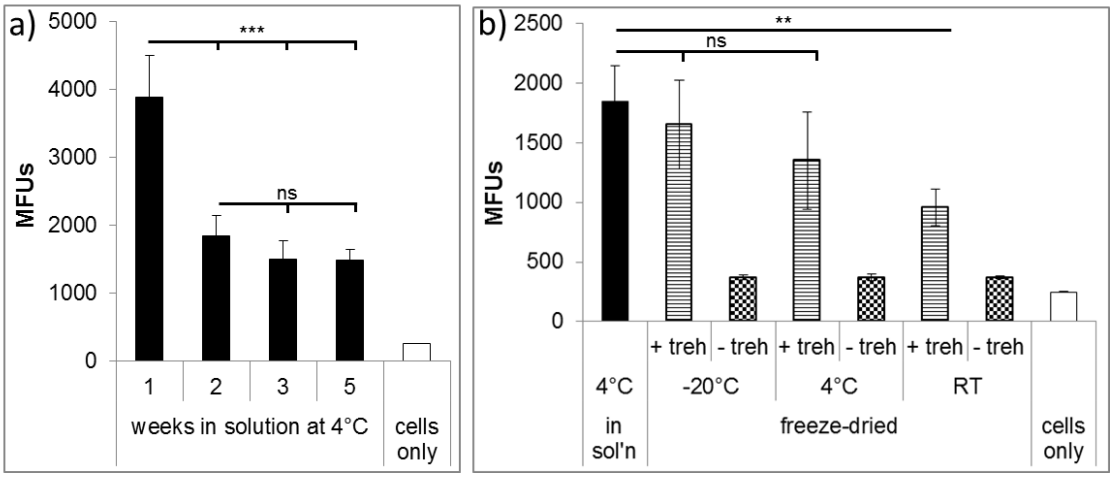

Figure 14. Effect of storage conditions on CD44v6+ cell binding of v6 Fab-PLGA NPs. a) Binding of v6 Fab-PLGA NPs stored in solution (water) to MKN74-CD44v6+ cells over time. b) In a parallel study, v6 Fab-PLGA NPs were freeze-dried with or without 10% trehalose (treh) and stored at -20 °C, 4 °C or room temperature (RT) for two weeks. n=3 formulation replicates. Error bars represent the standard deviation. MFUs = mean fluorescence units. ns = P-value >0.05. ** = P-value ≤0.01. *** = P-value ≤0.001.

Overall, these results suggest that freeze-drying NPs decorated with antibodies on their surface is a viable storage strategy similar to freeze-drying antibodies within NPs [180]. The possible explanations for the reduction in binding as storage temperature increased has to do with the structural integrity of either the Fab, the PLGA NPs, the covalent linkage of the Fab to the NPs, or any combination of the three. With these specific NPs, freeze-drying may be unnecessary as the highest binding was observed with NPs that were maintained at a high concentration in solution at 4 °C. Though, it should be considered that freeze-drying may help prevent bacterial contamination and/or aggregation common when biotherapeutics are stored in solution. It may also prevent premature release of an encapsulated drug and/or degradation of the material. Freeze-

drying can potentially allow for the NPs to be formulated within a pill for oral delivery or within a biosensor/lateral flow assay.

Only found one study was found that employed freeze-drying to (PLGA) NPs decorated with an antibody, but targeting was not evaluated neither before or after [198]. As the novelty and clinical impact of cryopreservation of antibody-decorated NPs is high, it is hoped this preliminary data sparks further investigation. Regardless, these results further verify our previous studies with nanoencapsulated biotherapeutics [180, 183].

In summary, the v6 Fab-PLGA NPs developed herein demonstrate valuable physical, biological and technological characteristics. They have morphology, size, PdI and charge typical of most PLGA-based NPs. The negative charge especially aids in reducing non-specific cell binding. Biologically, the v6 Fab-PLGA NPs bind specifically to CD44v6 when presented as a peptide and on the surface of cells. Importantly, they have nominal binding to cells that do not express CD44v6. The live cell binding studies also show that the NPs can be internalized in CD44v6-expressing cells. They are not cytotoxic and withstand SIF exposure but not in the presence of pancreatin. Technologically, the v6 Fab-PLGA NPs can be produced by nanoprecipitation and w/o/w double emulsion to harbor either hydrophobic or hydrophilic drugs, respectively, and they retain CD44v6 targeting after cryopreservation and short term storage in the cold.

5. Conclusions

The v6 Fab-PLGA NPs display many favorable qualities as a potential CD44v6-targeted drug and/or diagnostic delivery agent. The NPs were designed with immediate administration into humans in mind. As they are non-toxic, decorated with a fully human antibody fragment and the functional material (PLGA) is approved by the FDA/EMA, we would expect nominal issues (e.g. immunogenicity) in humans. Their PEGylation status also confers them with added “stealth” qualities to minimize phagocytic recognition for enhanced circulation times or, alternatively, for mucus penetration in the gastro-intestinal administration. Additionally, the NPs bind CD44v6+ cells in the presence of serum; therefore, it is expected that they would maintain CD44v6 targeting in circulation. Oral/rectal administration is possible, but inclusion of enzyme inhibitors would be needed to minimize damage to the NPs. Independent of the route of administration, the resistance of the v6 Fab-PLGA NPs to cryopreservation, and that trehalose is a widely-used excipient [199], suggests that they could be resuspended on demand or possibly incorporated within a pill/capsule. In their current state as fluorescent NPs, they can be

used mainly in diagnostics to target CD44v6-expressing tumors such as HNSCC tumors for which the Fab was originally developed [40]. However, they have the capacity to harbor hydrophobic or hydrophilic drugs depending on the production method, and, as such, could act in theranostics as well. Importantly, the core materials of the nanosystem developed herein (PLGA + fluorophore + maleimide functional groups) allow for tethering of the whole range of targeting ligands from peptides, proteins, nucleic acids, small molecules and, of course, other antibodies.

Given the many roles of CD44v6 in (metastatic) carcinoma, we envision the v6 Fab-PLGA NPs possibly targeting CSCs within the tumor [21] or that have escaped into circulation [27]. These NPs can potentially be used as an *in vivo* diagnostic from parenteral or oral/rectal administration. It may also be possible to incorporate these NPs within a biosensor [145] to detect CD44v6-expressing cells *ex vivo* (e.g. liquid biopsy). The epitope that the Fab was developed against [164] corresponds to the interaction region between CD44v6 and c-Met/VEGFR-2 [200], but the Fab itself has not been tested for its ability to disrupt this interaction or inhibit HGF/VEGF signaling, similar to anti-CD44v6 antibodies [10] or a five amino acid peptide derived from CD44v6 [12, 36, 37]. Thus, it may be possible for the v6 Fab-PLGA NPs to act synergistically with the Fab in a therapeutic context, similar to some ADCs [172], by inhibiting the above receptor interaction/ligand binding and delivering a therapeutic payload. Although the speculations above require experimental proof, the NPs developed herein present clinical potential and provide a launching point for future improvements and therapeutic and/or diagnostic opportunities.

CHAPTER V

Concluding remarks and future perspectives

1. Concluding remarks

Variant isoforms of CD44 expressing the v6 exon (CD44v6) are well-studied, cell surface, transmembrane glycoproteins that have a role in several of the malignant processes associated with cancers of the epithelium, thus making CD44v6 a potential target for therapy and/or diagnosis. Exploiting combined targeted drug delivery and nanomedicine represents a viable strategy in detecting CD44v6 expression in human tumors. Focusing on materials and ligands that are human compatible, while maintaining novelty, helps refine biomedical engineering design parameters. Targeting ligands based on recombinant monoclonal antibodies and aptamers each have the potential for low immunogenicity and high target specificity and affinity as well as other advantages and disadvantages. Taking all this into consideration, ligand-decorated nanocarriers that target CD44v6-expressing cells that simultaneously bypass normal cells could be a good tool in the oncology clinic.

The two main objectives of this thesis were to identify and characterize a novel ligand specific to human CD44v6 and to develop and characterize a polymeric nanocarrier that targets human CD44v6 for delivery of a drug and/or diagnostic. Ideally, the novel ligand identified in the first aim would then be used as the targeting ligand to be tethered to the nanocarrier.

RNA aptamers were chosen as the novel anti-human CD44v6 ligand type because there were none found in the literature or in the patent landscape, and they provided an opportunity to explore an emerging molecular recognition technology. The experimental design behind the selection process (i.e. SELEX) was based on the tools available (e.g. CD44v6-derived peptide and the CD44v6-overexpressing cells) and on the successful identification of the anti-CD44v6 Fab, AbD15179. Once overcoming initial technical hurdles, the procedures for the peptide and cell SELEX were straight forward, and quality control gels suggested that aptamer retrieval and subsequent amplification were successful. Due to the nature of classical SELEX (i.e. without deep sequencing), it was necessary to perform many rounds of SELEX before determining whether CD44v6-specific aptamers were being enriched.

CD44v6 enrichment was not demonstrated when fluorescently labeled polyclonal aptamers from the peptide SELEX outputs were tested for binding to CD44v6-derived peptide or CD44v6-expressing cells. It is possible that there were some technical issues (e.g. improper aptamer labeling or aptamer quantities) leading to this conclusion. However, when the binding assay exploiting AbD15179 as a positive control failed, the validity of the capture step of the peptide SELEX was placed under serious doubt and

undermined the resulting outputs. In hindsight, this control assay should have been performed before the peptide SELEX procedure was implemented. Although, deep sequencing and bioinformatics (e.g. APTANI) could elucidate sequence enrichment, but only synthesis and characterization of enriched monoclonal sequences would verify whether the SELEX protocols identified CD44v6-specific RNA aptamers or not.

AbD15179 was used as a known targeting ligand for nanocarrier funtionalization during parallel proof-of-concept studies while the identification of an anti-CD44v6 RNA aptamer was under investigation. The re-engineering of AbD15179 to express three C-terminal cysteines did not affect the binding affinity to the CD44v6-derived peptide or the CD44v6-expressing cells compared to the original Fab as seen in the Nestor group studies; thus allowing us to proceed with the Fab-decorated nanocarrier studies.

Initial nanocarrier studies utilized fluorescent, amine-modified, polystyrene latex FluoSpheres® because of their fluorescence, defined size and surface properties. Here, the idea was to conjugate the Fab to the FluoSpheres® using a maleimide-based linker containing 24 PEG chains (SMPEG24). Unfortunately, the FluoSpheres® proved to be difficult to work with due to their large tendency to aggregate and not dissociate during the washing steps. These issues are assumed to be the main reason why no specific binding was observed on the CD44v6-expressing cells. After exhaustive efforts to address the aggregation problems failed, similar design strategies were implemented with polymeric (i.e. PLGA-based) nanoparticles (NPs).

PLGA was chosen as the polymeric nanomaterial due to its many favorable properties in drug/diagnostic delivery in humans and because of the expertise within the Nanomedicines and Translational Drug Delivery group at i3S. PLGA NPs now incorporated PEG and maleimide directly into production bypassing the need for a linker. They were produced by nanoprecipitation within a 2% PVA solution as the surfactant. Different molar ratios of Fab to PLGA were also investigated. All attempts to demonstrate specific binding of v6 Fab-decorated NPs developed using this strategy failed.

It was only when the v6 Fab-decorated PLGA-FKR648-PEG-Mal NPs were produced in Pluronic F127 did they achieve specific binding to the CD44v6-expressing cells. Once this was demonstrated and reproduced, further optimization and characterization of the v6 Fab-PLGA NPs could progress. These NPs demonstrated expected sizes of 200-300 nm, negative zeta-potential and spherical morphology. Because a plateau of cell binding was not reached when investigating the molar ratio of Fab:PLGA, it is probable that more Fab may be able to be conjugated to the NPs resulting in even higher binding values. Because this novel nanosystem maintains targeting in the

presence of serum, is composed of an approved material (i.e. PLGA) and contains a fully human Fab, it is expected that it would be well tolerated in humans. The mid-term storage study suggests that the NPs could be stable for longer term storage in solution, but the cryopreservation study is more interesting. Cryopreserved NPs maintained cell targeting but was reduced with increasing storage temperature. Most likely this is due to degradation and/or instability of the Fab that could have been caused by impurities/contamination in either the Fab or the trehalose or only because of temperature.

The change in surfactant from PVA to F127 prompted the focused study of investigating the impact that common surfactants and their concentration have on downstream target recognition. The results confirmed that v6 Fab-decorated NPs produced in 2% PVA do not bind to the CD44v6-expressing cells. This study also demonstrated that the 0.5% F127 that was used during the production of the v6 Fab-PLGA NPs for the majority of the experiments in Chapter IV was not ideal.

Reviewing the objective of targeting cells expressing CD44v6, it is important to step back and re-evaluate the relevancy of CD44v6 as a target. The lack of specific isoform (e.g. CD44v3-v10) and/or glycoform targeting leading to targeting of multiple proteins could be a hurdle. Within a given cancer origin, there may be more than one v6 exon-expressing isoform with different functions. In the context of CRC, the study from Todaro *et al*. is pretty convincing where they show the role of the tumor micronenvironment in the re-education of CD44v6- progenitor cells into cancer stem cells leading to increased metastasis. However, low expression of CD44v6 in the normal crypt stem cell population of the stomach and intestine may be problematic in both diagnosis and therapy. The biggest reason for hesitation to target CD44v6 in drug delivery is the probable skin toxicity due to keratinocyte expression as evidenced in the phase I clinical trials with bivatuzumab mertansine; yet, this may be reduced by non-parenteral routes of administration. Though, CD44v6 may be best served in targeted therapy due to its role as an RTK co-receptor. Similar to the CD44v6-derived five amino acid peptide that blocks the c-Met-mediated signaling, AbD15179 could behave similarly since the binding epitope overlaps with that of the peptide. Additionally, the diagnostic value of CD44v6 still remains. The work of da Cunha *et al*. clearly shows the increasing expression of CD44v6 in GC as malignancy increases, and the original purpose of AbD15179 was in the *in vivo* radiolabeling of HNSCC. Given the above conclusions, the nanosystem developed herein may be best utilized in its current form as a vehicle to deliver a diagnostic agent or AbD15179 itself and not necessarily as a drug delivery agent.

Overall, the thesis-related research achieved one of the two goals. A novel ligand that is specific to human CD44v6 was not identified. The second aim of developing a human compatible, polymeric nanocarrier that targets human CD44v6 was achieved. In their present form, the v6 Fab-PLGA NPs demonstrated favorable physicochemical, biological and technological qualities that allow them to potentially be used in the oncology clinic as an (*in vivo*) diagnostic tool. Though, their use in drug delivery requires further investigation and optimization.

2. Future perspectives

As with most scientific and technological advancements, improvements in, and applications of, this research could definitely be explored. In the case of the anti-CD44v6 RNA aptamer identification, all of the outputs from each round of both peptide and cell SELEX are still available. None of the cell SELEX outputs were tested for enrichment; therefore, one could fluorescently label, for example, rounds 0, 4 and 7 and see if there is increased binding to the peptide or cells as was done for the peptide SELEX outputs. Alternatively, one could perform the deep sequencing and bioinformatics on some of the outputs and synthesize and characterize some of the promising sequences, as stated previously. Because the tools (peptide and cells) are robust and available, the SELEX protocols could be repeated with some adjustments. Specifically, the cell SELEX protocol should incorporate total elution from the v6-expressing cells in the first few rounds before performing the antibody elution in later rounds. This would help to maintain more diversity in the beginning of the SELEX and allow for more possible clones to be eluted during the antibody competing rounds. The capture step of the peptide SELEX quality control assay failed to demonstrate AbD15179 binding, and plate/plastic-based ELISA works well to demonstrate AbD15179 binding to the peptide. Therefore, adsorbing the peptide to plastic to capture the CD44v6-specific aptamers could replace the in solution-based approach to aptamer-peptide capture with magnetic beads. Lastly, if an anti-CD44v6 aptamer is identified, it could be used to decorate nanoparticles as was originally intended or possibly as therapeutic agent on its own. With that in mind, it should be noted that AbD15179 may also act as a therapeutic as it recognizes an epitope that is associated with the c-Met interaction and may function similarly as the five amino-acid currently under clinical trials.

The weaknesses of the targeted nanosystem, lack of evidence of specific drug (i.e. paclitaxel) delivery to CD44v6-expressing cells and *in vivo* studies, should be addressed first. In the case of the drug delivery studies, shorter conjugation times and/or the use of cryopreservation could minimize the presumed premature release of the drug during

storage prior to addition to the cells. Alternatively, drugs with different chemical and/or biological properties could be explored, because the v6 Fab-PLGA NPs can be used to encapsulate hydrophobic or hydrophilic drugs. As an example in translating other similar work, a monoclonal antibody could be encapsulated in the v6 Fab-PLGA NPs for localized and sustained release in the presence of a CD44v6-expressing tumor but outside the cell or could be for intracellular delivery as a signaling pathway disruptor or to engage TRIM21 for directed degradation.

In vivo studies could initially focus on tumor models and essentially replicate the *in vitro* cell-based studies but in rodents. Because the v6 Fab-PLGA NPs are fluorescent with FKR648, systemically-delivered NP targeting could be monitored in SCID mice harboring MKN74 tumors with or without CD44v6 overexpression in real time. Independent of whether or not the *in vitro* drug delivery assays demonstrate CD44v6-expressing cell cytotoxicity, drug-encapsulated NPs could also be delivered systemically and tumor volume could be assessed in the same *in vivo* tumor model. This could also open up the possibility for a theranostic approach where the same NPs could treat the tumor and monitor its progression at the same time. Of course, rodent studies would need to be highly convincing before proceeding to non-human primates or humans.

A possible application of the v6 Fab-PLGA NPs is to diagnose gastric or colorectal cancer from oral, and not systemic, administration. That is why the simulated intestinal fluid studies were performed. Though, several hurdles would need to be addressed before embarking on these studies. First, an appropriate model where the tumor cells are orthotopically implanted or derived from chemical or genetic manipulation needs to be established such that the GI tract tumor has a chance of being reached from the luminal side. Second, the optimal mucopenetrating ability of the NPs should be established *in vitro* by empirically adjusting the amount and/or MW of the PEG chains. Lastly, the NPs would need to be protected from the low pH and enzymes of the stomach through pre-preparation of the GI environment or through microencapsulation of the NPs. Once these are established, the NPs could be administered by oral gavage and monitored for tumor recognition and biodistribution.

Longer term storage in solution studies could also be implemented. At the same time, the release profile of the encapsulating drug as well as any dissociation of the Fab should be investigated in parallel. More importantly, the cryopreservation of the NPs should be more thoroughly studied. The use of different amounts of trehalose and cryopreservants as well as optimizing the steps of the lyophilization process could be tested following the studies of Pedro Fonte and colleagues. Ideally, a formulation would

be achieved where the NPs could be stored at room temperature. In this state, it is envisioned that the NPs could be incorporated within a pill/capsule or within a powder meant for inhalation.

As the nanosystem developed here was produced in microgram quantities at a time, it is important to investigate the scaling up of the system. This would be informative for providing sufficient quantities for *in vivo* studies, both pre-clinical and clinical. For example, a microfluidizer could be incorporated to automate the nanoprecipitation, NP washing and downstream Fab conjugation and purification.

The nanosystem developed herein should also be considered as being modular. Because these NPs are functionalized with maleimide, it is possible to conjugate other thiol-bearing ligand types (e.g. aptamers, proteins or peptides) or other antibodies or fragments against different targets (e.g. stromal cell-related targets) to the NPs, bearing in mind a proper site-oriented bioconjugation protocol. Also, these NPs are able to be produced to harbor hydrophobic or hydrophilic drugs. Alternatively, other maleimide-modified nanomaterials (e.g. liposomes) may be used with the engineered v6 Fab.

The work developed in this thesis laid a solid foundation for future exploration as outlined above. The identification of novel anti-CD44v6 aptamers should be revisited to bypass the licensing restrictions of AbD15179 and to provide a competing, and possibly better, molecular recognition technology to that of antibodies. Due to the limitations of the nanomaterial and CD44v6 as a relevant/safe target, the drug delivery potential of the nanosystem should be re-evaluated, and more focus should be placed on *in vivo* diagnosis with different modes of administration. Finally, the v6 nanosystem combined with the cell-based tools should be used as a model to investigate technological aspects of targeted NP development akin to the surfactant and cryopreservation studies.[201]

REFERENCES

[1] Zöller M. 2011. CD44: can a cancer-initiating cell profit from an abundantly expressed molecule? *Nat Rev Cancer*. 11:254-67.
[2] Morath I, Hartmann TN, Orian-Rousseau V. 2016. CD44: More than a mere stem cell marker. *Int J Biochem Cell Biol*. 81:166-73.
[3] Screaton GR, Bell MV, Jackson DG, Cornelis FB, Gerth U, Bell JI. 1992. Genomic structure of DNA encoding the lymphocyte homing receptor CD44 reveals at least 12 alternatively spliced exons. *Proc Natl Acad Sci U S A*. 89:12160-4.
[4] Günthert U, Hofmann M, Rudy W, Reber S, Zöller M, Hauβmann I, Matzku S, Wenzel A, Ponta H, Herrlich P. 1991. A new variant of glycoprotein CD44 confers metastatic potential to rat carcinoma cells. *Cell*. 65:13-24.
[5] Orian-Rousseau V. 2015. CD44 acts as a signaling platform controlling tumor progression and metastasis. *Front Immunol*. 6:154.
[6] Orian-Rousseau V. 2010. CD44, a therapeutic target for metastasising tumours. *Eur J Cancer*. 46:1271-7.
[7] Wielenga VJM, Heider K-H, Johan G, Offerhaus A, Adolf GR, van den Berg FM, Ponta H, Herrlich P, Pals ST. 1993. Expression of CD44 variant proteins in human colorectal cancer is related to tumor progression. *Cancer Res*. 53:4754-6.
[8] Arch R, Wirth K, Hofmann M, Ponta H, Matzku S, Herrlich P, Zöller M. 1992. Participation in normal immune responses of a metastasis-inducing splice variant of CD44. *Science*. 257:682-5.
[9] Volz Y, Koschut D, Matzke-Ogi A, Dietz Marina S, Karathanasis C, Richert L, Wagner Moritz G, Mély Y, Heilemann M, Niemann Hartmut H, Orian-Rousseau V. 2015. Direct binding of hepatocyte growth factor and vascular endothelial growth factor to CD44v6. *Biosci Rep*. 35.
[10] Orian-Rousseau V, Chen L, Sleeman JP, Herrlich P, Ponta H. 2002. CD44 is required for two consecutive steps in HGF/c-Met signaling. *Genes Dev*. 16:3074-86.
[11] Hasenauer S, Malinger D, Koschut D, Pace G, Matzke A, von Au A, Orian-Rousseau V. 2013. Internalization of Met requires the co-receptor CD44v6 and its link to ERM proteins. *PloS one*. 8:e62357.
[12] Tremmel M, Matzke A, Albrecht I, Laib AM, Olaku V, Ballmer-Hofer K, Christofori G, Héroult M, Augustin HG, Ponta H, Orian-Rousseau V. 2009. A CD44v6 peptide reveals a role of CD44 in VEGFR-2 signaling and angiogenesis. *Blood*. 114:5236-44.
[13] Bradley CA, Salto-Tellez M, Laurent-Puig P, Bardelli A, Rolfo C, Tabernero J, Khawaja HA, Lawler M, Johnston PG, Van Schaeybroeck S, consortium M. 2017. Targeting c-MET in gastrointestinal tumours: rationale, opportunities and challenges. *Nat Rev Clin Oncol*. 14:562-76.
[14] Olaku V, Matzke A, Mitchell C, Hasenauer S, Sakkaravarthi A, Pace G, Ponta H, Orian-Rousseau V. 2011. c-Met recruits ICAM-1 as a coreceptor to compensate for the loss of CD44 in Cd44 null mice. *Mol Biol Cell*. 22:2777-86.
[15] Orian-Rousseau V, Morrison H, Matzke A, Kastilan T, Pace G, Herrlich P, Ponta H. 2007. Hepatocyte growth factor-induced Ras activation requires ERM proteins linked to both CD44v6 and F-actin. *Mol Biol Cell*. 18:76-83.
[16] Cheng C, Yaffe MB, Sharp PA. 2006. A positive feedback loop couples Ras activation and CD44 alternative splicing. *Genes Dev*. 20:1715-20.
[17] Psaila B, Lyden D. 2009. The metastatic niche: adapting the foreign soil. *Nat Rev Cancer*. 9:285.
[18] Jung T, Castellana D, Klingbeil P, Hernández IC, Vitacolonna M, Orlicky DJ, Roffler SR, Brodt P, Zöller M. 2009. CD44v6 dependence of premetastatic niche preparation by exosomes. *Neoplasia*. 11:1093-105.

[19] da Cunha CB, Oliveira C, Wen X, Gomes B, Sousa S, Suriano G, Grellier M, Huntsman DG, Carneiro F, Granja PL, Seruca R. 2010. De novo expression of CD44 variants in sporadic and hereditary gastric cancer. *Lab Invest*. 90:1604-14.
[20] Carneiro P, Figueiredo J, Bordeira-Carriço R, Fernandes MS, Carvalho J, Oliveira C, Seruca R. 2013. Therapeutic targets associated to E-cadherin dysfunction in gastric cancer. *Expert Opin Ther Targets*. 17:1187-201.
[21] Todaro M, Gaggianesi M, Catalano V, Benfante A, Iovino F, Biffoni M, Apuzzo T, Sperduti I, Volpe S, Cocorullo G, Gulotta G, Dieli F, De Maria R, Stassi G. 2014. CD44v6 is a marker of constitutive and reprogrammed cancer stem cells driving colon cancer metastasis. *Cell Stem Cell*. 14:342-56.
[22] Thiery JP. 2002. Epithelial-mesenchymal transitions in tumour progression. *Nat Rev Cancer*. 2:442-54.
[23] Medema JP. 2013. Cancer stem cells: the challenges ahead. *Nat Cell Biol*. 15:338-44.
[24] Pattabiraman DR, Weinberg RA. 2014. Tackling the cancer stem cells - what challenges do they pose? *Nat Rev Drug Discov*. 13:497-512.
[25] Zeuner A, Todaro M, Stassi G, De Maria R. 2014. Colorectal cancer stem cells: from the crypt to the clinic. *Cell Stem Cell*. 15:692-705.
[26] Fruman DA, Rommel C. 2014. PI3K and cancer: Lessons, challenges and opportunities. *Nat Rev Drug Discov*. 13:140-56.
[27] Grillet F, Bayet E, Villeronce O, Zappia L, Lagerqvist EL, Lunke S, Charafe-Jauffret E, Pham K, Molck C, Rolland N, Bourgaux JF, Prudhomme M, Philippe C, Bravo S, Boyer JC, Canterel-Thouennon L, Taylor GR, Hsu A, Pascussi JM, Hollande F, Pannequin J. 2017. Circulating tumour cells from patients with colorectal cancer have cancer stem cell hallmarks in ex vivo culture. *Gut*. 66:1802-10.
[28] Bar JK, Grelewski P, Popiela A, Noga L, Rabczynski J. 2004. Type IV collagen and CD44v6 expression in benign, malignant primary and metastatic ovarian tumors: correlation with Ki-67 and p53 immunoreactivity. *Gynecol Oncol*. 95:23-31.
[29] Kawano T, Nakamura Y, Yanoma S, Kubota A, Furukawa M, Miyagi Y, Tsukuda M. 2004. Expression of E-cadherin, and CD44s and CD44v6 and its association with prognosis in head and neck cancer. *Auris Nasus Larynx*. 31:35-41.
[30] Vizoso FJ, Fernandez JC, Corte MD, Bongera M, Gava R, Allende MT, Garcia-Muniz JL, Garcia-Moran M. 2004. Expression and clinical significance of CD44V5 and CD44V6 in resectable colorectal cancer. *J Cancer Res Clin Oncol*. 130:679-86.
[31] Afify AM, Craig S, Paulino AFG, Stern R. 2005. Expression of hyaluronic acid and its receptors, CD44s and CD44v6, in normal, hyperplastic, and neoplastic endometrium. *Ann Diagn Pathol*. 9:312-8.
[32] Heider KH, Kuthan H, Stehle G, Munzert G. 2004. CD44v6: A target for antibody-based cancer therapy. *Cancer Immunol Immunother*. 53:567-79.
[33] Orian-Rousseau V, Ponta H. 2015. Perspectives of CD44 targeting therapies. *Arch Toxicol*. 89:3-14.
[34] Tijink BM, Buter J, de Bree R, Giaccone G, Lang MS, Staab A, Leemans CR, van Dongen GA. 2006. A phase I dose escalation study with anti-CD44v6 bivatuzumab mertansine in patients with incurable squamous cell carcinoma of the head and neck or esophagus. *Clin Cancer Res*. 12:6064-72.
[35] Riechelmann H, Sauter A, Golze W, Hanft G, Schroen C, Hoermann K, Erhardt T, Gronau S. 2008. Phase I trial with the CD44v6-targeting immunoconjugate bivatuzumab mertansine in head and neck squamous cell carcinoma. *Oral Oncol*. 44:823-9.
[36] Matzke A, Herrlich P, Ponta H, Orian-Rousseau V. 2005. A five-amino-acid peptide blocks Met- and Ron-dependent cell migration. *Cancer Res*. 65:6105-10.
[37] Matzke-Ogi A, Jannasch K, Shatirishvili M, Fuchs B, Chiblak S, Morton J, Tawk B, Lindner T, Sansom O, Alves F, Warth A, Schwager C, Mier W, Kleeff J, Ponta H, Abdollahi A, Orian-Rousseau V. 2016. Inhibition of tumor growth and metastasis in pancreatic cancer models by interference with CD44v6 signaling. *Gastroenterol*. 150:513-25.e10.

[38] Sandstrom K, Haylock AK, Spiegelberg D, Qvarnstrom F, Wester K, Nestor M. 2012. A novel CD44v6 targeting antibody fragment with improved tumor-to-blood ratio. *Int J Oncol*. 40:1525-32.
[39] Prassler J, Thiel S, Pracht C, Polzer A, Peters S, Bauer M, Norenberg S, Stark Y, Kolln J, Popp A, Urlinger S, Enzelberger M. 2011. HuCAL PLATINUM, a synthetic Fab library optimized for sequence diversity and superior performance in mammalian expression systems. *J Mol Biol*. 413:261-78.
[40] Haylock AK, Spiegelberg D, Nilvebrant J, Sandstrom K, Nestor M. 2014. In vivo characterization of the novel CD44v6-targeting Fab fragment AbD15179 for molecular imaging of squamous cell carcinoma: A dual-isotope study. *EJNMMI Res*. 4:11.
[41] Haylock AK, Spiegelberg D, Mortensen AC, Selvaraju RK, Nilvebrant J, Eriksson O, Tolmachev V, Nestor MV. 2016. Evaluation of a novel type of imaging probe based on a recombinant bivalent mini-antibody construct for detection of CD44v6-expressing squamous cell carcinoma. *Int J Oncol*. 48:461-70.
[42] Barenholz Y. 2012. Doxil® — The first FDA-approved nano-drug: Lessons learned. *J Control Release*. 160:117-34.
[43] Singal PK, Iliskovic N. 1998. Doxorubicin-induced cardiomyopathy. *N Engl J Med*. 339:900-5.
[44] Blanco E, Shen H, Ferrari M. 2015. Principles of nanoparticle design for overcoming biological barriers to drug delivery. *Nat Biotechnol*. 33:941-51.
[45] Anselmo AC, Mitragotri S. 2016. Nanoparticles in the clinic. *Bioeng Transl Med*. 1:10-29.
[46] Fernandes E, Ferreira JA, Andreia P, Luís L, Barroso S, Sarmento B, Santos LL. 2015. New trends in guided nanotherapies for digestive cancers: A systematic review. *J Control Release*. 209:288-307.
[47] das Neves J, Amiji MM, Bahia MF, Sarmento B. 2010. Nanotechnology-based systems for the treatment and prevention of HIV/AIDS. *Adv Drug Deliv Rev*. 62:458-77.
[48] Costa A, Pinheiro M, Magalhaes J, Ribeiro R, Seabra V, Reis S, Sarmento B. 2016. The formulation of nanomedicines for treating tuberculosis. *Adv Drug Deliv Rev*. 102:102-15.
[49] Kalepu S, Nekkanti V. 2015. Insoluble drug delivery strategies: Review of recent advances and business prospects. *Acta Pharmaceutica Sinica B*. 5:442-53.
[50] Vasconcelos T, Marques S, das Neves J, Sarmento B. 2016. Amorphous solid dispersions: Rational selection of a manufacturing process. *Adv Drug Deliv Rev*. 100:85-101.
[51] Shao K, Singha S, Clemente-Casares X, Tsai S, Yang Y, Santamaria P. 2015. Nanoparticle-based immunotherapy for cancer. *ACS Nano*. 9:16-30.
[52] Gonzalez-Delgado JA, Kennedy PJ, Ferreira M, Tome JP, Sarmento B. 2016. Use of photosensitizers in semisolid formulations for microbial photodynamic inactivation. *J Med Chem*. 59:4428-42.
[53] Kemp JA, Shim MS, Heo CY, Kwon YJ. 2016. “Combo” nanomedicine: Co-delivery of multi-modal therapeutics for efficient, targeted, and safe cancer therapy. *Adv Drug Deliv Rev*. 98:3-18.
[54] Sharma P, Brown S, Walter G, Santra S, Moudgil B. 2006. Nanoparticles for bioimaging. *Adv Colloid Interface Sci*. 123–126:471-85.
[55] Sosnik A, das Neves J, Sarmento B. 2014. Mucoadhesive polymers in the design of nano-drug delivery systems for administration by non-parenteral routes: A review. *Prog Polym Sci*. 39:2030-75.
[56] Sarmento B, Ribeiro A, Veiga F, Sampaio P, Neufeld R, Ferreira D. 2007. Alginate/chitosan nanoparticles are effective for oral insulin delivery. *Pharm Res*. 24:2198-206.
[57] Araújo F, Shrestha N, Shahbazi MA, Liu D, Herranz-Blanco B, Makila EM, Salonen JJ, Hirvonen JT, Granja PL, Sarmento B, Santos HA. 2015. Microfluidic assembly of a

multifunctional tailorable composite system designed for site specific combined oral delivery of peptide drugs. *ACS Nano*. 9:8291-302.
[58] Gomes MJ, Fernandes C, Martins S, Borges F, Sarmento B. 2016. Tailoring lipid and polymeric nanoparticles as siRNA carriers towards the blood-brain barrier – From targeting to safe administration. *J Neuroimmune Pharmacol*.1-13.
[59] Sawyers C. 2004. Targeted cancer therapy. *Nature*. 432:294.
[60] Yang JC, Haworth L, Sherry RM, Hwu P, Schwartzentruber DJ, Topalian SL, Steinberg SM, Chen HX, Rosenberg SA. 2003. A randomized trial of bevacizumab, an anti–vascular endothelial growth factor antibody, for metastatic renal cancer. *N Engl J Med*. 349:427-34.
[61] Burger RA, Brady MF, Bookman MA, Fleming GF, Monk BJ, Huang H, Mannel RS, Homesley HD, Fowler J, Greer BE, Boente M, Birrer MJ, Liang SX. 2011. Incorporation of bevacizumab in the primary treatment of ovarian cancer. *N Engl J Med*. 365:2473-83.
[62] Karapetis CS, Khambata-Ford S, Jonker DJ, O'Callaghan CJ, Tu D, Tebbutt NC, Simes RJ, Chalchal H, Shapiro JD, Robitaille S, Price TJ, Shepherd L, Au H-J, Langer C, Moore MJ, Zalcberg JR. 2008. K-ras mutations and benefit from cetuximab in advanced colorectal cancer. *N Engl J Med*. 359:1757-65.
[63] Jonker DJ, O'Callaghan CJ, Karapetis CS, Zalcberg JR, Tu D, Au H-J, Berry SR, Krahn M, Price T, Simes RJ, Tebbutt NC, van Hazel G, Wierzbicki R, Langer C, Moore MJ. 2007. Cetuximab for the treatment of colorectal cancer. *N Engl J Med*. 357:2040-8.
[64] Bonner JA, Harari PM, Giralt J, Azarnia N, Shin DM, Cohen RB, Jones CU, Sur R, Raben D, Jassem J, Ove R, Kies MS, Baselga J, Youssoufian H, Amellal N, Rowinsky EK, Ang KK. 2006. Radiotherapy plus cetuximab for squamous-cell carcinoma of the head and neck. *N Engl J Med*. 354:567-78.
[65] Bae YH, Park K. 2011. Targeted drug delivery to tumors: Myths, reality and possibility. *J Control Release*. 153:198-205.
[66] Bertrand N, Wu J, Xu X, Kamaly N, Farokhzad OC. 2014. Cancer nanotechnology: The impact of passive and active targeting in the era of modern cancer biology. *Adv Drug Deliv Rev*. 66:2-25.
[67] Hrkach J, Von Hoff D, Mukkaram Ali M, Andrianova E, Auer J, Campbell T, De Witt D, Figa M, Figueiredo M, Horhota A, Low S, McDonnell K, Peeke E, Retnarajan B, Sabnis A, Schnipper E, Song JJ, Song YH, Summa J, Tompsett D, Troiano G, Van Geen Hoven T, Wright J, LoRusso P, Kantoff PW, Bander NH, Sweeney C, Farokhzad OC, Langer R, Zale S. 2012. Preclinical development and clinical translation of a PSMA-targeted docetaxel nanoparticle with a differentiated pharmacological profile. *Sci Transl Med*. 4:128ra39.
[68] Farokhzad OC, Cheng J, Teply BA, Sherifi I, Jon S, Kantoff PW, Richie JP, Langer R. 2006. Targeted nanoparticle-aptamer bioconjugates for cancer chemotherapy in vivo. *Proc Natl Acad Sci U S A*. 103:6315-20.
[69] Nichols JW, Bae YH. 2014. EPR: Evidence and fallacy. *J Control Release*. 190:451-64.
[70] Danhier F. 2016. To exploit the tumor microenvironment: Since the EPR effect fails in the clinic, what is the future of nanomedicine? *J Control Release*. 244:108-21.
[71] Shi J, Kantoff PW, Wooster R, Farokhzad OC. 2017. Cancer nanomedicine: progress, challenges and opportunities. *Nat Rev Cancer*. 17:20-37.
[72] Peer D, Karp JM, Hong S, Farokhzad OC, Margalit R, Langer R. 2007. Nanocarriers as an emerging platform for cancer therapy. *Nat Nanotechnol*. 2:751-60.
[73] Janeway CA, Travers P, Walport M, Shlomchik MJ. Immunobiology: The immune system in health and disease: Garland New York; 2001.
[74] Martins JP, Kennedy PJ, Santos HA, Barrias C, Sarmento B. 2016. A comprehensive review of the neonatal Fc receptor and its application in drug delivery. *Pharmacol Ther*. 161:22-39.

[75] Roopenian DC, Akilesh S. 2007. FcRn: The neonatal Fc receptor comes of age. *Nat Rev Immunol*. 7:715-25.
[76] Rogers LM, Veeramani S, Weiner GJ. 2014. Complement in monoclonal antibody therapy of cancer. *Immunol Res*. 59:203-10.
[77] Mallery DL, McEwan WA, Bidgood SR, Towers GJ, Johnson CM, James LC. 2010. Antibodies mediate intracellular immunity through tripartite motif-containing 21 (TRIM21). *Proc Natl Acad Sci U S A*. 107:19985-90.
[78] James LC, Keeble AH, Khan Z, Rhodes DA, Trowsdale J. 2007. Structural basis for PRYSPRY-mediated tripartite motif (TRIM) protein function. *Proc Natl Acad Sci U S A*. 104:6200-5.
[79] Vaysburd M, Watkinson RE, Cooper H, Reed M, O'Connell K, Smith J, Cruickshanks J, James LC. 2013. Intracellular antibody receptor TRIM21 prevents fatal viral infection. *Proc Natl Acad Sci U S A*. 110:12397-401.
[80] Foss S, Watkinson R, Sandlie I, James LC, Andersen JT. 2015. TRIM21: A cytosolic Fc receptor with broad antibody isotype specificity. *Immunol Rev*. 268:328-39.
[81] Tonegawa S. 1983. Somatic generation of antibody diversity. *Nature*. 302:575-81.
[82] Holliger P, Hudson PJ. 2005. Engineered antibody fragments and the rise of single domains. *Nat Biotechnol*. 23:1126-36.
[83] Hamers-Casterman C, Atarhouch T, Muyldermans S, Robinson G, Hamers C, Songa EB, Bendahman N, Hamers R. 1993. Naturally occurring antibodies devoid of light chains. *Nature*. 363:446-8.
[84] Greenberg AS, Avila D, Hughes M, Hughes A, McKinney EC, Flajnik MF. 1995. A new antigen receptor gene family that undergoes rearrangement and extensive somatic diversification in sharks. *Nature*. 374:168-73.
[85] Köhler G, Milstein C. 1975. Continuous cultures of fused cells secreting antibody of predefined specificity. *Nature*. 256:495-7.
[86] Orlandi R, Güssow DH, Jones PT, Winter G. 1989. Cloning immunoglobulin variable domains for expression by the polymerase chain reaction. *Proc Natl Acad Sci U S A*. 86:3833-7.
[87] Sastry L, Alting-Mees M, Huse WD, Short JM, Sorge JA, Hay BN, Janda KD, Benkovic SJ, Lerner RA. 1989. Cloning of the immunological repertoire in Escherichia coli for generation of monoclonal catalytic antibodies: Construction of a heavy chain variable region-specific cDNA library. *Proc Natl Acad Sci U S A*. 86:5728-32.
[88] Ward ES, Gussow D, Griffiths AD, Jones PT, Winter G. 1989. Binding activities of a repertoire of single immunoglobulin variable domains secreted from Escherichia coli. *Nature*. 341:544-6.
[89] Huse WD, Sastry L, Iverson SA, Kang AS, Alting-Mees M, Burton DR, Benkovic SJ, Lerner RA. 1989. Generation of a large combinatorial library of the immunoglobulin repertoire in phage lambda. *Science*. 246:1275-81.
[90] Nelson B, Sidhu SS. Synthetic antibody libraries. In: Voynov V, Caravella AJ, editors. Therapeutic proteins: Methods and protocols. Totowa, NJ: Humana Press; 2012. p. 27-41.
[91] Knappik A, Ge L, Honegger A, Pack P, Fischer M, Wellnhofer G, Hoess A, Wölle J, Plückthun A, Virnekäs B. 2000. Fully synthetic human combinatorial antibody libraries (HuCAL) based on modular consensus frameworks and CDRs randomized with trinucleotides. *J Mol Biol*. 296:57-86.
[92] Rothe C, Urlinger S, Löhning C, Prassler J, Stark Y, Jäger U, Hubner B, Bardroff M, Pradel I, Boss M, Bittlingmaier R, Bataa T, Frisch C, Brocks B, Honegger A, Urban M. 2008. The human combinatorial antibody library HuCAL GOLD combines diversification of all six CDRs according to the natural immune system with a novel display method for efficient selection of high-affinity antibodies. *J Mol Biol*. 376:1182-200.
[93] McCafferty J, Griffiths AD, Winter G, Chiswell DJ. 1990. Phage antibodies: Filamentous phage displaying antibody variable domains. *Nature*. 348:552-4.
[94] Clackson T, Hoogenboom HR, Griffiths AD, Winter G. 1991. Making antibody fragments using phage display libraries. *Nature*. 352:624-8.

[95] Barbas 3rd CF, Kang AS, Lerner RA, Benkovic SJ. 1991. Assembly of combinatorial antibody libraries on phage surfaces: the gene III site. *Proc Natl Acad Sci U S A*. 88:7978-82.
[96] Marks JD, Hoogenboom HR, Bonnert TP, McCafferty J, Griffiths AD, Winter G. 1991. By-passing immunization: Human antibodies from V-gene libraries displayed on phage. *J Mol Biol*. 222:581-97.
[97] Hoogenboom HR. 2005. Selecting and screening recombinant antibody libraries. *Nat Biotechnol*. 23:1105-16.
[98] Zhao A, Tohidkia MR, Siegel DL, Coukos G, Omidi Y. 2016. Phage antibody display libraries: a powerful antibody discovery platform for immunotherapy. *Crit Rev Biotechnol*. 36:276-89.
[99] Smith GP. 1985. Filamentous fusion phage: Novel expression vectors that display cloned antigens on the virion surface. *Science*. 228:1315-7.
[100] Burton DR, Barbas 3rd CF, Persson MA, Koenig S, Chanock RM, Lerner RA. 1991. A large array of human monoclonal antibodies to type 1 human immunodeficiency virus from combinatorial libraries of asymptomatic seropositive individuals. *Proc Natl Acad Sci U S A*. 88:10134-7.
[101] Boder ET, Wittrup KD. 1997. Yeast surface display for screening combinatorial polypeptide libraries. *Nat Biotechnol*. 15:553-7.
[102] Chao G, Lau WL, Hackel BJ, Sazinsky SL, Lippow SM, Wittrup KD. 2006. Isolating and engineering human antibodies using yeast surface display. *Nat Protoc*. 1:755-68.
[103] Sun Y, Ban B, Bradbury A, Ansari GAS, Blake DA. 2016. Combining yeast display and competitive FACS to select rare hapten-specific clones from recombinant antibody libraries. *Anal Chem*. 88:9181-9.
[104] Li H, Sethuraman N, Stadheim TA, Zha D, Prinz B, Ballew N, Bobrowicz P, Choi B-K, Cook WJ, Cukan M, Houston-Cummings NR, Davidson R, Gong B, Hamilton SR, Hoopes JP, Jiang Y, Kim N, Mansfield R, Nett JH, Rios S, Strawbridge R, Wildt S, Gerngross TU. 2006. Optimization of humanized IgGs in glycoengineered Pichia pastoris. *Nat Biotechnol*. 24:210-5.
[105] Beerli RR, Bauer M, Buser RB, Gwerder M, Muntwiler S, Maurer P, Saudan P, Bachmann MF. 2008. Isolation of human monoclonal antibodies by mammalian cell display. *Proc Natl Acad Sci U S A*. 105:14336-41.
[106] Ernest SS, Maurice Z. 2014. Antibody library display on a mammalian virus vector: combining the advantages of both phage and yeast display into one technology. *Curr Drug Discov Technol*. 11:48-55.
[107] Zhang H, Wilson IA, Lerner RA. 2012. Selection of antibodies that regulate phenotype from intracellular combinatorial antibody libraries. *Proc Natl Acad Sci U S A*. 109:15728-33.
[108] Yea K, Zhang H, Xie J, Jones TM, Yang G, Song BD, Lerner RA. 2013. Converting stem cells to dendritic cells by agonist antibodies from unbiased morphogenic selections. *Proc Natl Acad Sci U S A*. 110:14966-71.
[109] Zhang H, Yea K, Xie J, Ruiz D, Wilson IA, Lerner RA. 2013. Selecting agonists from single cells infected with combinatorial antibody libraries. *Chem Biol*. 20:734-41.
[110] Xie J, Zhang H, Yea K, Lerner RA. 2013. Autocrine signaling based selection of combinatorial antibodies that transdifferentiate human stem cells. *Proc Natl Acad Sci U S A*. 110:8099-104.
[111] Yea K, Zhang H, Xie J, Jones TM, Lin CW, Francesconi W, Berton F, Fallahi M, Sauer K, Lerner RA. 2015. Agonist antibody that induces human malignant cells to kill one another. *Proc Natl Acad Sci U S A*. 112:E6158-65.
[112] Xie J, Yea K, Zhang H, Moldt B, He L, Zhu J, Lerner RA. 2014. Prevention of cell death by antibodies selected from intracellular combinatorial libraries. *Chem Biol*. 21:274-83.
[113] Carlson ED, Gan R, Hodgman CE, Jewett MC. 2012. Cell-free protein synthesis: Applications come of age. *Biotechnol Adv*. 30:1185-94.

[114] Stech M, Kubick S. 2015. Cell-free synthesis meets antibody production: A review. *Antibodies (Basel)*. 4:12.
[115] Hanes J, Pluckthun A. 1997. In vitro selection and evolution of functional proteins by using ribosome display. *Proc Natl Acad Sci U S A*. 94:4937-42.
[116] Fukuda I, Kojoh K, Tabata N, Doi N, Takashima H, Miyamoto-Sato E, Yanagawa H. 2006. In vitro evolution of single-chain antibodies using mRNA display. *Nucleic Acids Res*. 34:e127.
[117] He M, Taussig MJ. 1997. Antibody-ribosome-mRNA (ARM) complexes as efficient selection particles for in vitro display and evolution of antibody combining sites. *Nucleic Acids Res*. 25:5132-4.
[118] Stafford RL, Matsumoto ML, Yin G, Cai Q, Fung JJ, Stephenson H, Gill A, You M, Lin SH, Wang WD, Masikat MR, Li X, Penta K, Steiner AR, Baliga R, Murray CJ, Thanos CD, Hallam TJ, Sato AK. 2014. In vitro Fab display: a cell-free system for IgG discovery. *Protein Eng Des Sel*. 27:97-109.
[119] Cai Q, Hanson JA, Steiner AR, Tran C, Masikat MR, Chen R, Zawada JF, Sato AK, Hallam TJ, Yin G. 2015. A simplified and robust protocol for immunoglobulin expression in Escherichia coli cell-free protein synthesis systems. *Biotechnol Prog*. 31:823-31.
[120] Zemella A, Thoring L, Hoffmeister C, Kubick S. 2015. Cell-free protein synthesis: Pros and cons of prokaryotic and eukaryotic systems. *ChemBioChem*. 16:2420-31.
[121] Stech M, Hust M, Schulze C, Dübel S, Kubick S. 2014. Cell-free eukaryotic systems for the production, engineering, and modification of scFv antibody fragments. *Eng Life Sci*. 14:387-98.
[122] Scheid JF, Mouquet H, Ueberheide B, Diskin R, Klein F, Oliveira TYK, Pietzsch J, Fenyo D, Abadir A, Velinzon K, Hurley A, Myung S, Boulad F, Poignard P, Burton DR, Pereyra F, Ho DD, Walker BD, Seaman MS, Bjorkman PJ, Chait BT, Nussenzweig MC. 2011. Sequence and structural convergence of broad and potent HIV antibodies that mimic CD4 binding. *Science*. 333:1633-7.
[123] Boder ET, Midelfort KS, Wittrup KD. 2000. Directed evolution of antibody fragments with monovalent femtomolar antigen-binding affinity. *Proc Natl Acad Sci U S A*. 97:10701-5.
[124] Smith ES, Mandokhot A, Evans EE, Mueller L, Borrello MA, Sahasrabudhe DM, Zauderer M. 2001. Lethality-based selection of recombinant genes in mammalian cells: Application to identifying tumor antigens. *Nat Med*. 7:967-72.
[125] Hanes J, Schaffitzel C, Knappik A, Plückthun A. 2000. Picomolar affinity antibodies from a fully synthetic naive library selected and evolved by ribosome display. *Nat Biotechnol*. 18:1287-92.
[126] Nelson AL, Dhimolea E, Reichert JM. 2010. Development trends for human monoclonal antibody therapeutics. *Nat Rev Drug Discov*. 9:767-74.
[127] Bradbury AR, Sidhu S, Dübel S, McCafferty J. 2011. Beyond natural antibodies: The power of in vitro display technologies. *Nat Biotechnol*. 29:245-54.
[128] Clynes RA, Towers TL, Presta LG, Ravetch JV. 2000. Inhibitory Fc receptors modulate in vivo cytotoxicity against tumor targets. *Nat Med*. 6:443-6.
[129] Rouet R, Lowe D, Christ D. 2014. Stability engineering of the human antibody repertoire. *FEBS Lett*. 588:269-77.
[130] Bunka DHJ, Stockley PG. 2006. Aptamers come of age – at last. *Nat Rev Microbiol*. 4:588.
[131] Keefe AD, Pai S, Ellington A. 2010. Aptamers as therapeutics. *Nat Rev Drug Discov*. 9:537-50.
[132] Lao Y-H, Phua KKL, Leong KW. 2015. Aptamer nanomedicine for cancer therapeutics: Barriers and potential for translation. *ACS Nano*. 9:2235-54.
[133] Sun H, Zu Y. 2015. Aptamers and their applications in nanomedicine. *Small*. 11:2352-64.
[134] Sun H, Zhu X, Lu PY, Rosato RR, Tan W, Zu Y. 2014. Oligonucleotide Aptamers: New Tools for Targeted Cancer Therapy. *Mol Ther Nucleic Acids*. 3.

[135] Tuerk C, Gold L. 1990. Systematic evolution of ligands by exponential enrichment: RNA ligands to bacteriophage T4 DNA polymerase. *Science*. 249:505-10.
[136] Ozer A, Pagano JM, Lis JT. 2014. New technologies provide quantum changes in the scale, speed, and success of SELEX methods and aptamer characterization. *Mol Ther Nucleic Acids*. 3:e183.
[137] Darmostuk M, Rimpelova S, Gbelcova H, Ruml T. 2015. Current approaches in SELEX: An update to aptamer selection technology. *Biotechnol Adv*. 33:1141-61.
[138] Dao P, Hoinka J, Takahashi M, Zhou J, Ho M, Wang Y, Costa F, Rossi JJ, Backofen R, Burnett J, Przytycka TM. 2016. AptaTRACE elucidates RNA sequence-structure motifs from selection trends in HT-SELEX experiments. *Cell Systems*. 3:62-70.
[139] Caroli J, Taccioli C, De La Fuente A, Serafini P, Bicciato S. 2016. APTANI: a computational tool to select aptamers through sequence-structure motif analysis of HT-SELEX data. *Bioinformatics*. 32:161-4.
[140] Lambert JM. 2013. Drug-conjugated antibodies for the treatment of cancer. *Br J Clin Pharmacol*. 76:248-62.
[141] Brannon-Peppas L, Blanchette JO. 2004. Nanoparticle and targeted systems for cancer therapy. *Adv Drug Deliv Rev*. 56:1649-59.
[142] Hrkach J, Von Hoff D, Ali MM, Andrianova E, Auer J, Campbell T, De Witt D, Figa M, Figueiredo M, Horhota A, Low S, McDonnell K, Peeke E, Retnarajan B, Sabnis A, Schnipper E, Song JJ, Song YH, Summa J, Tompsett D, Troiano G, Van Geen Hoven T, Wright J, LoRusso P, Kantoff PW, Bander NH, Sweeney C, Farokhzad OC, Langer R, Zale S. 2012. Preclinical development and clinical translation of a PSMA-targeted docetaxel nanoparticle with a differentiated pharmacological profile. *Sci Transl Med*. 4:128ra39.
[143] Lundqvist M, Stigler J, Elia G, Lynch I, Cedervall T, Dawson KA. 2008. Nanoparticle size and surface properties determine the protein corona with possible implications for biological impacts. *Proc Natl Acad Sci U S A*. 105:14265-70.
[144] Kennedy PJ, Oliveira C, Granja PL, Sarmento B. 2018. Monoclonal antibodies: Technologies for early discovery and engineering. *Crit Rev Biotechnol*. 38:394-408.
[145] Arruebo M, Valladares M, González-Fernández Á. 2009. Antibody-conjugated nanoparticles for biomedical applications. *J Nanomater*. 2009:1-24.
[146] Park JW, Hong K, Kirpotin DB, Colbern G, Shalaby R, Baselga J, Shao Y, Nielsen UB, Marks JD, Moore D, Papahadjopoulos D, Benz CC. 2002. Anti-HER2 immunoliposomes: Enhanced efficacy attributable to targeted delivery. *Clin Cancer Res*. 8:1172-81.
[147] Elias DR, Poloukhtine A, Popik V, Tsourkas A. 2013. Effect of ligand density, receptor density, and nanoparticle size on cell targeting. *Nanomedicine*. 9:194-201.
[148] Sapsford KE, Algar WR, Berti L, Gemmill KB, Casey BJ, Oh E, Stewart MH, Medintz IL. 2013. Functionalizing nanoparticles with biological molecules: Developing chemistries that facilitate nanotechnology. *Chem Rev*. 113:1904-2074.
[149] Kumar S, Aaron J, Sokolov K. 2008. Directional conjugation of antibodies to nanoparticles for synthesis of multiplexed optical contrast agents with both delivery and targeting moieties. *Nat Protoc*. 3:314-20.
[150] Antunes F, Andrade F, Sarmento B. Chitosan-based nanoparticulates for oral delivery of biopharmaceuticals. Chitosan-based systems for biopharmaceuticals: John Wiley & Sons, Ltd; 2012. p. 225-41.
[151] Sokolov K, Follen M, Aaron J, Pavlova I, Malpica A, Lotan R, Richards-Kortum R. 2003. Real-time vital optical imaging of precancer using anti-epidermal growth factor receptor antibodies conjugated to gold nanoparticles. *Cancer Res*. 63:1999-2004.
[152] Yao VJ, D'Angelo S, Butler KS, Theron C, Smith TL, Marchio S, Gelovani JG, Sidman RL, Dobroff AS, Brinker CJ, Bradbury AR, Arap W, Pasqualini R. 2016. Ligand-targeted theranostic nanomedicines against cancer. *J Control Release*.

[153] Cheng Z, Al Zaki A, Hui JZ, Muzykantov VR, Tsourkas A. 2012. Multifunctional nanoparticles: Cost versus benefit of adding targeting and imaging capabilities. *Science*. 338:903-10.
[154] van der Meel R, Vehmeijer LJ, Kok RJ, Storm G, van Gaal EV. 2013. Ligand-targeted particulate nanomedicines undergoing clinical evaluation: Current status. *Adv Drug Deliv Rev*. 65:1284-98.
[155] Pearson RM, Juettner V, Hong S. 2014. Biomolecular corona on nanoparticles: A survey of recent literature and its implications in targeted drug delivery. *Front Chem*. 2:108.
[156] Salvati A, Pitek AS, Monopoli MP, Prapainop K, Bombelli FB, Hristov DR, Kelly PM, Aberg C, Mahon E, Dawson KA. 2013. Transferrin-functionalized nanoparticles lose their targeting capabilities when a biomolecule corona adsorbs on the surface. *Nat Nanotechnol*. 8:137-43.
[157] Dai Q, Walkey C, Chan WCW. 2014. Polyethylene glycol backfilling mitigates the negative impact of the protein corona on nanoparticle cell targeting. *Angew Chem Int Ed Engl*. 53:5093-6.
[158] Roth F, De La Fuente AC, Vella JL, Zoso A, Inverardi L, Serafini P. 2012. Aptamer-mediated blockade of IL4Rα triggers apoptosis of MDSCs and limits tumor progression. *Cancer Res*. 72:1373-83.
[159] Daftarian P, Kaifer AE, Li W, Blomberg BB, Frasca D, Roth F, Chowdhury R, Berg EA, Fishman JB, Al Sayegh HA, Blackwelder P, Inverardi L, Perez VL, Lemmon V, Serafini P. 2011. Peptide-conjugated PAMAM dendrimer as a universal DNA vaccine platform to target antigen-presenting cells. *Cancer Res*. 71:7452-62.
[160] Kennedy PJ, Oliveira C, Granja PL, Sarmento B. 2017. Antibodies and associates: Partners in targeted drug delivery. *Pharmacol Ther*.
[161] Polz MF, Cavanaugh CM. 1998. Bias in template-to-product ratios in multitemplate PCR. *Appl Environ Microbiol*. 64:3724-30.
[162] Williams R, Peisajovich SG, Miller OJ, Magdassi S, Tawfik DS, Griffiths AD. 2006. Amplification of complex gene libraries by emulsion PCR. *Nat Methods*. 3:545-50.
[163] Levay A, Brenneman R, Hoinka J, Sant D, Cardone M, Trinchieri G, Przytycka TM, Berezhnoy A. 2015. Identifying high-affinity aptamer ligands with defined cross-reactivity using high-throughput guided systematic evolution of ligands by exponential enrichment. *Nucleic Acids Res*. 43:e82.
[164] Nilvebrant J, Kuku G, Bjorkelund H, Nestor M. 2012. Selection and in vitro characterization of human CD44v6-binding antibody fragments. *Biotechnol Appl Biochem*. 59:367-80.
[165] Sefah K, Shangguan D, Xiong X, O'Donoghue MB, Tan W. 2010. Development of DNA aptamers using Cell-SELEX. *Nat Protoc*. 5:1169-85.
[166] Lv L, Liu H-G, Dong S-Y, Yang F, Wang Q-X, Guo G-L, Pan Y-F, Zhang X-H. 2016. Upregulation of CD44v6 contributes to acquired chemoresistance via the modulation of autophagy in colon cancer SW480 cells. *Tumor Biol*. 37:8811-24.
[167] Saito S, Okabe H, Watanabe M, Ishimoto T, Iwatsuki M, Baba Y, Tanaka Y, Kurashige J, Miyamoto Y, Baba H. 2013. CD44v6 expression is related to mesenchymal phenotype and poor prognosis in patients with colorectal cancer. *Oncol Rep*. 29:1570-8.
[168] Okayama H, Kumamoto K, Saitou K, Hayase S, Kofunato Y, Sato Y, Miyamoto K, Nakamura I, Ohki S, Sekikawa K, Takenoshita S. 2009. CD44v6, MMP-7 and nuclear Cdx2 are significant biomarkers for prediction of lymph node metastasis in primary gastric cancer. *Oncol Rep*. 22:745-55.
[169] Yamaguchi A, Goi T, Yu J, Hirono Y, Ishida M, Iida A, Kimura T, Takeuchi K, Katayama K, Hirose K. 2002. Expression of CD44v6 in advanced gastric cancer and its relationship to hematogenous metastasis and long-term prognosis. *J Surg Oncol*. 79:230-5.

[170] Wang J-L, Su W-Y, Lin Y-W, Xiong H, Chen Y-X, Xu J, Fang J-Y. 2017. CD44v6 overexpression related to metastasis and poor prognosis of colorectal cancer: A meta-analysis. *Oncotarget*. 8:12866-76.
[171] Reichert JM. 2017. Antibodies to watch in 2017. *MAbs*. 9:167-81.
[172] Kennedy PJ, Oliveira C, Granja PL, Sarmento B. 2017. Antibodies and associates: Partners in targeted drug delivery. *Pharmacol Ther*. 177:129-45.
[173] Li Y, Wang J, Wientjes MG, Au JLS. 2012. Delivery of nanomedicines to extracellular and intracellular compartments of a solid tumor. *Adv Drug Deliv Rev*. 64:29-39.
[174] Araújo F, das Neves J, Martins JP, Granja PL, Santos HA, Sarmento B. 2017. Functionalized materials for multistage platforms in the oral delivery of biopharmaceuticals. *Prog Mater Sci*. 89:306-44.
[175] Kwon EJ, Lo JH, Bhatia SN. 2015. Smart nanosystems: Bio-inspired technologies that interact with the host environment. *Proc Natl Acad Sci U S A*. 112:14460-6.
[176] Lee Y, Graeser R, Kratz F, Geckeler KE. 2011. Paclitaxel-loaded polymer nanoparticles for the reversal of multidrug resistance in breast cancer cells. *Adv Func Mater*. 21:4211-8.
[177] Sivaram AJ, Wardiana A, Howard CB, Mahler SM, Thurecht KJ. 2017. Recent advances in the generation of antibody–nanomaterial conjugates. *Adv Healthc Mater*. in press.
[178] Gärtner F, David L, Seruca R, Machado JC, Sobrinho-Simões M. 1996. Establishment and characterization of two cell lines derived from human diffuse gastric carcinomas xenografted in nude mice. *Virchows Arch*. 428:91-8.
[179] Govender T, Stolnik S, Garnett MC, Illum L, Davis SS. 1999. PLGA nanoparticles prepared by nanoprecipitation: drug loading and release studies of a water soluble drug. *J Control Release*. 57:171-85.
[180] Sousa F, Cruz A, Fonte P, Pinto IM, Neves-Petersen MT, Sarmento B. 2017. A new paradigm for antiangiogenic therapy through controlled release of bevacizumab from PLGA nanoparticles. *Sci Rep*. 7:3736.
[181] Gomes MJ, Kennedy PJ, Martins S, Sarmento B. 2017. Delivery of siRNA silencing P-gp in peptide-functionalized nanoparticles causes efflux modulation at the blood-brain barrier. *Nanomedicine (Lond)*. 12:1385-99.
[182] Almeida A, Silva D, Goncalves V, Sarmento B. 2017. Synthesis and characterization of chitosan-grafted-polycaprolactone micelles for modulate intestinal paclitaxel delivery. *Drug Deliv Transl Res*. 8:387-97.
[183] Fonte P, Soares S, Sousa F, Costa A, Seabra V, Reis S, Sarmento B. 2014. Stability study perspective of the effect of freeze-drying using cryoprotectants on the structure of insulin loaded into PLGA nanoparticles. *Biomacromolecules*. 15:3753-65.
[184] Nair DP, Podgórski M, Chatani S, Gong T, Xi W, Fenoli CR, Bowman CN. 2014. The Thiol-Michael addition click reaction: A powerful and widely used tool in materials chemistry. *Chem Mater*. 26:724-44.
[185] Sato S, Yokozaki H, Yasui W, Nikai H, Tahara E. 1999. Silencing of the CD44 gene by CpG methylation in a human gastric carcinoma cell line. *Jpn J Cancer Res*. 90:485-9.
[186] Danhier F, Ansorena E, Silva JM, Coco R, Le Breton A, Préat V. 2012. PLGA-based nanoparticles: An overview of biomedical applications. *J Control Release*. 161:505-22.
[187] Martins C, Sousa F, Araújo F, Sarmento B. 2017. Functionalizing PLGA and PLGA derivatives for drug delivery and tissue regeneration applications. *Adv Healthc Mater*. in press.
[188] Suk JS, Xu Q, Kim N, Hanes J, Ensign LM. 2016. PEGylation as a strategy for improving nanoparticle-based drug and gene delivery. *Adv Drug Deliv Rev*. 99:28-51.
[189] Gref R, Lück M, Quellec P, Marchand M, Dellacherie E, Harnisch S, Blunk T, Müller RH. 2000. 'Stealth' corona-core nanoparticles surface modified by polyethylene glycol (PEG): influences of the corona (PEG chain length and surface density) and of the core composition on phagocytic uptake and plasma protein adsorption. *Colloids Surf B Biointerfaces*. 18:301-13.

[190] Menon JU, Kona S, Wadajkar AS, Desai F, Vadla A, Nguyen KT. 2012. Effects of surfactants on the properties of PLGA nanoparticles. *J Biomed Mater Res A*. 100A:1998-2005.
[191] Fonseca C, Simões S, Gaspar R. 2002. Paclitaxel-loaded PLGA nanoparticles: preparation, physicochemical characterization and in vitro anti-tumoral activity. *J Control Release*. 83:273-86.
[192] Heinz H, Pramanik C, Heinz O, Ding Y, Mishra RK, Marchon D, Flatt RJ, Estrela-Lopis I, Llop J, Moya S, Ziolo RF. 2017. Nanoparticle decoration with surfactants: Molecular interactions, assembly, and applications. *Surf Sci Rep*. 72:1-58.
[193] Owens DE, Peppas NA. 2006. Opsonization, biodistribution, and pharmacokinetics of polymeric nanoparticles. *Int J Pharm*. 307:93-102.
[194] Danhier F, Lecouturier N, Vroman B, Jérôme C, Marchand-Brynaert J, Feron O, Préat V. 2009. Paclitaxel-loaded PEGylated PLGA-based nanoparticles: In vitro and in vivo evaluation. *J Control Release*. 133:11-7.
[195] Afify A, Durbin-Johnson B, Virdi A, Jess H. 2016. The expression of CD44v6 in colon: from normal to malignant. *Ann Diagn Pathol*. 20:19-23.
[196] Landry FB, Bazile DV, Spenlehauer G, Veillard M, Kreuter J. 1996. Degradation of poly(d,l-lactic acid) nanoparticles coated with albumin in model digestive fluids (USP XXII). *Biomaterials*. 17:715-23.
[197] Fonte P, Reis S, Sarmento B. 2016. Facts and evidences on the lyophilization of polymeric nanoparticles for drug delivery. *J Control Release*. 225:75-86.
[198] Jahan ST, Haddadi A. 2015. Investigation and optimization of formulation parameters on preparation of targeted anti-CD205 tailored PLGA nanoparticles. *Int J Nanomedicine*. 10:7371-84.
[199] Ohtake S, Wang YJ. 2011. Trehalose: Current use and future applications. *J Pharm Sci*. 100:2020-53.
[200] Spiegelberg D, Nilvebrant J. 2017. CD44v6-targeted imaging of head and neck squamous cell carcinoma: Antibody-based approaches. *Contrast Media Mol Imaging*. 2017:14.
[201] Jung T, Gross W, Zoller M. 2011. CD44v6 coordinates tumor matrix-triggered motility and apoptosis resistance. *J Biol Chem*. 286:15862-74.